Thesis presented by

Abdenor FELLAH

for the degree of

Doctor of Philosophy

PHYSICAL AND CHEMICAL ATTACHMENT OF PECTINS TO SUBSTRATES : METHODS, CHARACTERISATION AND APPLICATION

MASSEY UNIVERSITY, NEW ZEALAND

MASSEY UNIVERSITY
TE KUNENGA KI PŪREHUROA

&

FONTERRA, NEW ZEALAND

Fonterra
Dairy for life

Research conducted in : Institute of Fundamental Sciences (IFS)
Massey University, Palmerston North

Supervision : Ass. Prof. Martin.A.K WILLIAMS

Co-supervision : Dr. Don OTTER and Dr. Yacine HEMAR

July, 2011

SUMMARY

The plant cell wall is a complex biological matrix in which pectic polysaccharides play an instrumental role in regulating mechanical properties. Nanomechanical studies of single chains hold the promise of enabling the comprehension of fundamental aspects concerning the structural, mechanical and binding properties of pectin at an unprecedented level of molecular detail, using measured single polysaccharide force-extension behavior as a signature. However, before such promise can be fulfilled, a better understanding of the attachment of the polymer under study to the substrates between which it is stretched is required.

Herein, chemoselective methodologies have been developed to covalently couple one end of a pectin chain onto a solid support. Prior to immobilization, pectin fine structure was investigated using accurate and non-invasive infrared spectroscopy. Comparison of experimental results with the predictions of quantum chemical calculations carried out using density functional theory confirmed this technique as an effective tool for the characterization of pectin fine structure. Subsequently, following appropriate functionalization of the support, pectin chains were anchored to polystyrene beads, specifically through their reducing end. These methods were shown to be efficient using IR spectroscopy, once more coupled with quantum chemical calculations, with the formation of specific newly introduced bonds being demonstrated.

Finally, single-molecule force spectroscopy was used to stretch single pectin molecules covalently bonded to substrates using the previously described method applied to glass surfaces. Compared to physisorption, which was also extensively studied, tethering the pectin non-reducing end appeared to increase the average stretch length and improved significantly the probability of stretching a single chain to high forces.

To my joy, my pride, my everything,

my baby boys

ETHAN et RUBEN…

(and the little one coming)…

AKNOWLEDGMENTS

Surprisingly (yeah right!), this part is kind of a relief, even if I don't really know where to start. Some many people to thank...

I have to start with "the boss". Bill, you will never know how much I am grateful. When I decided to come to New Zealand, there was a little bit of fear. Life in the other side of the world, down under ... And the language. And the kiwi accent!!! The first English word I heard here was from you. And immediately I had a good feeling. My supervisor is the best in the world. Not only for his scientific knowledge (thank you for all your help, all your support, all the interesting meetings that always made me feel better afterwards when I was feeling I was getting nowhere,...) but also for his "human side" (I don't think I have ever seen you in a bad day...). Priceless...

Special thanks to my co-supervisors Yacine (Djazaïr, Djazaïr !!!) and Donn, who have always been there for me with their support, help and scientific suggestions.

I would also like to thank everyone at the Institute of Fundamental Science and Fonterra, for making my stay in New Zealand very interesting and rewarding.

This work was financially supported by the Foundation for Research, Science and Technology, and Fonterra, without which my project would not have been possible.

I would also like to thank all the member of the "pectin" group for their ideas... and morning tea discussions. Steve, Erich,... Especially Padmesh and Naser (Djazaïr, Djazaïr (bis)). A few articles together... and some really good moments all over Aotearoa...

"La patience est un arbre dont les racines sont amères et les fruits doux".

Cette thèse est la face visible de l'iceberg. Je ne peux omettre ici la partie émergée : tous les enseignants de Physique-Chimie au lycée de Gagny, Majdi Hochlaf, prof à Marne-La-Vallée, tous mes potes à la fac de Marne-La-Vallée, Régis, Mathias,… et surtout mon 'binôme' Jean-Michel pour tous les bons moments passés ensemble (comme quoi des supporters de l'OM et du PSG peuvent s'entendre !!!) et son aide précieuse (si tu vois ce que je veux dire !!!).

Sans oublier toutes les personnes ici en nz qui m'ont permis d'en arriver la : Mickael et Laureline, Ali,… J'en oublie certainement…Merci sincèrement pour votre aide très précieuse.

Un petit mot pour ma famille adore en France. Toujours la pour moi, même quand je décidai de partir à près de 20000km, la tête à l'envers…Mon ange-frère Yassin, mon frère adore Sif pour toute son aide avec les programmes de calcul qui m'ont sauve un nombre incalculable d'heures (promis, je vais réduire les demandes d'aide informatique!!!), mes belles sœurs Jess et Tif et mon beau-frère (un jour peut-être ?) Eddy pour tout leur support émotionnel quand tout n'allait pas pour le mieux. Et, en dernier mais pas le moindre, ma sœur adorée Suad, sans qui cette thèse n'aurait probablement jamais vu le jour… Je vous adore.

To finish, I would like to thank my beautiful wife Melissa for her support throughout my PhD. The good times (many), also the hard ones (few?)… A big big big thank you to Uncle Phil for his kindness and help.

Last but not least, my kids. Ethan, Ruben, the 3rd one coming… You are my joy, my pride,… my everything. I love you so much. This thesis is for you, my baby boys…

CONTENTS

LIST OF FIGURES

LIST OF TABLES

ABBREVIATIONS

AFM	Atomic Force Microscopy
CI	Confidence Interval
DLS	Dynamic Light Scattering
DFT	Density Functional Theory
DM	Degree of Methyl-esterification
Fig.	Figure
HG	Homogalacturonan
HM	Highly Methyl-esterified
Gal*p*A	Galactopyranosyluronic acid
Kdo	Ketodeoxymannooctulopyranosylonic acid
LM	Lowly Methyl-esterified
NMR	Nuclear Magnetic Resonance
OT	Optical Tweezers
PFM	Peak Fitting Module
PG	Polygalacturonase
PGL	Pectate Lyase
PL	Pectin Lyase
Pka	Dissociation constant
PME	Polymethylesterase
PMG	Polymethylgalacturonase
RA	Reductive Amination
RG I	Rhamnogalacturonan I
RG II	Rhamnogalacturonan II
Rha	Rhamnose
SMFS	Single molecule force spectroscopy
SPM	Scanning Probe Microscopy
STM	Scanning Tunneling Microscope
TF	Thiazolidine Formation

CHAPTER 1.

Biopolymers are used to a major extent in the food and other industries (pharmaceuticals, cosmetics, etc…). In general, they can be utilized as thickening and/or gelling agents, for the stabilization of emulsions (Dickinson et al., 2000; McClements, 2006), for syneresis control (Sanli et al., 2011; Schenkel et al., 2010), as suspending agents (Dlamini et al., 2007), and for coating and binding (Marciano et al., 2008), amongst many other uses.

A major advantage of biopolymers is that they are natural ingredients, which is often required for 'consumer-friendly' labels. The molecular and functional properties of biopolymers depend on the extraction, purification and processing treatments used to produce functional ingredients. This provides food scientists with a large palette of potential biopolymer-based functional ingredients to design improved or novel food.

Amongst the plant cell components, the cell walls, whose most prominent components are polysaccharides (hemicellulose, cellulose, pectin), have the most important influence on the textural properties of plant tissues. Multiple biological functions have been attributed to pectins, most of them related to cell wall mechanical properties: regulation of cell expansion (Cosgrove, 2000), cell adhesion (Willats, 2001), etc…

1. BACKGROUND: PECTIN

1.1. Generalities

Pectin was discovered in the 18th century (Vauquelin, 1790) and was first characterized as the active fruit component responsible for gel formation in the 19th century by Henri Braconnot. In his 1825 communication (Braconnot, 1825), he reported about an acid he found in so many plants that he studied the molecule and emphasized on its gelling properties, naming it pectin acid from the Greek word *pectic* which means *coagulum*.

Pectic substances are integral structural components of plant cells and play an important role as cementing material in the middle lamella of primary cell walls (Fig. 1.1.).

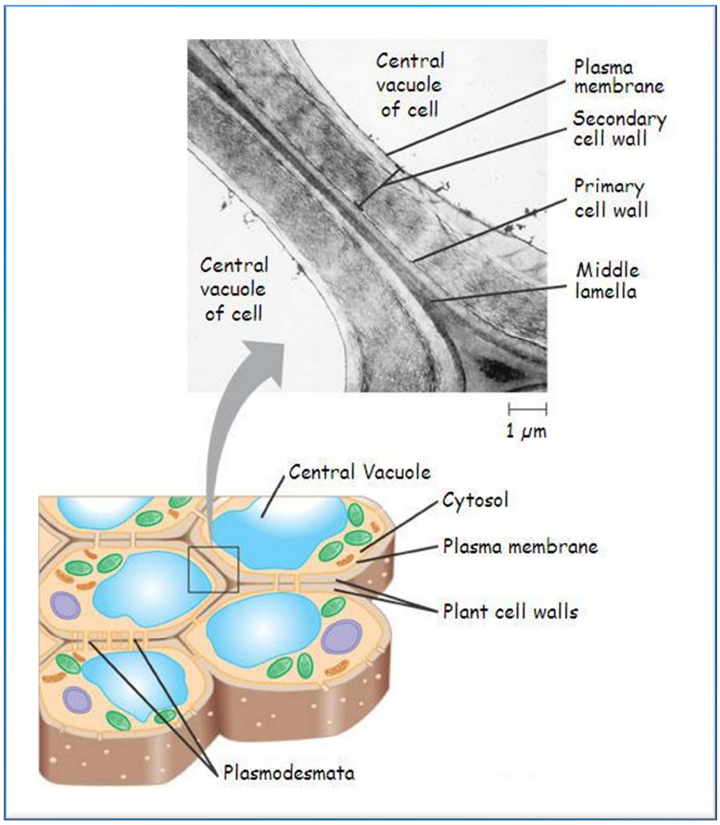

Fig. 1. 1. Plant cells diagram. Contact between cells is maintained by the middle lamella and the cell corners are often filled with pectin-rich polysaccharides.

1.2. Structure and properties

Pectins are structurally complex polymers. The backbone is composed of (1→4) linked α-D-galacturonic acid units interrupted by single (1→2) linked α-L-rhamnose residues (Colquhoun et al., 1990). Three pectic polysaccharides (homogalacturonan, rhamnogalacturonan I and substituted galacturonans) have been isolated from primary cell walls and structurally characterized (Visser and Voragen, 1996).

Homogalacturonan (HG) is a linear chain of (1→4) linked α-D-galactopyranosyluronic acid (Gal*p*A) units in which some of the carboxyl groups may be substituted by methyl ester groups and HG may, depending on the plant source be partially *O*-acylated, whilst rhamnogalacturonan I (RG I) consists of the repeating dissacharide →4)- α-D- Gal*p*A-(1→2)- α-L-Rha (1→(Fig. 1.2.) to which a variety of different glycan chains (principally arabinan and galactan) are attached to the rhamnose residues.

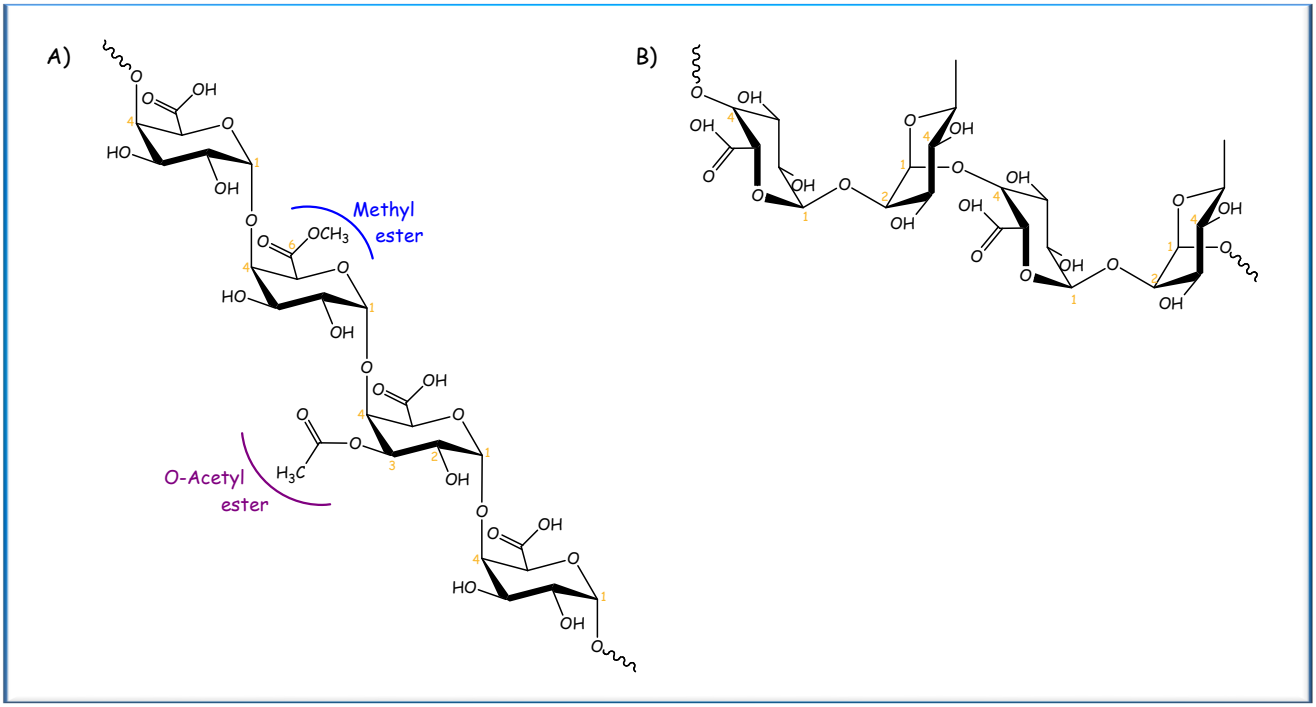

Fig. 1. 2. The primary structure of pectin. A) HG is a linear polymer of GalpA residues. Some of these residues are esterified with methanol on C-6 and with acetic acid on C-2 and C-3. B) RG I is composed of rhamnose and GalpA units. Sidechains of neutral sugar can be attached to C-4 of the rhamnose residues.

The confusingly named rhamnogalacturonan II (RG II) has a backbone of HG rather than RG, with complex side chains attached to the GalpA residues (Ridley et al., 2001; Willats et al., 2001; Willats et al., 2006), as shown in Fig. 1.3.

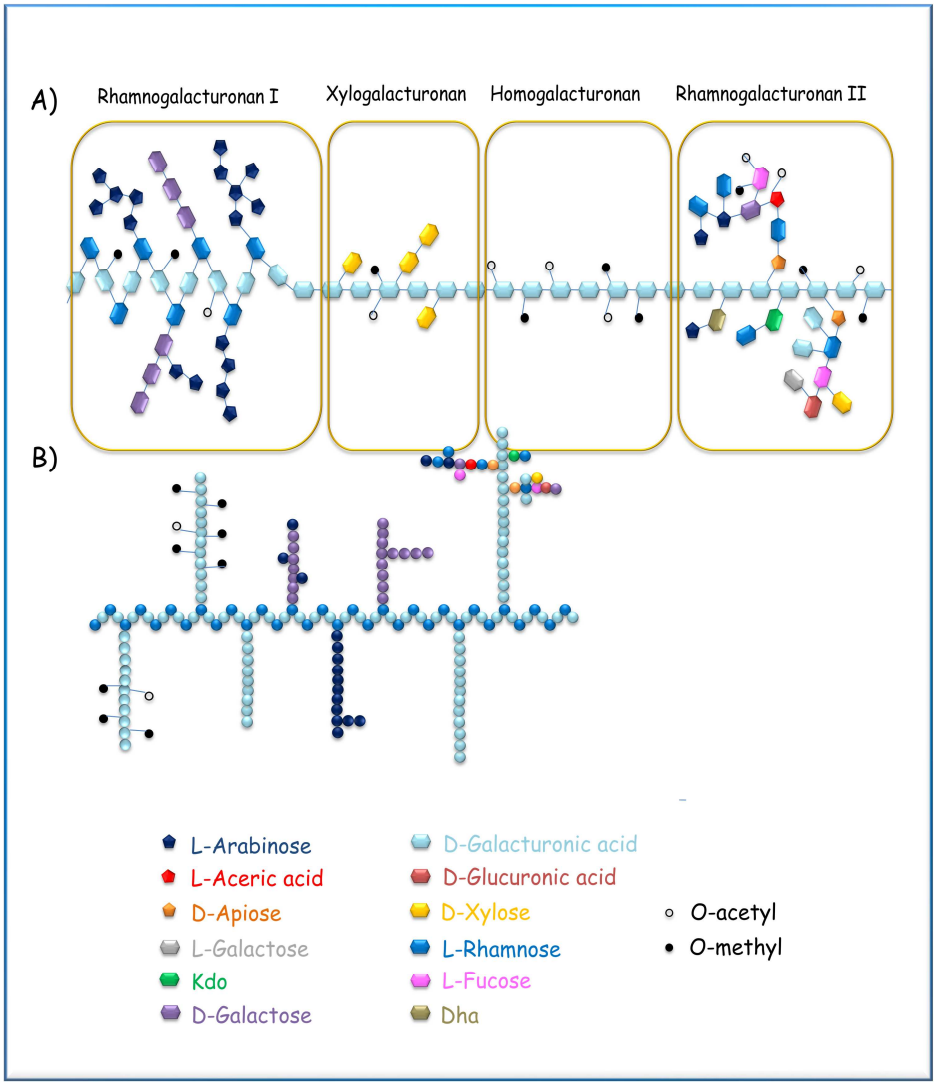

Fig. 1. 3. Schematic representation of the basic structure of pectin. A) Conventional Structure. B) Proposed alternative structure. The polymers shown here are intended only to illustrate some of the major domains found in most pectins rather than definitive structures.

The number and distribution of residues in the rhamnose region (hairy region) are dependent on the source of pectin whereas the galacturonic region (smooth region) is estimated to be a minimum of 72-100 Gal*p*A units independent of the pectin origin (Axelos et al., 1989; Ryden and Selvendran, 1990; Thibault et al., 1993). Many biological functionalities are linked to the smooth region (Willats et al., 2001; Parre et al., 2005) whereas no functionality has been clearly assigned to the hairy region (Willats et al., 2001; Perez et al., 2003).

The degree of methyl-esterification (DM) is defined by the ratio of methyl-esterified galacturonic acid residues to the total galacturonic acid units present in the pectin sample. By convention, highly methyl-esterified pectins (HM pectins) have a methyl ester content greater than 50% (Fig. 1.4B.) while lowly methyl-esterified pectins have a methyl ester content less than 50%(Fig. 1.4A.).

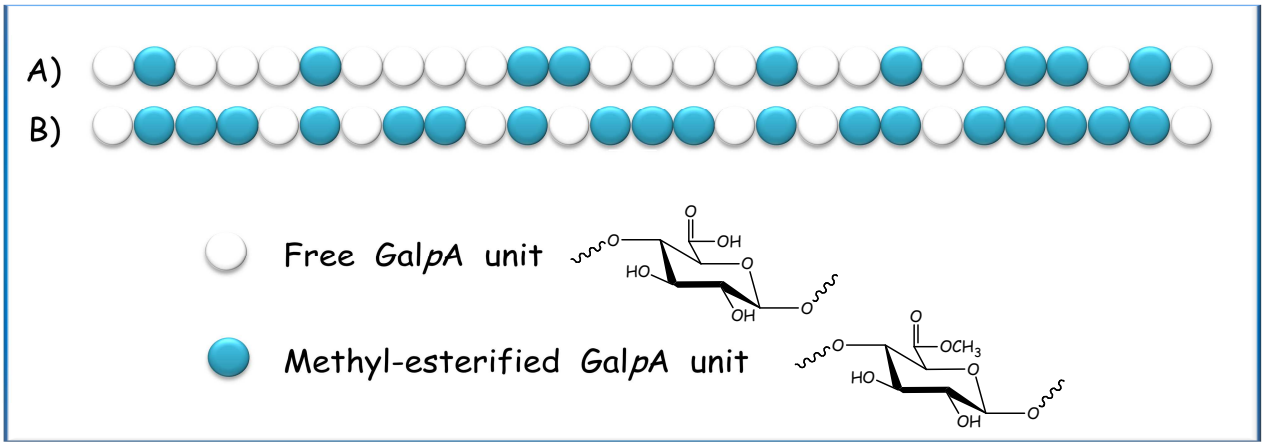

Fig. 1. 4. Schematic representation of A) a low DM pectin. B) a high DM pectin.

1.3. Extraction

The main sources of commercial pectins are citrus (lemon, lime, orange and grapefruit) peel and apple pomace, using the waste from the fruit juice industry as raw material (May, 1990). To a minor extent, pectin is also extracted from sugar-beet, potato fibres, onions, and sunflower heads, as a by-product of oil production (Joyce and Luzio, 2000).

Several extraction processes exist but they all involve 3 main steps (Sakai and Okushima, 1980; May, 1990; Iglesias and Lozano, 2004) :

(i) aqueous extraction from the raw material, performed by acid treatment (pH 1.5 to 3) at high temperature (70 to 90°C). This step enables extraction and solubilisation of pectin materials from plant tissues. Under these conditions, degradation reactions such as de-esterification and depolymerisation will occur. Therefore, the extraction conditions,

namely temperature, time and pH, should be carefully controlled to achieve the desired final properties of the product.

(ii) purification of the extract from the peel or pomace residue by filtration or centrifugation process.

(iii) isolation of the pectin from the purified extract by precipitation with alcohol or by precipitation with an insoluble salt by addition of a polyvalent cation. The precipitate obtained is washed with alcohol and pressed to remove insoluble impurities, and finally dried and milled to yield powdered pectin with a typically high DM.

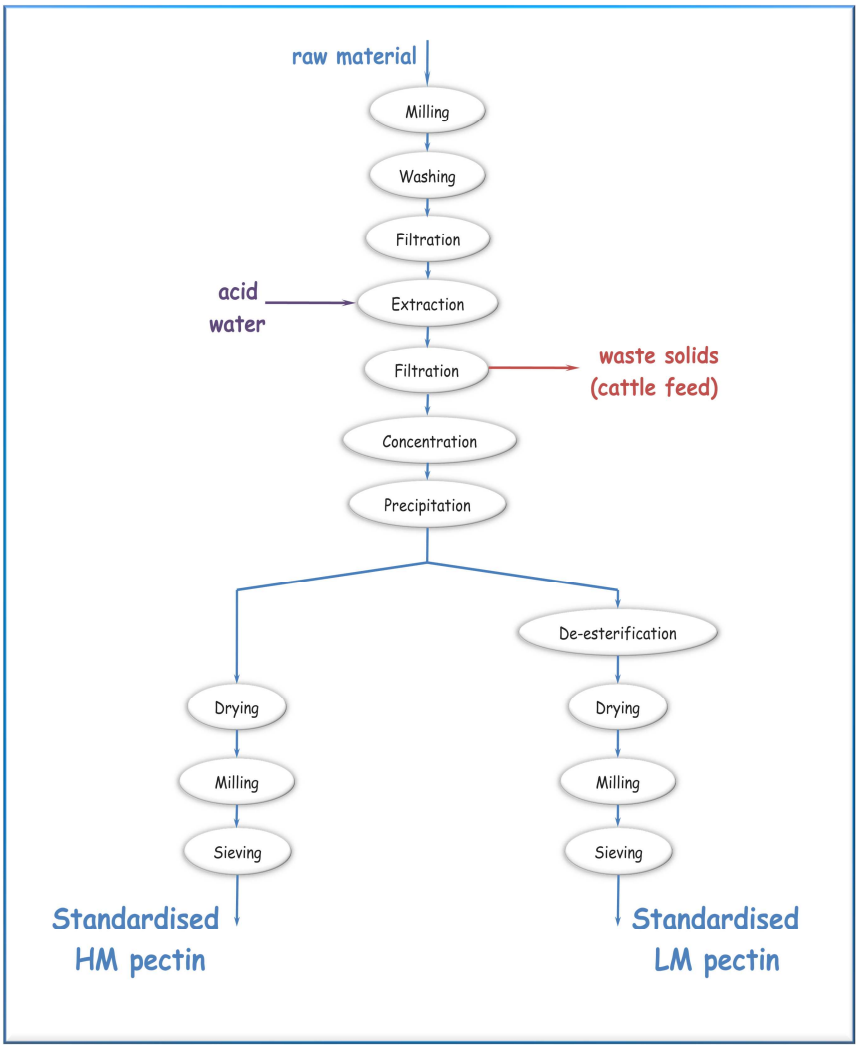

Fig. 1. 5. Schematic representation of the steps involved during the extraction and production of pectin.

As extracted from the raw materials, commercial pectins have a typical DM between 55 and 75%. The intramolecular distribution of the free carboxyl groups along the galacturonic main chain is usually heterogeneous and dependent on the deesterification method used (Taylor, 1982; Daas et al., 2001).

1.4. Structural modification

The fine structure of the extracted pectins is commonly modified with regards to their methyl ester content and sometimes with regard to their intramolecular methyl ester distribution.
LM pectins are generally obtained by controlled acid deesterification but other means, namely alkali, enzymes and ammonia, can be used. The method using ammonia produces a different type of LM pectins in which some of the carboxylic groups have been amidated (Black & Smith, 1972).

1.4.1. Acid deesterification

Treatment of pectin with acid at low temperatures leads to substantial deesterification with little chain breakdown. However, under extreme conditions decarboxylation may occur as well as chain breakdown (Stutz and Deuel, 1958). The deesterification by acid is considered to be totally random and the resulting LM pectin is assumed to have the remaining methyl ester groups in a random manner (Speiser et al., 1947). One of the disadvantages of acid deesterification is the long reaction time required to produce a suitable low DM. Shorter analysis time can be achieved but only with considerable depolymerisation (Woodmanser & Baker, 1949). This disadvantage combined with the need for acid resistant equipment has led to a closer examination of the other deesterification methods.

1.4.2. Alkaline deesterification

Alkaline deesterification, classical method of splitting ester links, is a random process that can result in decreased molecular weight due to depolymerisation of the pectin backbone glycosidic bonds by β-elimination (Renard & Thibault, 1996).

The rate of alkaline deesterification is more rapid than in the case of acid deesterification and reaction times of the order of 1-2h are sufficient to lower the DM from 80 to 10% (Vollmert, 1950).

Because preservation of pectin's molecular weight is desirable for functional properties such as gelation, enzymatic deesterification represents an attractive alternative to chemical deesterification.

Pectinases are an enzyme group that catalyses pectic substance degradation through deesterification reactions (esterases) and depolymerisation (hydrolases and lyases). Fig. 1.6. shows the action mode of the most studied esterases.

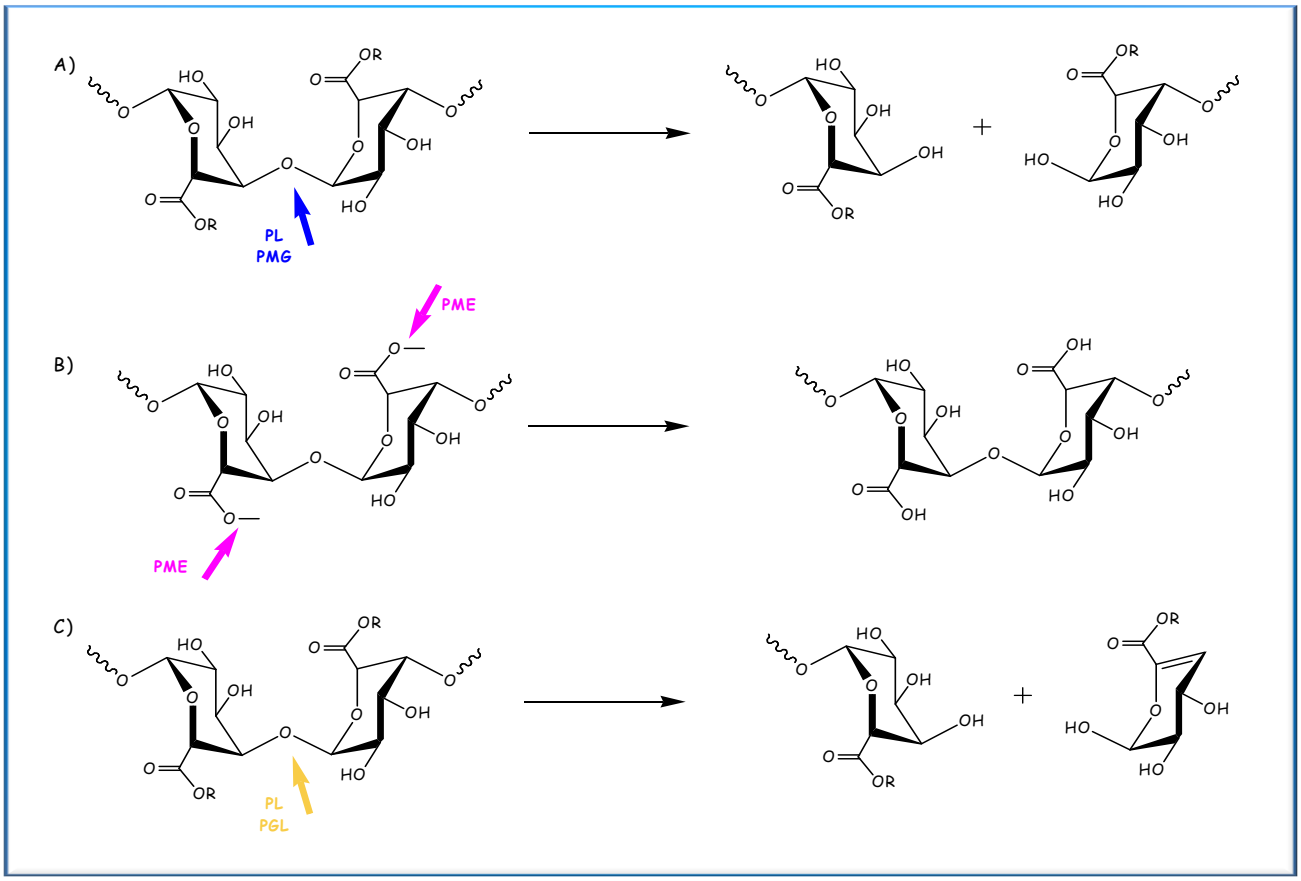

Fig. 1. 6. Mode of action of pectinases. A) R=H for PG and CH_3 for PMG. B) PME. C) R=H for PGL and CH_3 for PL.

1.4.3. Enzymatic deesterification

Pectin methyl esterase (PME) catalyses the hydrolysis of the methyl ester bonds of pectin forming pectic acid and methanol and altering the degree and the pattern of methyl esterification. The action pattern by which such degradations proceed may be divided into 3 types (Greenwood & Milne, 1968):

(i) *single-chain mechanism*: the formation of the complex enzyme-substrate is followed by the complete conversion of the contiguous sites before the enzyme diffuses away to attack another substrate molecule.

(ii) *multi-chain mechanism*: the enzyme dissociates from the substrate after each reaction resulting in splitting a single bond.

(iii) *multiple-attack mechanism*: the enzyme catalyses the transformation of a limited average number of residues for every active enzyme-substrate-complex formed.

PMEs are ubiquitous enzyme in the plant kingdom and in several plant pathogenic bacteria and fungi. The action of plant PMEs with pH optima in the neutral to alkaline region leads to pectins with a blockwise arrangement of free carboxyl groups by single-chain (Massiot et al., 1997; Ralet et al., 2001; Kim et al., 2005) or multiple-attack mechanism (Grasdalen et al., 1996; Ralet & Thibault, 2002). Fungal PMEs from different *Aspergillus Niger* strains with acidic pH optima act following a multiple-chain mechanism generating pectin with a random distribution of deesterified pectin (Kohn et al., 1983; Ishii et al., 1979; Baron et al., 1980).

1.4.4. Backbone degradation

Polymethylgalacturonase (PMG) and Polygalacturonase (PG) catalyzes the hydrolytic cleavage of (1→4)-α-glycosidic bonds in pectin backbone, preferentially highly esterified pectin for PMG, forming respectively 6-methyl-D-galacturonate and D-galacturonate.

Both groups of hydrolase enzymes can act in endo- or exo- mode. Endo-PG and endo-PMG catalyze random cleavage of substrate, exo-PG and exo-PMG catalyze hydrolytic cleavage at substrate non-reducing end producing monogalacturonate or digalacturonate in some cases (Kashyap et al., 2001; Kester et al., 1996).

Pectate lyase (PGL) and pectin lyase (PL) catalyzes the random cleavage of pectin, preferentially HM pectin in the case of PL, producing respectively methyloligogalacturonates and unsaturated Δ-4,5-D-galacturonate, through transelimination of glycosidic linkages. Pectate lyases are classified as endo-PGLs that act towards substrate in a random way and exo-PGLs that catalyze the substrate cleavage from the non-reducing end while all described pectin lyases are endo-PLs.

1.5. Properties and applications

1.5.1. Chemical properties

The dissociation constant (pK_a) of the carboxyl group of HG is independent of the pectin concentration, DM, degree of amidation or degree of polymerization, and has a value around 2.9 to 3.2, close to the pK_a value of the monomeric acid (Ravanat et al., 1980). For a given pH, the ionization degree increases with increasing pectin concentration. The apparent pK_a depends on the effective charge density of the pectin, and thus decreases when the degree of ionization decreases, or when the DM increases (Speiser et al., 1945).

1.5.2. Gelation

Pectins are widely used in the food industry for their gelling properties. A gel is formed when portions of HG are crossed-linked to form a three dimensional crystalline network in which water and solutes are trapped. Various factors determine gelling properties including temperature, pectin type, DM, pH, sugar and other solutes, and calcium.

The two classical types of pectin gels are those obtained from LM pectins on addition of calcium ions, over a wide range of pH with or without sugar (Fig. 1.7.) or from HM pectins by the cross-

linking of HG by hydrogen bridges and hydrophobic forces between methoxyl groups both promoted by high sugar concentration and low pH.

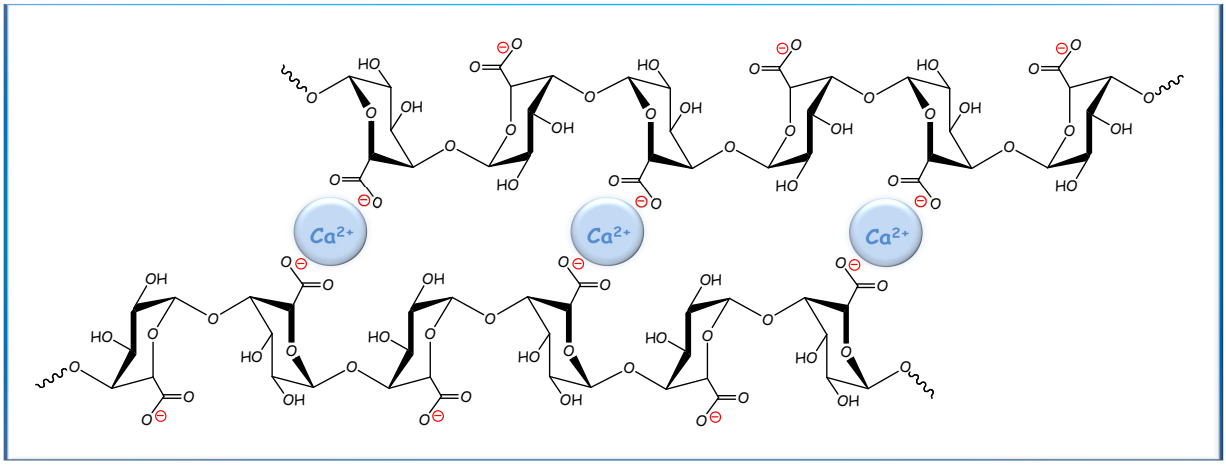

Fig. 1. 7. Interaction through insertion of calcium ions between the unesterified carboxyl groups of the GalpA units of two pectin HG chains.

Therefore, LM pectins can be used in low-calorie jams and jellies. Calcium-sensitive (CS) pectins also have been described in which HM pectins can gel in the presence of calcium without the addition of sucrose as long as blocks of deesterified pectin are present (Joye & Luzio, 2000). CS pectins retain more water than LM pectin, making them softer and more commercially desirable for dietetic food and many other applications (Willats et al., 2001).

1.5.3. Applications

In addition to the important physiological functions (gelation, cell adhesion,…), pectins have also an important roles in many fields :

(i) they are involved in interactions between plants and pathogenic agents (Talmadge et al., 1973; Albersheim et al., 1981);

(ii) the amount and nature of pectin are determinant for the texture of fruits and vegetables during their growth, ripening, storage and processing (Knee, 1978);

(iii) as they are extracted commercially, they are applied as additives in many fields, as stabilizers, thickeners and mainly as gelling agents;

(iv) they have an important role as nutritional fibre (Cummings et al. 1979) and may have interesting therapeutical properties (Pfeffer et al., 1981).

2. PRESENT WORK

The aim of this study was to covalently attach pectin to substrates specifically through the reducing end sugar residue in order to facilitate experiments examining, for example, the response of pectin chains to mechanical stretching using Atomic Force Microscopy.
Infrared Spectroscopy was used to investigate the nature of the coupling formed between the polysaccharide and the substrate as it is a fast and easy-to-use analysis technique, and uniquely offers the opportunity to observe the chemical nature of any covalent linkage formed between the support and the pectin.

Firstly, the structure of pectin was investigated using Infrared Spectroscopy. The study showed that the reported methodology previously used to determine the degree of methylesterification of pectin requires careful attention and sample handling, in particular to the moisture content and the ionisation state of the pectin. An alternative methodology was developed based on the assessment of the magnitude of antisymetric vibration stretches of the methyl ester groups relative to those in the backbone and proved to be a more useful tool to determine the structure of pectin.

Then polystyrene beads were used as a support to anchor different pectins because of their large surface area maximizing the IR signal, and their use in light-scattering techniques and various biophysical experiments. New hydrazide supports were prepared, designed for chemoselective immobilization of pectins macromolecules via the reducing end. Indeed the IR spectrum showed the formation of a new bond during the covalent attachment, also present in theoretical calculations. While using silica beads as a further example substrate proved problematic for IR studies, dynamic light scattering studies showed results consistent with the Infrared Spectroscopy results on the polystyrene beads.

Finally, the coupling technique was applied to glass surfaces and such systems used to stretch pectin macromolecules with Atomic Force Microscopy. The results were compared to studies performed on physically adsorbed pectins on substrates.

3. THESIS OUTLINE

The majority of the following chapters are or will be published in relevant journals and are included in an article format. Therefore some introduction and experimental details are unavoidably repeated between chapters. The major introduction and materials chapters are included as a preamble in order to give a larger overview of the necessary theory and literature than what is found in the other chapters.

4. REFERENCES

Albersheim, P.; Danville, A.G.; McNeil, M.; Valent, B.S.; Hahn, M.G.; Lyon, G.; Sharp, J.K.; Desjardins, A.E.; Spellman, M.W.; Ross, L.M.; Robertsen, B.K.; Aman, P. and Franzen, L.E. (1981) Structure and function of complex carbohydrates active in regulating plant-microbe interactions. *Pure and Applied Chemistry*, **53** (1), 79-88.

Axelos, M.A.V.; Thibault, J.F. and Lefebvre, J. (1989) Structure of citrus pectins and viscometric study of their solution properties. *International Journal of Biological Macromolecules*, **11** (3), 186-191.

Baron, A.; Rombouts, F; Drilleau, J.F. and Pilnik, W. (1980) Purification et propriétés de la pectinestérase produite par *Aspergillus Niger*. *Lebensmittel Wissenschaft + Technologie*, **13**, 330-333.

Black, S.A. and Smit, C.J.B. (1972) The effect of demethylation procedures on the quality of low-ester pectins used in dessert gels. *Journal of Food Science*, **37** (5), 730-732.

Bracannot, H. (1825) Recherches sur un nouvel acide universellement repandu dans tous les vegetaux. *Annales de Chimie et de Physique (serie 2)*, **28**, 173

Colquhoun, I.J.; de Ruiter, G.A.; Schols, H.A. and Voragen, A.G.J. (1990) Hairy (ramified) regions of pectins. 3. Identification by NMR-spectroscopy of oligosaccharides obtained by treatment of the hairy regions of apple pectin with rhamnogalacturonase. *Carbohydrate Research*, **206** (1), 131.

Cosgrove, D.J. (2000) Expansive growth of plant cell walls. *Plant Physiology and Biochemistry*, **38** (1-2), 109-124.

Cummings, J.H.; Southgate, D.A.T.; Branch, W.G.; Wiggins, W.J.; Houston, H.; Jenkis, D.J.A.; Livraj, T. and Hill, M.J. (1979) Digestion of pectin in the human gut and its effect on calcium-absorption and large bowel function. *British Journal of Nutrition*, **42**, 515-524.

Daas, P.J.H.; Boxma, B.; Hopman, A.M.C.P.; Voragen, A.G.J. and Schols, H.A. (2001) Non-esterified galacturonic acid sequence homology of pectins. *Biopolymers*, **58** (1), 1-8.

Dickinson, E. and James, J.D. (2000) Influence of high-pressure treatment on β-lactoglobulin-pectin associations in emulsions and gels. *Food hydrocolloids*, **14** (4), 365-376.

Dlamini, A.M.; Peiris, P.; Bavor, J.H. and Kailasapathy, K. (2007) Characterization of the exopolysaccharide produced by a whey utilizing strain of Klebsiella oxytoca. *African Journal of Biotechnology*, **6** (22), 2603-2611.

Grasdalen, H.; Andersen, A.K. and Larsen, B. (1996) NMR spectroscopy studies of the action pattern of tomato pectinesterase : generation of block structure in pectin by a multiple-attack mechanism. *Carbohydrate Research*, **289**, 105-114.

Greenwood, C.T. and Milne, E.A. (1968) Starch degrading and synthesizing enzymes : a discussion of their properties and action pattern. *Advances in Carbohydrate Chemistry*, **23**, 281-366.

Iglesias, M.T. and Lozano, J.E. (2004) Extraction and characterization of sunflower pectin. *Journal of Food Engineering*, **62**, 215-223.

Ishii, S.; Kiho, K.; Sugiyama, S. and Sugimoto, H. (1979) Low-methoxyl pectin prepared by pectinesterase form *Aspergillus japonicus*. *Journal of Food Science*, **44** (2), 611-614.

Jayani, R.S.; Saxena, S. and Gupta, R. (2005) Microbial pectinolytic enzymes : a review. *Process Biochemistry*, **40** (9), 2931-2944.

Joyce, D.D. and Luzio, G.A. (2000) Process for selective extraction of pectins from plant material by differential pH. *Carbohydrate Polymers*, **43**, 337-342.

Joye, D.D. and Luzio, G.A. (2000) Process for selective extraction of pectins from plant material by differential pH. *Carbohydrate Polymers*, **43**, 337-342.

Kashyap, D.R.; Vohra, P.K. and Tewari, R. (2001) Application of pectinases in the commercial sector : a review. *Bioresource Technology*, **77** (3), 215-227.

Kester, H.C.M.; Kusters-Van Someren, M.A.; Muller, Y. and Visser, J. (1996) Primary structure and characterization of an exopolygalacturonase from *Aspergillus Tubingensis*, **240**, 738-746.

Knee, M. (1978) Properties of polygalacturonate and cell adhesion in apple fruit cortical tissue. *Phytochemistry*, **17** (8), 1257-1260.

Kohn, R.; Markovic, O. and Machova, E. (1983) Deesterification mode of pectin by pectin esterases of *Aspergillus foetidus*, tomatoes and alfalfa. Collection of Czechoslovak Chemical Communications, **48** (3), 790-797.

Knee, M. (1978) Metabolism of polymethylgalacturonate in apple fruit corical tissue during ripening. *Phytochemistry*, **17** (8), 1261-1264.

Kim, Y.; Teng, Q. and Wicker, L. (2005) Action pattern of Valencia orange PME de-esterification of high methoxyl pectin and characterization of modified pectins. *Carbohydrate* Research, **340**(17), 2620-2629.

Marciano, A.; Chefetz, B. and Gedanken, A. (2008) Differential adsorption of silver nanoparticles to the inner and outer surfaces of the agave Americana cuticle. *The Journal of Physical Chemistry*, **112** (46), 18082-18086.

Massiot, P.; Perron, V.; Barron, A. and Drilleau, J.F. (1997) Release of methanol and depolymerisation of highly methyl esterified apple pectin with an endopolygalacturonase from *Aspergillus niger* and

pectin methylesterases from *A.Niger* or from orange. *Lebensmittel Wissenschaft und Technology*, **30**(7), 697-702.

McClements, D.J. (2006) Non-covalent interactions between proteins and polysaccharides. *Biotechnology advances,* **24** (6), 621-625.

May, C.D. (1990) Industrial pectins : Sources, production and applications. *Carbohydrate Polymers*, **12**, 79-99.

Parre, E. and Geitmann, A. (2005) Pectin and the role of the physical properties of the cell wall in pollen tube growth of *Solanum Chacoense*. *Planta*, **220** (4), 582-592.

Perez, S.; Rodriguez-Carvajal, M.A. and Doco, T. (2003) A complex plant cell wall polysaccharide ; rhamnogalacturonan II. A structure in the quest of a function. *Biochimie*, **85** (1-2), 109-121.

Pfeffer, P.E.; Doner, L.W.; Hoagland, P.D. and McDonald, G.G. (1981) Molecular interactions with dietary fibre components – Investigation of the possible association of pectin and bile-acids. *Journal of Agricultural and Food Chemistry*, **29** (3), 455-461.

Ralet, M.C.; Dronnet, V.; Buchholt, H.C. and Thibault, J.F. (2001) Enzymatically and chemically de-esterified lime pectins : characterization, polyelectrolyte behavior and calcium binding properties. *Carbohydrate Research*, **336**, 117-125.

Ralet, M.C. and Thibault, J.F. (2002) Interchain heterogeneity of enzymatically deesterified lime pectins. *Biomacromolecules*, **3**(5), 917-925.

Ravanat, G.; Rinaudo, M. (1980) Investigation on oligo- and polygalacturonic acids by potentiometry and circular dichroism. *Biopolymers*, **19** (12), 2209-2222.

Renard, C.M.G.C. and Thibault, J.F. (1996) Pectins in mild alkaline conditions : β-elimination and kinetics of demethylation. In *Pectins and Pectinases*, *Progress in Biotechnology Vol. 14*, Elsevier, Amsterdam.

Ridley, B.L.; O'Neill, M.A. and Mohnen, D. (2001) Pectins : structure, biosynthesis and oligogalacturonide-related signaling. *Phytochemistry*, **57** (6), 929-967.

Ryden, P. and Selvendran, R.R. (1990) Structural features of cell-wall polysaccharides of potato (*solanum tuberosum*). *Carbohydrate Research*, **195** (2), 257-272.

Sakai, T. and Okushima, M. (1980) Microbial production of pectin from citrus peel. *Applied and Environmental Microbiology*, **39** (4), 908-912.

Sanli, T.; Sezgin, E.; Deveci, O.; Senel, E. and Benli, M. (2011) Effect of using transglutaminase on physical, chemical and sensory properties of set-type yoghurt. *Food hydrocolloids*, **25** (6), 1477-1481.

Schenkel, P. and Hinrichs, J. (2010) Integrating new technologies of milk pre-treament in soft cheese manufacture – a systematic approach. *Milchwissenschaft*, **65** (4), 385-388.

Speiser, R.; Hills, C.H. and Eddy, C.R. (1945) The acid behavior of pectinic acids. *The Journal of Physical Chemistry*, **49** (4), 328-343.

Speiser, R.; Copley, M.J. and Nutting, G.C. (1947) Effect of molecular association and charge distribution on the gelation of pectin. *The Journal of Physical Chemistry*, **51** (1), 117-133.

Stoddart, R.W.; Barrett, A.J. and Northcote, D.H. (1967) Pectic polysaccharides of growing plant tissues. *Biochemical Journal*, **102** (1), 194-204.

Stutz, E. and Deuel, H. (1958) Über die saure Decarboxylierung von Hexuronsäuren. *Helvetica Chimica Acta*, ***41*** (6), 1722-1730.

Talmadge, K.W.; Keegstra, K.; Bauer, W.D. and Albersheim, P. (1973) Structure of plant cell walls. 1. Macromolecular components of walls of suspension-cultured sycamore cells with a detailed analysis of pectic polysaccharides. *Plant Physiology*, **51**, 158-173.

Taylor, A.J. (1982) Intramolecular distribution of carboxyl groups in low methoxyl pectins – a review. *Carbohydrate Polymers*, **2** (1), 9-17.

Thibault, J.F.; Renard, C.M.G.C.; Axelos, M.A.V.; Roger, P. and Crepeau, M.J. (1993) Studies of the length of homogalacturonic regions in pectin by acid hydrolysis. *Carbohydrate Research*, **238** (15), 271-286.

Visser, J. and Voragen, A.G.J. (1996) Pectins and pectinases. *Progress in Biotechnology Vol. 14*, Elsevier, Amsterdam.

Vauquelin, M. (1790) Analyse du tamrin. *Annali Di Chimica*, **5** (92), 106.

Vollmert, B. (1950) Uber den alkalischen pektinabbau. *Makromolekulare Chemie*, **5** (2), 110-127.
Willats, W.G.T.; McCartney, L.; Mackie, W and Knox, J.P. (2001) Pectin : cell biology and prospects for functional analysis. *Plant Molecular biology*, **47**, 9-27.

Willats, W.G.T.; Orfila, C.; Limberg, G.; Buchholt, H.C.; Van Alebeek, G.J.W.M.; Voragen, A.G.J., Marcus, S.E.; Christensen, T.M.I.E.; Mikkelsen, J.D.; Murray, B.S. and Knox, J.P. (2001) Modulation of the degree and pattern of methyl-esterification of pectin homogalacturonan in plant cell walls – Implications for pectin methyl esterase action, matrix properties and cell adhesion. *Journal of Biological Chemistry*, **276** (22), 19404-19413.

Woodmansee, C.W. and Baker, G.L. (1949) High-Polymer, acid-demethylated pectinates and their gelation. *Food Technology*, **3** (3), 82-85.

CHAPTER 2.

This chapter briefly reviews the techniques and instrumention used in this work. Further details on the procedures are reported in the relevant chapters.

1. CAPILLARY ELECTROPHORESIS

1.1. Theory

Pectin fine structure, in particular the degree of methylesterification (DM), can be determined using several methods such as titration (Schultz, 1981) or NMR spectroscopy (Rosenbohm, 2003). These methods are rather time consuming and can hardly be automated. Other methods using High Performance Liquid Chromatography (HPLC) (Voragen et al., 1986; Levigne et al., 2002) and Gas Chromatography (GC) (Huisman et al., 2004; Walter et al., 1983) analyzing the methanol content after saponification of the pectins have been developed. Recently, Capillary Electrophoresis (CE) has been used to determine the inter- and intra-molecular DM distributions of pectins (Ström et al, 2004; Goubet et al., 2005). Separation of charged components with CE is rapid and efficient. Another advantage of CE to the other methods is that the HG content of the samples is not required to calculate the DM whereas it has to be known prior to analyzing using the other methods.

In CE, separation of analyte ions is performed in an electrolyte solution (background electrolyte) present in a narrow fused-silica capillary. The ends of the capillary are immersed into vials (inlet and outlet) filled with electrolyte solution, which also contain electrodes connected to a high voltage supply (Fig. 2.1.).

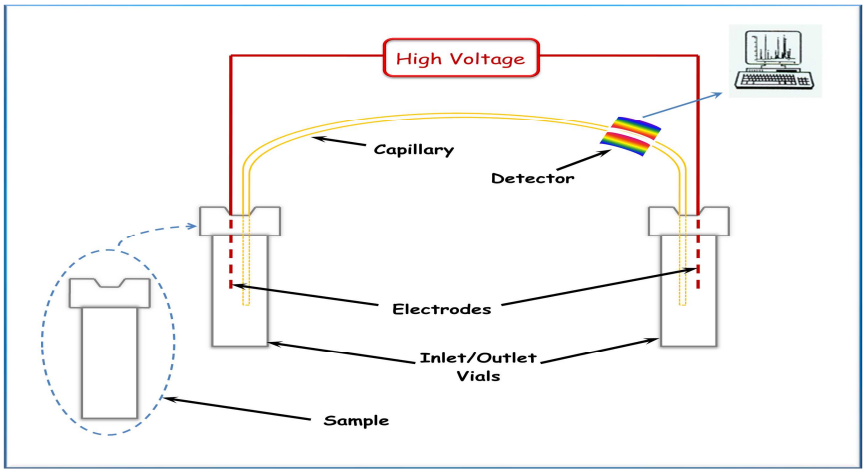

Fig. 2. 1. Typical CE instrumentation. A computer is used to collect and treat the data after detection.

The sample solution is introduced into the capillary as a small plug by applying pressure (hydrodynamic injection) or voltage (electrokinetic injection). Subsequently, with the application of high voltage (3-30 kV) across the capillary, zones of analyte are formed and migrate toward the outlet side of the capillary. Before reaching the end of the capillary, the separated analyte bands are detected directly through the capillary wall by UV/Vis or fluorescence.

When the voltage is applied to the circuit, one electrode becomes net negative and the other net positive. The capillary wall's immobile silanol anions pair with mobile buffer cations, forming an electrical double layer along the wall. The remaining buffer cations are attracted to the negative electrode, dragging the bulk buffer solution with them. This is the *electroosmotic flow (EOF)*.
The separation is based on the differences in electrophoretic mobility, which is directly proportional to the charge on the molecule, and inversely proportional to the viscosity of the solvent and radius of the atom. The velocity at which the ion moves is directly proportional to the elctrophoretic mobility and the magnitude of the electric field (Fig. 2.2.)

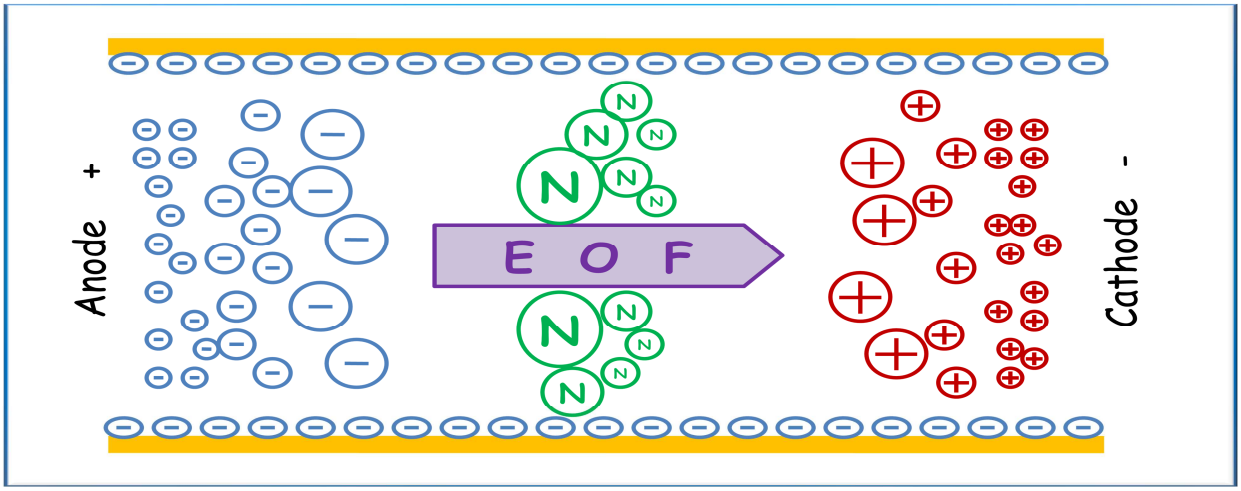

Fig. 2. 2. Schematic of the double layer on the capillary surface.

Anions are attracted to the positively charged anode, but get swept to the cathode as well owing to the EOF. Cations with the largest charge-to-mass ratio separate out first, followed by cations with reduced ratios, neutral species (which travel at the same velocity as the EOF), anions with smaller charge-to-mass ratios, and finally anions with greater ratios. The electroosmotic velocity can be adjusted by altering the pH, the solvent viscosity, the ionic strength, the voltage and the dielectric constant of the buffer.

The electrophoretic mobility μ_p can be experimentally determined from the migration time and the field strength:

$$\mu_p = \frac{L \,.\, L_t}{V}\left[\frac{1}{t} - \frac{1}{t_{EOF}}\right]$$

→ L , distance from the inlet to the detection point
L_t , total length of the capillary
V , applied voltage
t_{EOF} , EOF elution time
t , time required for the analyte to reach the detection point (migration time)

Pectins possess both charge and UV-Vis chromophore (carboxylate group of Gal*p*A unit), which are prerequisites for the direct use of CE.

1.2. Experimental section

This section demonstrates the use of CE in the measurement of pectin fine structure.

1.2.1. Set up

Materials : All pectins used in this section were obtained treatment of the same mother pectin, Apple pectin, from Fluka (DM 78%, Gal*p*A content of ≈ 90%, M_W≈30-100 kDa).
Plant pectin methylesterase was purchased from Sigma Aldrich. Polygacturonase (pure endo-PG II isoform from *Aspergillus Niger*) was kindly provided by Jacques Benen, University of Wageningen, Netherlands.

Alkali deesterification : Mother pectin (Apple pectin) was dispersed in deionized water to a final concentration of 0.5%, heated and kept under stirring at 60°C until complete dissolution was obtained. The solution was then cooled to below 4°C. The deesterification process started as pH was adjusted to 10.5 with a 1 M NaOH solution. The pH was kept constant at 10.5 until the required amount of NaOH had been added to reach the desired DM values. The reaction was carried out under stirring and between 0 and 4°C to prevent β-elimination. On completion of the reaction the samples were dialysed against deionized water in order to remove excess salt and freeze-dried.

Enzymatic deesterification: Apple pectin was deesterified with PME (0.5 mg per gram of pectin) at pH 7 and 30°C because of the increased risk of β-elimination as pH increases. The pH was kept constant by the addition of a 0.1 M NaOH solution and car was taken that the pH did not exceed 7. When the required DM was obtained, the reaction was stopped by addition of HCl (pH≈4) and the enzyme inactivated at 90°C for 3 minutes. The modified pectins were then dialyzed against deionized water and freeze-dried.

Digestion : Pectins were digested in a 50 mM acetate buffer (pH 4.2) at 30°C for 12 hours using 20 µL of endo-PG II solution (0.094 mg/mL) for 1mL of pectin substrate (0.5% w/w). The reaction was stopped by denaturation of the enzyme at 90°C for 3 minutes.

Capillary Electrophoresis: All CE experiments were carried out using an Agilent $HP^{3D}CE$ with a diode array detector (DAD), Agilent technologies. Electrophoresis was carried out in a fused silica capillary of internal diameter 50 µm and a total length of 46.5 cm (40 cm from inlet the detector) with an extended light-path detection window (150 µm) and was thermo statistically controlled at 25°C.

Phosphate buffer at pH 7.0 was used as a background electrolyte (BGE) and was prepared by mixing 0.2 M Na_2HPO_4 and 0.2 M NaH_2PO_4 in appropriate ratios and subsequently reducing the ionic strength to 50 or 90 mM. At pH 7.0, the unmethylated GalA residues are fully charged, and while the polysaccharides studied here are susceptible to base-catalyzed β-elimination above pH 4.5, no problems were encountered during the CE runs of some 20 min at room temperature. All new capillaries were conditioned by rinsing for 30 min with 1 M NaOH, 30 min with a 0.1 M NaOH solution, 15 min with water, and 30 min with BGE. All solutions were filtered through 0.2 µm filters. Between runs, the capillary was washed for 2 min with 1 M NaOH, 2 min with 0.1 M NaOH, 1 min with water, and 2 min with BGE. Detection was carried out using UV absorbance at 191 nm with a bandwidth of 2 nm. Samples were loaded hydrodynamically (various injection times at 5000 Pa, typically giving injection volumes of the order of 10 nL) and, typically, electrophoresed across a potential difference of 20 kV. All experiments were carried out at normal polarity (inlet anodic). Electrophoretic mobilities μ_p, are related to the migration times of the injected samples relative to a neutral marker, t and t_{EOF}, respectively, by the equation stated above.

1.2.2.Intermolecular methyl ester distribution determination

When the chain contains more than 25 Gal*p*A units, the electrophoretic mobility depends only on the DM, which can then be determined by comparison with standard samples of known DM (Fig. 2.3.)

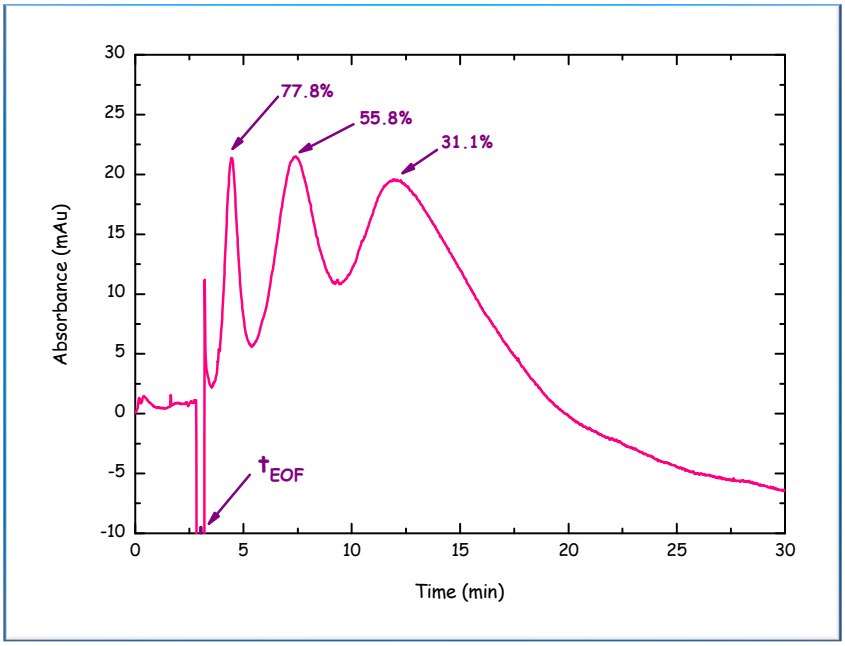

Fig. 2. 3. Electrophoregram of 3 different pectins of known DM.

A linear fit between the DM and the reduced electromobility is determined from this standards electrophoregram. It is then trivial to convert an experimentally measured electrophoregram into a DM distribution.

The electrophoretic mobility of the pectins is independent of the intramolecular methyl ester distribution and only dependant on the DM (Williams et al., 2003); so that CE can be used as a tool for DM determination irrespective of whether the pectins have a random or blocky methyl ester distribution. However, the width of the peaks reflects the intermolecular methylester distribution (Zhong et al., 1998; Williams et al., 2003); alkali deesterified pectins have a narrower intermolecular methyl ester distribution (Fig. 2.4B.) than enzyme deesterified pectins (Fig. 2.4A.), which agrees to the proposed reaction mechanisms : multiple-attack mechanism for alkali deesterification and single-chain mechanism for PME deesterification.

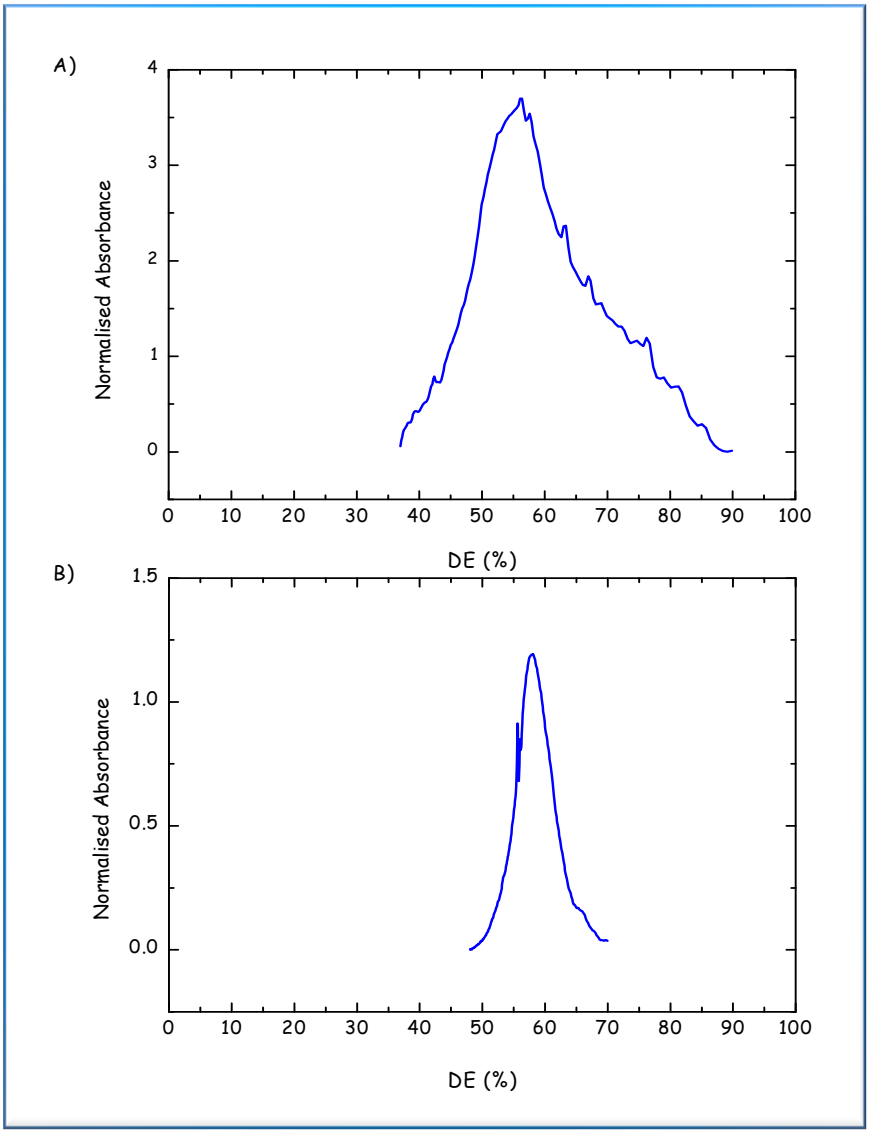

Fig. 2. 4. Intermolecular DM distribution for DM 57 % pectins produced with different patterns of intramolecular deesterification. A) Enzymatic deesterification. B) Alkali deesterification.

1.2.3. Intramolecular methyl ester distribution determination

It is important to point out that the electrophoretic mobility is independent of the pectin length only above a certain degree of polymerization. Below the small oligomers may adopt different conformational shapes, which will change their frictional force (as stated previously, the electrophoretic mobility is determined by both the charge and the size of the solutes).

This characteristic can be used to determine the intramolecular methylester distribution by studying the pectic oligomers produced by digestion of pectins with various pectin-degrading enzymes, such as PG or PL. Due to the site specificity of these enzymes, the oligomers produced will reflect the variation in the intramolecular methyl ester distribution.

The observed digest pattern (Fig. 2.5.) is identical to those obtained in previous studies (Williams et al, 2001; 2002) using the same experimental conditions (endo-PG II enzyme and CE conditions).

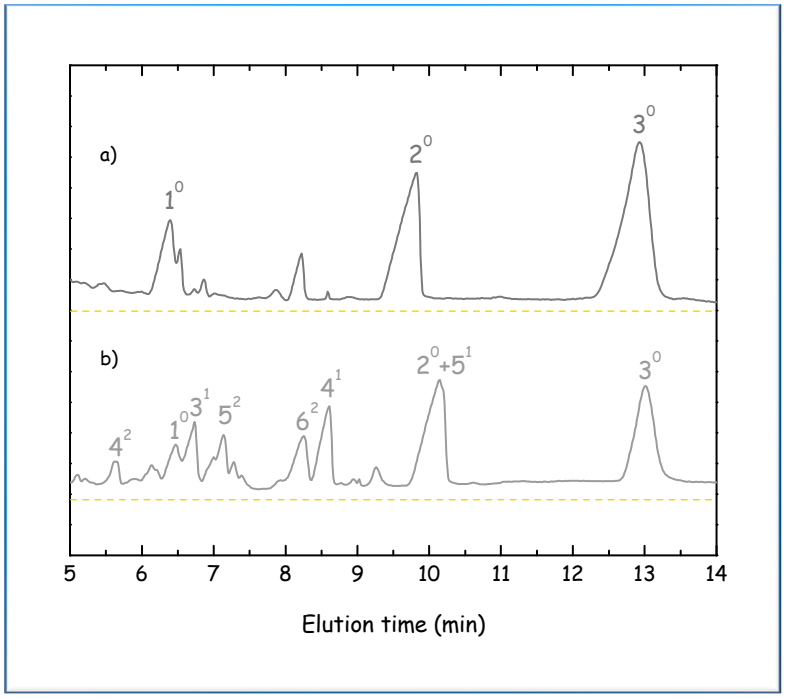

Fig. 2. 5. Electrophoregram obtained upon PG digestion of a) PME deesterified pectin and b) alkali deesterified pectin.

The difference in the ratio of esterified and unesterified oligomers can clearly be seen in this electrophoregram, with no need to quantify the individual oligomers. The digest pattern of the PME deesterified pectin (Fig. 2.5a.) is relatively simple, almost entirely constituted of the monomer, dimer and trimer of Gal*p*A, which indicates that the pectin contains long unesterified blocks and therefore, fully digestible by the enzyme. The alkali deesterified pectin digest electrophoregram (Fig. 2.5b.) includes several unidentified peaks, whose early elution time indicates that they correspond to esterified oligomers with a small charge.

2. ATR/FT-IR SPECTROSCOPY

2.1. Introduction

Infrared (IR) spectroscopy is one of the most common, reliable and well recognized spectroscopic techniques used to characterize, identify and also quantify substances. One of its strengths is its ability as an analytical technique to obtain spectra from a very wide range of solids, liquids and gases. However, in many cases, some form of sample preparation is required in order to obtain a good quality spectrum. Traditionally, IR spectrometers have been used to analyze solids, liquids and gases by means of transmitting the infrared radiation directly through the sample. Where the sample is in a liquid or solid form, the intensity of the spectral features is determined by the thickness of the sample and typically, this sample thickness cannot be more than a few tens of micrometers.

Attenuated Total Reflectance has in recent years revolutionized solid and liquid sample analyses, combating the most challenging aspects of infrared analyses, namely sample preparation and spectral reproducibility.

2.2. Principle

At temperatures above absolute zero, all the atoms in molecules are in continuous vibration with respect to each other. When the frequency of a specific vibration is equal to the frequency of the IR radiation directed on the molecule, the radiation is absorbed by the molecule and the associated energy is converted into molecular vibrations (Skoog et al., 1998; Rouessac, 2007), the major being stretching and bending (Fig. 2.6.).

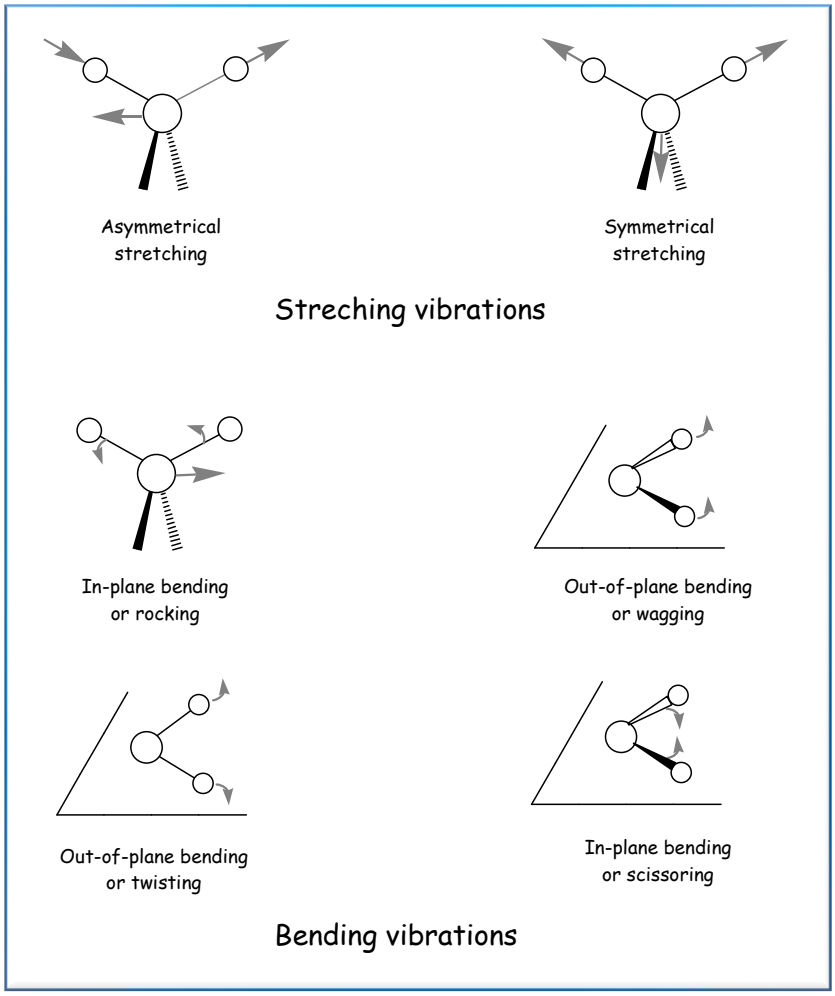

Fig. 2. 6. Major vibrational modes for a non-linear group.

ATR occurs when a beam of radiation enters from a more-dense (with a higher refractive index) into a less-dense medium (with a lower refractive index). The fraction of the incident beam reflected increases when the angle of incidence increases. All incident radiation is completely reflected at the interface when the angle of incidence is greater than the critical angle (a function of refractive index). The beam penetrates a very short distance beyond the surface and into a less dense medium before the complete reflection occurs. This penetration is called the evanescent wave and typically is at a depth of a few microns (Fig. 2.7.). Its intensity is reduced (attenuated) by the sample in regions of the IR spectrum where the sample absorbs. The attenuated energy from each evanescent wave is passed back to the IR beam, which then exits the opposite end of the crystal and is passed to the detector in the IR spectrometer. The system generates then an infrared spectrum.

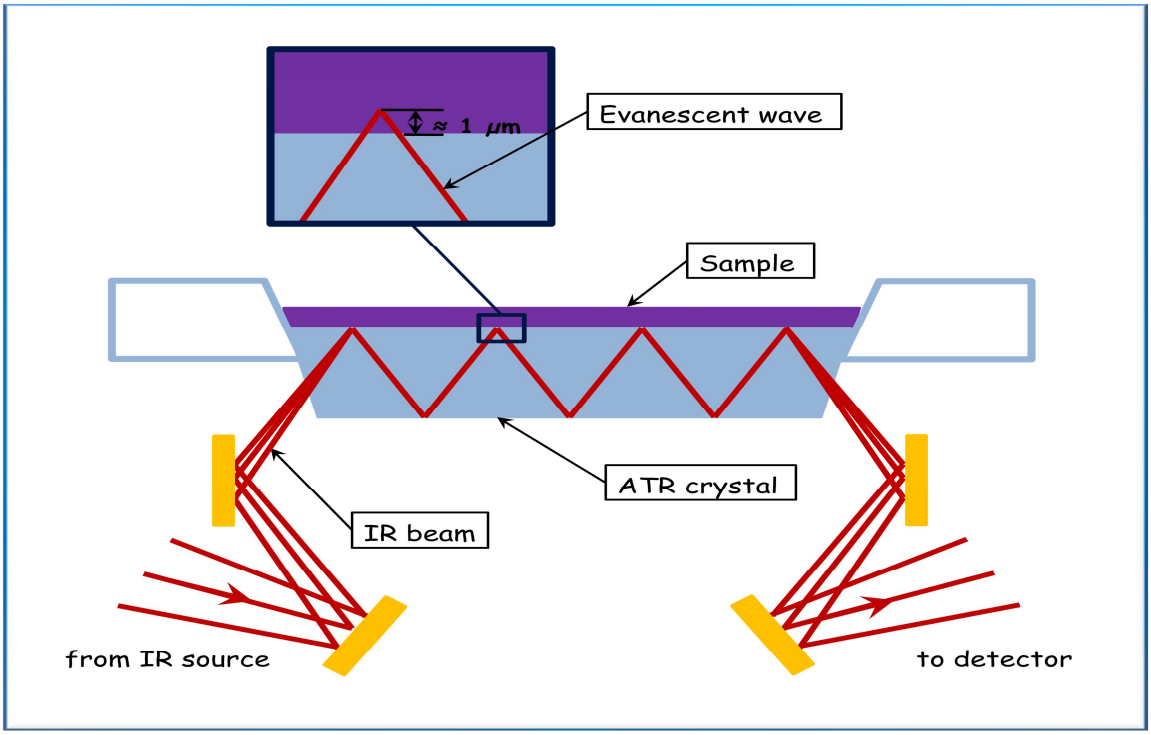

Fig. 2. 7. Schematic representation of multiple internal reflection in ATR.

For the technique to be successful, the sample must be in close contact (because the evanescent wave extends beyond the crystal 0.5-5 μm) with a high refractive index crystal, greater than that of the sample or else internal reflectance will not occur, such as germanium. The IR beam is directed onto the bevelled edge of the ATR crystal and internally reflected through the crystal with a single or multiple reflections. Both the number of reflections and the penetration depth decrease with increasing the angle of incidence. For a given angle, the higher length-to-thickness ratio of the ATR crystal gives higher number of reflections.

2.3. Transmission vs. ATR

In transmission, the most common form of solid sample preparation involves grinding the material to a fine powder, dispersing it in a matrix (KBr generally) and pressing into a transparent disk or pellet. Liquid compounds are usually examined as a thin film between 2 NaCl plates. Overall, sample preparation suffers from inevitable reproducibility issues given the complexity of the methods. In

addition, it can be very messy and time consuming and is further complicated by difficulties in getting sample to matrix ratios right and homogeneous throughout the sample.
ATR has revolutionized IR sampling (no preparation required) through time efficient sampling, sample recovery (non-destructive method), and improved sample-to-sample reproducibility and user-to-user variation.

The resulting ATR spectra resemble the conventional transmission spectra, but with some differences: the adsorption band positions are identical in the 2 spectra, but the relative intensities of corresponding bands are different.

3. ATOMIC FORCE MICROSCOPY

3.1. Introduction

Between 1966 and 1972, Russel D. Young, National Institute of Standards and Technology (US), developed the "Topographiner", a new surface microtopography instrument (Young, 1966; Young et al., 1971; Young et al., 1972). In 1982, Gerd Binning et Heinrich Rohrer (Binning et al., 1982) developed the Scanning Tunnelling Microscope (STM). Five years later, they were awarded the Nobel Prize for their invention. This microscope was the precursor of an all new class of microscope that revolutionized surface science: the Scanning Probe Microscopes (SPM), in which a proximal probe is exploited for investigating properties of surfaces with subnanometre resolution.
The Atomic Force Microscope (AFM) was also invented by Gerd Binning, Calvin Quate et Christophe Gerber in 1986 (Binning et al., 1986). While the STM could only image materials that conduct a tunnelling current, the AFM measures the force acting between a fine tip and a sample. The probing tip is attached to a cantilever-type spring. Interacting with the sample the cantilever deflects and the tip-sample interaction can be monitored with high resolution exploiting a laser beam impinging on the back of the cantilever. The beam is reflected towards a split detector.
The deflection detection initially used by Binning en 1986 was inspired by STM. The invention of a new detection method based on an optical lever, which amplifies cantilever deflections, accelerated the AFM development (Martin et al., 1987; McLelland et al., 1987).

A typical AFM system consists of a sharp tip mounted at the end of a flexible microcantilever, a piezoelectric actuator and a position sensitive photodetector for receiving a laser beam reflected off the end-point of the beam to provide cantilever deflection feedback (Fig. 2.8.).

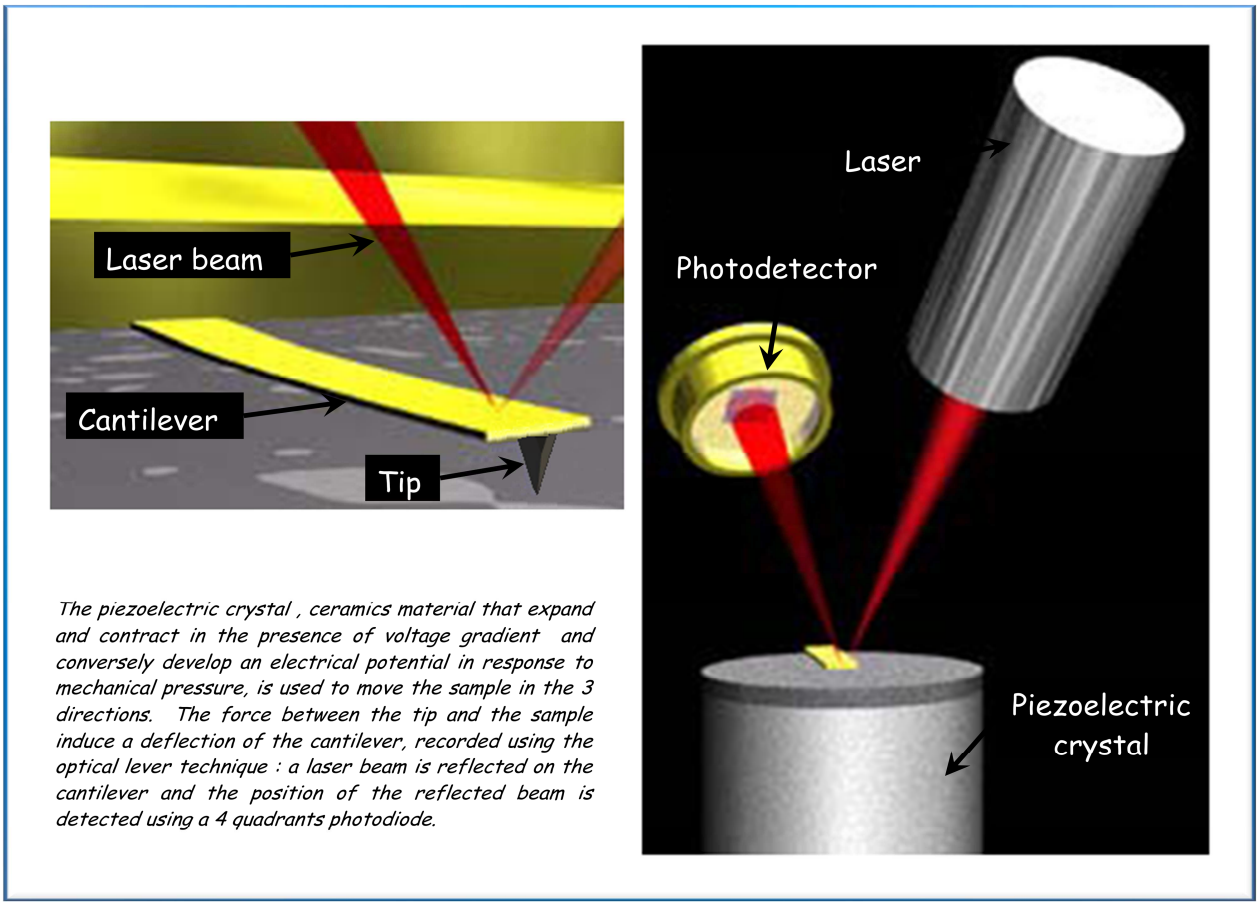

Fig. 2. 8. Atomic Force Microscope with optical lever deflection

The principle of AFM operation used to generate images is to scan, in a raster fashion, the tip in gentle contact with the sample. When interacting with the sample the cantilever deflects and the tip-sample interaction can be monitored with high resolution exploiting a laser beam impinging on the back of the cantilever. The beam is reflected towards a split photodetector configuring an optical lever. In almost all operating modes, a feedback circuit, connected to the cantilever deflection sensor, keeps tip-sample interaction at a fixed value controlling the tip-sample distance.

Depending on the force experienced by the tip-cantilever ensemble, 3 working modes can be defined:

(i) *contact mode* : the force between the tip and the sample is always repulsive and the tip is constantly in gentle contact with the sample. This mode provides high scan speeds, "atomic resolution" and easier scanning of rough samples with extreme changes in vertical topography. However, lateral forces can distort the image, capillary forces can cause large forces normal to the tip-sample interaction and combination of these forces reduces spatial resolution and can cause damage to soft samples.

(ii) *intermittent-contact mode (tapping mode):* the tip experiences both the attractive and repulsive force with the sample (oscillating probe). This mode provides higher lateral resolution, almost no lateral forces, lower forces and less damage to soft samples in air. However, the scan speed is slower than in contact mode.

(iii) *non-contact mode:* the tip experiences only an attractive force (Van Der Walls attraction) with the sample and never touches the sample. In this mode, low force is exerted on the sample surface and no damage is caused to soft samples. However, lateral resolution is lower, limited by tip-sample separation, scan speed is lower to avoid contact with fluid layer, and it is usually applicable only in extremely hydrophobic samples with a minimal fluid layer.

Although topographic mapping is still the dominant application, AFM is also a powerful tool for sensitive force measurements.

3.2. AFM force spectroscopy

In AFM force spectroscopy experiments. The cantilever and tip are moved directly towards the sample until they are in contact with it and then retracted again while the interaction between the tip and the sample is measured. This may be repeated at different locations to build up a map of

the tip-surface interaction, or can be repeated at the same point to give a full statistical understanding of the interaction.

The schematic diagram in Fig. 2.9. shows the movement of the cantilever and tip during the force spectroscopy experiment – towards the sample (the approach part) and then away again (the retract part).

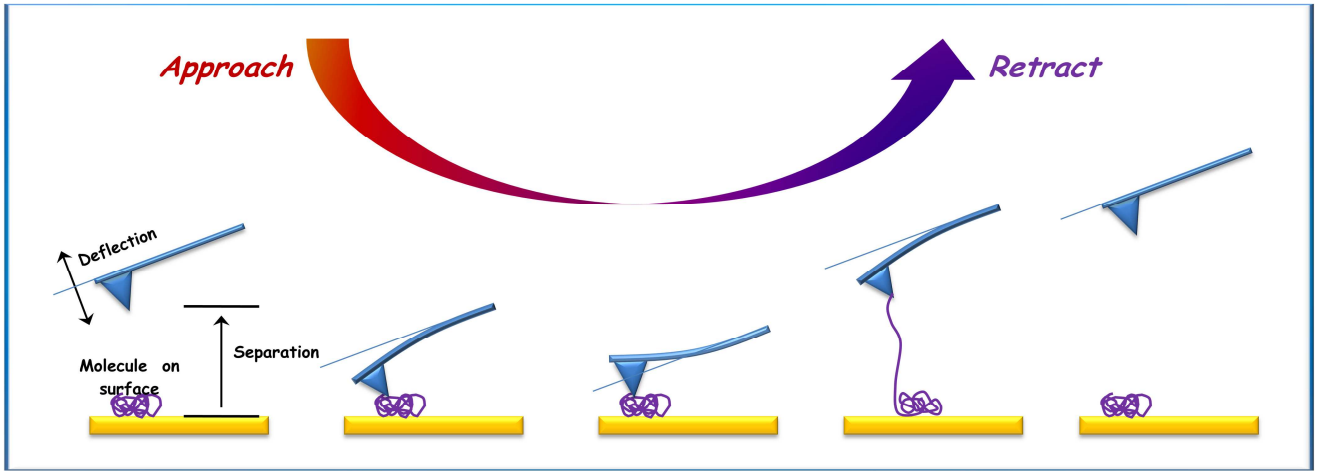

Fig. 2. 9. Schematic of an AFM force spectroscopy experiment. The tip is used to stretch a single molecule.

In Fig. 2.10., a typical force curve, that can be divided in several regions, is shown. Starting from the right (region I), the AFM tip is far from the sample and no interaction is detected (no deflection). The surface approaching the tip, no interaction is detected until the cantilever deflects towards the sample due to Van Der Walls forces, which cause the tip to snap into contact with the sample. After contact, approaching the surface further to the tip, a positive deflection of the cantilever arises (region II) due to repulsive forces. This is the contact region of the force curve, where elastic properties of the sample can be measured.. The surface is moved towards the sample until a preset force threshold is reached. The movement direction is then inverted and the surface starts moving away from the tip. Initially, the behaviour of the cantilever during withdrawal equals that described for the approach but, due to adhesion between the tip and sample, the cantilever starts to deflect negatively (region III) until the adhesion force is overcome by the cantilever restoring force and the contact breaks. The hysteretic behaviour of curves is largely due to capillary forces arising from the water film wetting both sample and probe.

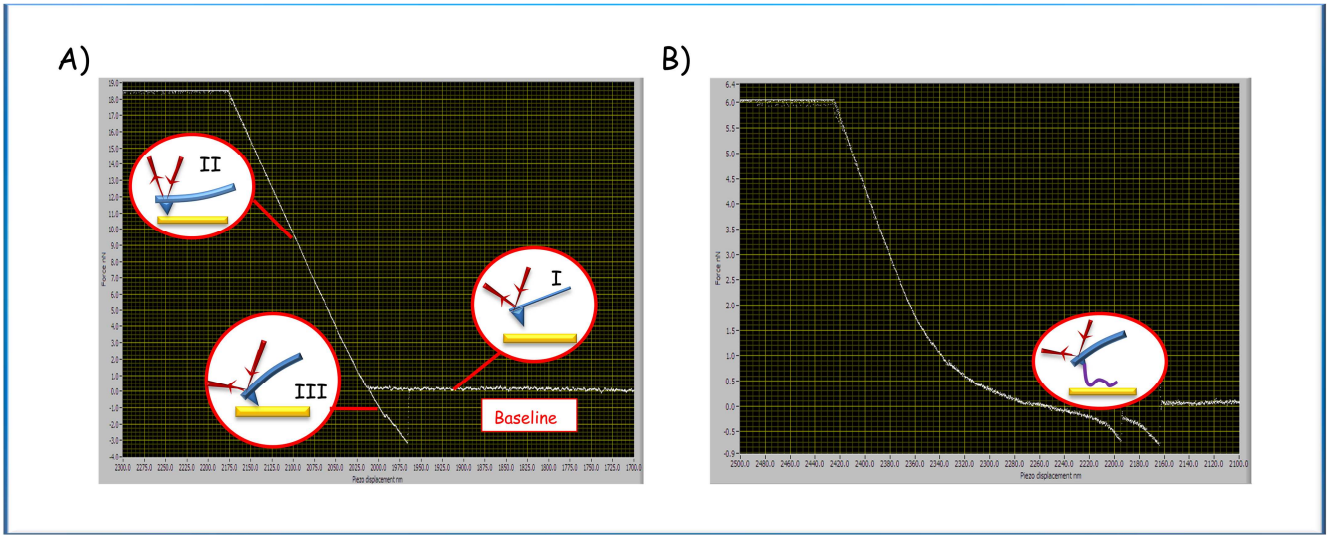

Fig. 2. 10. Schematics of force curves with the different regions of the approach and retract cycles.

If a tether is formed between the cantilever and the substrate during their contact, then the retraction of the piezoelectric crystal results in a force being exerted on the cantilever, mediated by the polymeric tether. When several molecules adsorbed onto the tip or when the molecule is attached to the surface at several points, multiple bridges can form during the contact with the surface, resulting in unbinding traces with multiple saw-toothed patterns, with the molecules loosing attachment successively (Fig. 2.10B.).

3.3. Calibration

3.3.1. Piezoelectric crystal

The z displacement of the piezoscanner is calibrated by scanning a surface (TGX1, Silicon-MDT Ltd, Moscow, Russia) with known step heights (Fig. 2.11.). When the calibrated scanner deflects the cantilever in the z direction, the optical readout may be calibrated and is normally given in nm.

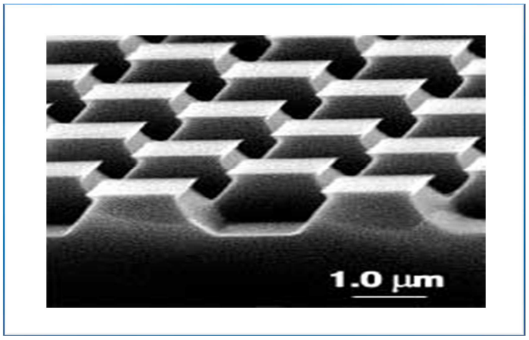

Fig. 2. 11. Silicon grating.

The setup parameters of the scanner were adjusted until the measured value agreed with the actual height.

The deflection of the cantilever spring is directly proportional to the tip-sample interaction force but there are 2 measurements required to convert the photodetector signal into a qualitative value of force.

3.3.2. Cantilever deflection

It is necessary, for each experiment, to calibrate the distance that the cantilever actually deflects for a certain measured change in photodetector voltage. This value depends on type of cantilever but also on the optical path of the AFM detection laser and will be slightly different each time the cantilever is mounted in the instrument.
A force curve between a plain cantilever tip and a bare hard substrate is used to determine the sensitivity of the experimental setup. This is a measurement of the deflection of the tip in nanometres for a given movement of the detection laser on the photodetector. The repulsive contact region (region II in Fig. 2.10.), where the deflection rises steeply upwards, is linear for a hard surface and tip. Therefore the software can easily determine the factor converting a voltage into a distance. (Fig. 2.12.).

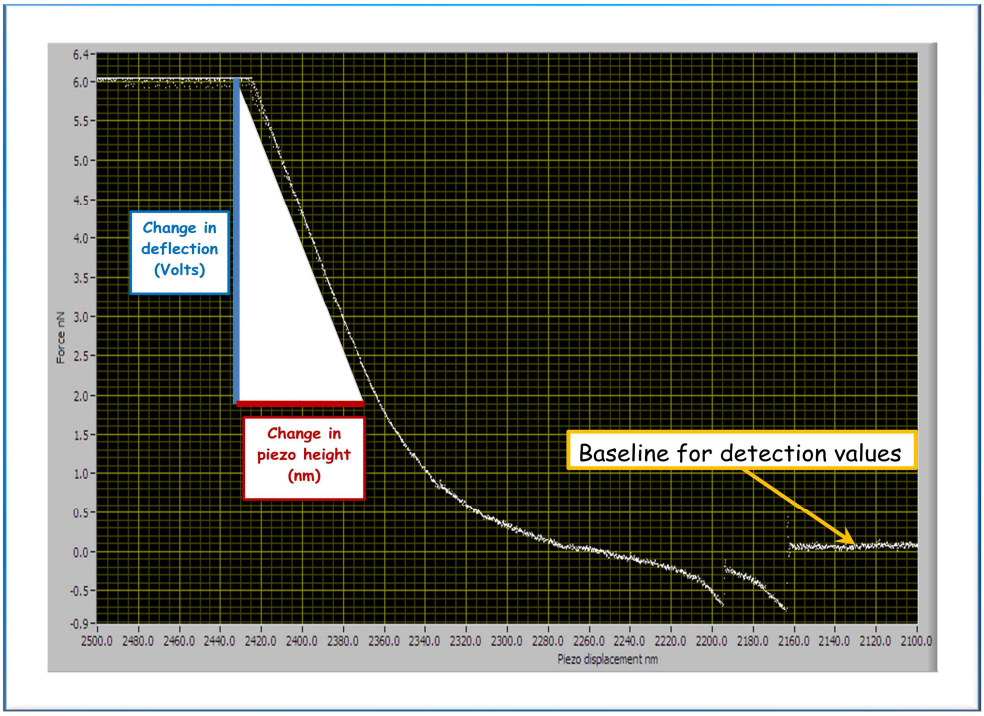

Fig. 2. 12. Sensitivity measurement.

3.3.3. Cantilever spring constant

For quantitative measurement, the spring constant of the cantilever must be calibrated, so that the deflection of the cantilever (Fig. 2.13.) can be converted into actual force values. There are various different ways of calibrating spring constants of cantilevers, the most common being the thermal noise method.

Here we use the thermal noise spectrum, plot of the cantilever fluctuations as a function of frequency (Fig. 2.14.).

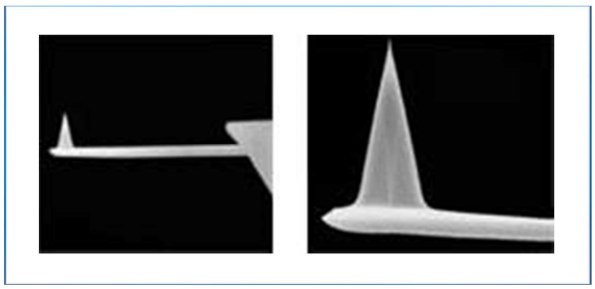

Fig. 2. 13. AFM tip (silicon nitride CSG11/CSG11Au,Silicon MDT Ltd).

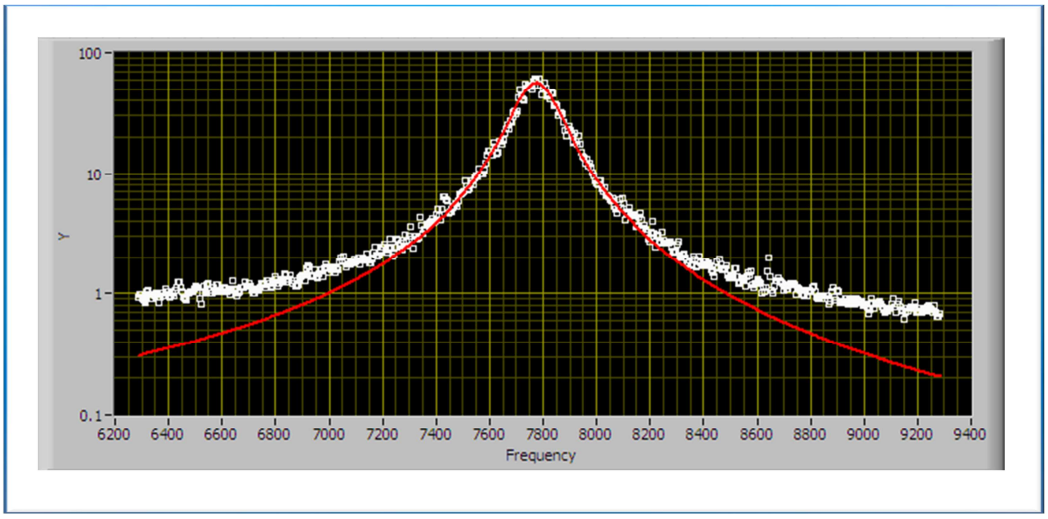

Fig. 2. 14. Thermal noise measurement showing the cantilever resonance peak and the Lorentz fit.

The amplitude of the fluctuations for a given temperature depends only on the spring constant of the cantilever. The thermal noise resonance curve can therefore be fitted to a Lorentzian function, which allows calculation of the spring constant (Sader et al., 2005).

4. DYNAMIC LIGHT SCATTERING

Dynamic Light Scattering (DLS) is a non-invasive technique for measuring particle size, typically in the sub-micron size range. Particles in suspension undergo random Brownian motion. If these particles are illuminated with a laser beam, the laser light is scattered. The intensity of the scattered light detected at a particular angle fluctuates at a rate that is dependent upon the

particle diffusion speed, which in turn is governed by particle size. Particle size data can therefore be generated from an analysis of the fluctuations in scattered light intensity.

A conventional DLS instrument is shown in Fig. 2.15. Laser light is scattered by the particles at all angles but is detected at only one, conventionally 90° (as shown). The measured intensity fluctuations of the scattered light are converted into electrical pulses, which are fed into a digital correlator. Particle size information is generated from the resulting data.

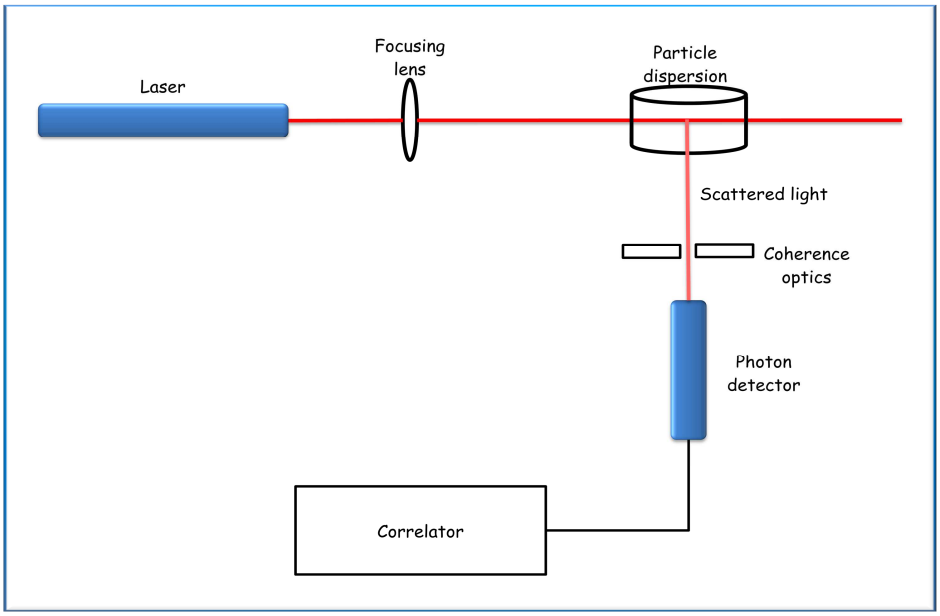

Fig. 2. 15. Schematic diagram of a conventional 90° dynamic light scattering instrument.

5. REFERENCES

Binning, G.; Quate, C.F. and Gerber, C. (1986) Atomic force microscope. Physical Review Letters, 56 (9), 930-933.

Binning, G.; Rohrer, H.; Gerber, C. and Weibel, E. (1982) Surface studies by scanning tunneling microscopy. *Physical Review Letters*, **49** (1), 57-61.

Goubet, F; Ström, A., Ralet, M.C.; Thibault, J.F. and Williams, M.A.K. (2005) An investigation of pectin methylesterification patterns by two independent methods : capillary electrophoresis and polysaccharide analysis using carbohydrate gel electrophoresis. *Carbohydrate Research*, **340** (6), 1193-1199.

Griffiths, P.R. and de Haseth, J.A. (2007) Fourier transform infrared spectrometry. *Wiley and Sons*, 2nd Edition.

Huisman, M.M.H.; Oosterveld, A.; Schols, H. A. (2004) New method for fast determination of the degree of methylation of pectins by headspace GC. *Food Hydrocolloids*, **18** (4), 665-668.

Levigne S. ; Thomas M. ; Ralet M. C. ; Quemener B. and Thibault J.-F. (2002). Determination of the degrees of methylation and acetylation of pectins using a C18 column and internal standards. *Food Hydrocolloids*, **16** (6), 547-550.

McLelland, G.M.; Erlandsson, R. and Chinag, S. (1987) Atomic force microscopy : general principles and a new implementation. *Review of Progress in Quantitative Nondestructive Evolution*, **6B**, 1307-1314.

Martin, Y.; Williams, C.C. and Wickramasinghe, H.K. (1987) Atomic force microscope – force mapping and profiling on a sub 100-Å scale. Journal of Applied Physics, 61 (0), 4723-4729.

Rosenbohm, C.; Lundt, I.; Christensen, T.M.I.E. and Young, N.W.G. (2003) Chemically methylated and reduced pectins : preparation, characterization by ^{1}H NMR spectroscopy, enzymatic degradation and gelling properties. *Carbohydrate Research*, **338** (7), 637-649.

Schultz, T.H. (1965) Determination of the degree of esterification of pectin. *Methods in Carbohydrate Chemistry*, **5**, 189-194.

Rouessac, F. and Rouessac, A. (2007) Chemical analysis : modern instrumentation methods and techniques. *Wiley and Sons, Ltd*, 2nd Edition.

Sader, J.E.; Pacifico, J.; Green, C.P. and Mulvaney, P. (2005) General scaling law for stiffness measurement of small bodies with applications to the atomic force microscope. Journal of Applied Physics, 97 (12), 124903.

Skoog, D.A.; Holler, J. and Crouch, S.R. (1998) Principles of instrumental analysis. *Brooks/Cole Pub Co*, 5th Edition.

Strom, A; Ralet, M.C.; Thibault, M.C. and Williams, M.A.K. (2005) Capillary electrophoresis of homogeneous pectin fractions. *Carbohydrate Polymers*, **60** (4), 467-473.

Voragen, A.G.J.; Schols, H.A. and Pilnik, W. (1986) Determination of the degree of methylation of pectins by HPLC. *Food Hydrocolloids*, **1** (1), 65-70.

Williams, M.A.K.; Buffet, M.G.C.; Foster, T.J. and Norton, I.T. (2001) Simulation of endo-PG digest patterns and implications for the determination of pectin fine structure. *Carbohydrate Research*, **334** (3), 243-250.

Williams, M.A.K.; Buffet, G.M.C. and Foster, T.J. (2002) Analysis of partially methylesterified galacturonic acid oligomers by capillary electrophoresis. *Analytical Biochemistry*, **301** (1), 117-122.

Williams, M.A.K.; Foster, T.J. and Schols, H.A. (2003) Elucidation of pectin methylester distributions by capillary electrophoresis. *Journal of Agricultural Food and Chemistry*, **51** (7), 1777-1781.

Young, R.D. (1996) Field emission ultramicrometer. *Review of Scientific Instruments*, **37** (3), 275-278.

Young, R.D.; Ward, J. and Scire, F. (1971) Observation of metal-vacuum-metal tunneling, field emission and the transition region. *Physical Review Letters*, **27** (14), 922-924.

Young, R.D., Ward, J. and Scire, F. (1972) The topographiner : an instrument for measuring surface microtopography. *Review for Scientific Instruments*, **43** (7), 999-1011.

Zhong, H.J.; Williams, M.A.K.; Goodall, D.M. and Hansen, M.E. (1998) Capillary electrophoresis studies of pectins. *Carbohydrate Research*, **308** (1-2), 1-8.

CHAPTER 3.

PECTIN FINE STRUCTURE : ATR/FT-IR DETERMINATION

This chapter has been published as :

Fellah, A.; Anjukandi, P.; Waterland, M.R. and Williams, M.A.K. (2009) Determining the degree of methylesterification of pectin by ATR/FT-IR: Methodology optimisation and comparison with theoretical calculations. *Carbohydrate Polymers*, **78**, 847-853.

1. ABSTRACT

The application of FT-IR to the study of the structure and interactions of the major plant-cell wall polysaccharide pectin has been reported for many decades. Nevertheless, here we show that the generally reported methodology for one of its most commonly utilized applications, the measurement of the degree of methylesterification (DM), requires careful interpretation and sample handling; including consideration of the moisture content and ionization state. We propose instead a different methodology based on the assessment of the magnitude of C–H stretches in the methyl groups relative to those in the backbone and demonstrate experimentally the advantage of this method. In addition, we add a theoretical dimension to our work, performing full quantum chemical (DFT) calculations of monomeric-, dimeric-, and trimeric-pectic compounds, in various states of partial methylesterification. These extensive calculations not only confirm the identity of the proposed methyl-band and illustrate its scaling with DM; but also demonstrate the success of the theoretical approach. Thus, DFT calculations are expected to be a valuable tool in the interpretation of IR spectra obtained from more complex systems such as polysaccharide conjugates.

2. INTRODUCTION

Amongst the plant cell components, the cell walls, comprised largely of cellulose, hemicelluloses and pectins, have the most important influence on the textural properties of plant tissues. This is manifest, for example, during the storage of fruits, when important physiological and textural changes in the cell wall composition and structure occur, due largely to enzymatic modification of the pectic molecules. While the detailed structure of the pectin macromolecular assembly in vivo is still a matter of debate to some extent (Vincken et al., 2003), most commercially available pectin samples can be considered as a collection of polymer chains each consisting of extended regions of homogalacturonan (HG) interspersed sparsely with regions of rhamonogalacturonan I (RGI) (Ralet & Thibault, 2002). HG consists of a linear backbone of (1,4)-linked a-D-galacturonic acid (GalA) residues, commonly partly methylesterified at C-6, while the RG-I backbone consists of 2)-a-L Rha-(1,4)-a-D-Gal*p*A-(1 repeats with no strong evidence that GalA units in RG-I domains are

methylesterified (Voragen et al., 1995). The rhamnosyl (Rha) residues of RG-I backbone are substituted, mainly at O-4, with several types of arabinose and galactose-containing neutral sugars side-chains (Voragen et al., 1995). Most of the functional uses of pectin are linked to the quantity of methylester groups (as well as their inter- and intra- molecular distribution) and measurement of the degree of methylesterification (DM), defined as the percentage of galacturonic acid residues carrying a methylester group, is a routine procedure in pectin analysis.

Several methods have been developed over the years for the DM determination. Acid-base titration was the first method used (Schulz, 1965) while later alternative methods using alkaline hydrolysis to split the ester linkage and subsequently estimate the quantity of methanol released using HPLC analysis, headspace GC, or NMR, have also been demonstrated (Voragen et al., 1986; Maness et al., 1990; Massiot et al., 1997; Bedouet et al., 2003; Rosenbohm et al., 2003; Huisman et al., 2004). These methods present certain disadvantages, mainly due to the complexity of the procedures involved and the ensuing sample destruction. Unlike many other natural polysaccharides, pectin has both charge and a UV chromophore (the carboxyl group) which makes Capillary Electrophoresis (CE) a practical analytical tool for its study (Zhong et al., 1996; Zhong et al., 1998; Ström & Williams, 2004; Ström et al., 2005). This technique provides a simple, rapid and non-destructive method for the quantitative detection and separation of pectins with different degrees of methylation in aqueous solution, with the advantage of gaining information regarding the distribution of the substituents; although its application to low DM samples is limited by counter-ion condensation.

Infrared spectroscopy has also been suggested as a useful and non-destructive tool to distinguish different pectins: (Haas & Jager, 1986; Monsoor et al., 2001; Barros et al., 2002; Synytsya et al., 2003). In particular Chatjigakis and Gnanasambandam (Chatjigakis et al., 1998; Gnanasambandam & Proctor, 2000) used Fourier transform infrared spectroscopy (FT-IR) to determine the degree of pectin methylesterification. They found that absorbance of the ester carbonyl groups ($COOCH_3$) increased with increase in degree of methylesterification and promisingly that the band area seemed linearly related to the DM, with bands occurring between 1730 and 1760 cm^{-1} and between 1620 and 1650 cm^{-1} indicating respectively the esterified carbonyl groups and carboxylic ions (COO^-). However, this technique does have certain disadvantages, in particular if other carboxylates and carbonyl groups are present and, as we will show, is crucially dependant on the presence of water and the pH and ionic conditions.

One objective of this current study was to develop a more robust method for the DM determination using Attenuated Total Reflectance Fourier Transform Infrared Spectroscopy (ATR/FT-IR), which, unlike other FT-IR methods does not require the sample to be heated, pressed or ground in order to collect the spectrum; (which takes time and can cause structural changes). It should be noted however that the general method expounded herein is based on spectral interpretation, and as such is applicable to the full range of IR techniques. It was hoped that developing such robust spectroscopy methods might prove of value in validating specific bond formation in proposed coupling reactions involving pectin macromolecules and substrates, which were been carried out in order to facilitate various biophysical experiments. Furthermore, with this in mind, the investigation of the utility of Density Functional Theory (DFT) for calculating features of the IR spectra of such complex polysaccharides was also of interest. While the question of the calculation of saccharide IR spectra has been considered before for single sugar rings of differing substitutions (Korolevich & Zhbankov, 1998; Korolevich & Zhbankov, 1999), the revolutionary development in recent years in available computational facilities and large clusters have made the simulations of comparatively large systems (such as the three sugar rings examined herein) possible. Of late, there have been extensive studies of the IR and Raman properties of other molecular systems using theoretical simulations (Krishnakumar et al., 2004; Krishnakumar & Prabhavathi, 2008).

3. EXPERIMENTAL

3.1. Samples

Pectin samples used in the analysis included pectins of DM 30%, 60% and 90% purchased from Sigma (P9311, P9436 and P9561); a sample of DM 78% purchased from Fluka (apple pectin); pectins of DM 35%, 71% and 74% kindly provided by Henk Schols of the University of Wageningen (F, C and X6904); samples of DM 35%, 37% and 48% kindly provided by CP Kelco (randomly distributed methyl groups, LM 12, and blocky samples, 0001-8-F and 0001-8-D, respectively); and samples of DM 58%, 62% and 65% with randomly distributed methyl groups, alkali de-esterified in previous studies (Vincent et al., 2009; Vincent & Williams, 2009). Additionally samples of polygalacturonic

acid (DM 0%) were also obtained from Sigma and Fluka, and mono- and di galacturonic acid were purchased from Sigma.

All the DMs were provided by the suppliers, with the exception of the homemade deesterified samples, which had their values determined by Capillary Electrophoresis (CE), as described previously (Williams et al., 2003). Previously documented data is also considered (Ström, 2006).

3.2. ATR/FT-IR spectroscopy and spectral analysis

Spectral acquisition was performed on solid samples using a Nicolet 5700 FT-IR spectrometer equipped with Omnic software (version 7.1) and a Smart Omni-Sampler (ATR cell with single reflectance germanium crystal). Each recorded spectrum is the average of 32 scans with a spectral resolution of 4 cm^{-1} from 400 to 4000 cm^{-1} on a dried sample, with a background spectrum recorded before each analysis. Three spectra were measured and each one was analyzed and fitted using Origin software (Version 7.5) equipped with Peak-Fitting Module (PFM).

Fitting involved first ensuring that the baseline was averaged to zero in the appropriate spectral range where no bands were detectable (1800–1900 cm^{-1}) followed by a normalization to the intensity by the largest peak. The spectral region for fitting was then selected (typically from 950 to 1900 cm^{-1}; or 950 to 1500 cm^{-1}). Typically an automated peak-picking algorithm found around 12 main peaks in such a region (peaks could be added or subtracted manually if required). Subsequently, Lorentzian peak shapes were selected and placed at the peak-picked positions whereupon their relative intensities and widths were modified by a fitting algorithm until a best fit was found, as determined by a minimized reduced chi squared. The peak areas of the component Lorentzians, centred at the peak-picked frequencies, are then output. The uncertainty in the repeat measurements performed on the same sample was less than 2%.

3.3. Drying and acidifying

The pectin samples were dissolved (0.5% w/w in MilliQ water) and the resultant solutions were Acidified by addition of 0.2 M HCl solution until low pH (≈1–2). They were then dialysed against MilliQ water, freeze-dried and finally dried under reduced pressure in a vacuum oven, at T=30–40 °C.

4. RESULTS AND DISCUSSION

Fig. 3.1A. shows the ATR/FT-IR spectra obtained from a number of representative pectin samples, with the inset revealing that indeed there appears to be a promising relationship between the DM and the relative contribution of the 2 peaks centred at about 1750 and 1630 cm^{-1} , due respectively to the infrared absorption of the carboxylic ester and the any protonated carboxylic acid groups, and to the infrared absorption of the carboxylic anion as reported previously (Bociek & Welti, 1975; Venyaminov & Kalnin, 1990) and discussed in the introduction.

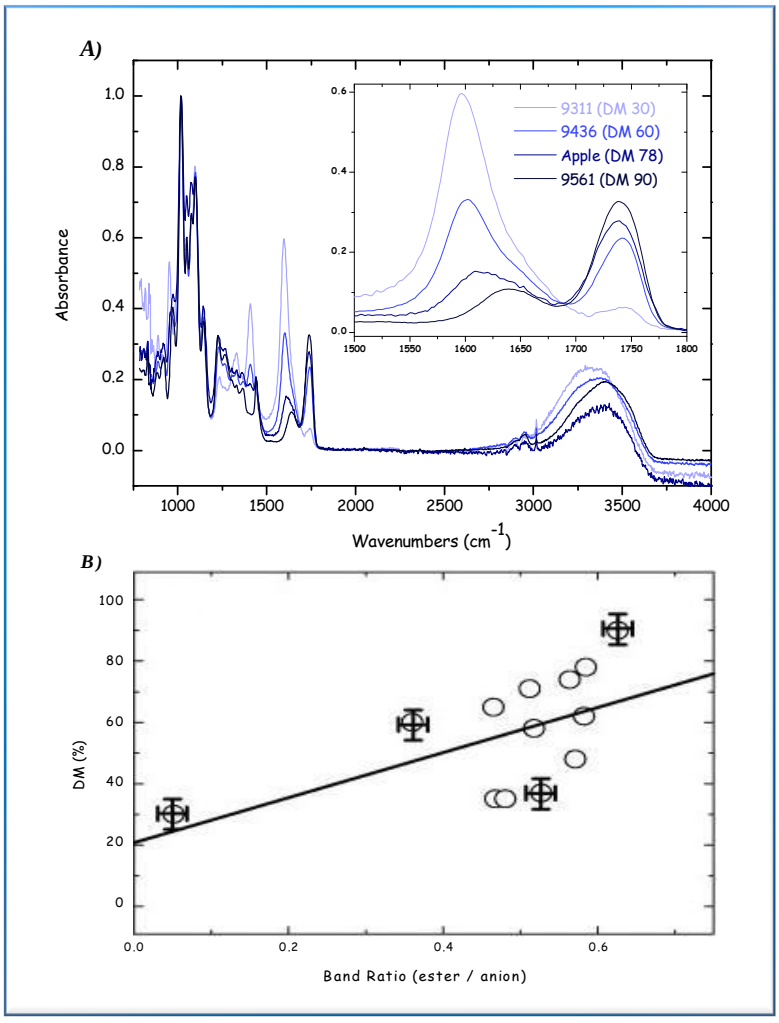

Fig. 3. 1. A) ATR/FT-IR spectra of pectins with different DM. Inset – the two peaks conventionally used to determine the DM. B) Regression analysis of suggested band ratio versus DM, carried out on crude samples using the peak areas of these carboxyl bands, at 1630 and 1750 cm^{-1}, obtained by peak fitting as described in Section III.B.

However, although a linear relationship between the DM and the ratio of the area underneath these peaks has been proposed (Chatjigakis et al., 1998) it was found here that when the results from a larger set of samples was studied (with no specific sample treatment protocol) that the relationship between the peak area ratio we obtained from spectral fitting, as described in Section III.B, and DM, did not seem to be strongly adhered to (Fig. 3.1B.); a linear regression yielding an R^2 value of 0.57. One explanation for this could possibly be interference either from other carboxylates and carbonyl ester groups, such as those from cell wall phenolics, or more concerningly from water (the in-plane deformation band of water $\delta(H_2O)$ occurs at 1645 cm^{-1}). As such, samples were extensively dried and while this improved the correlation between the ratio of the suggested band intensities and DM somewhat (data not shown), there were clearly still problems with obtaining accurate DM determinations.

Further examination of the results lead us to consider that the intensity of the symmetric (≈1450 cm^{-1}) and asymmetric (≈1630 cm^{-1}) carboxylate stretch modes are in fact very sensitive to the ratio of protonated to ionic carboxylate groups. By carefully precipitating and drying the pectins from acidified solutions, the carboxylic anion band largely disappears, and the band at 1750 cm^{-1} can be seen to increase owing to the presence of the newly formed carboxylic acid groups (Fig. 3.2.).

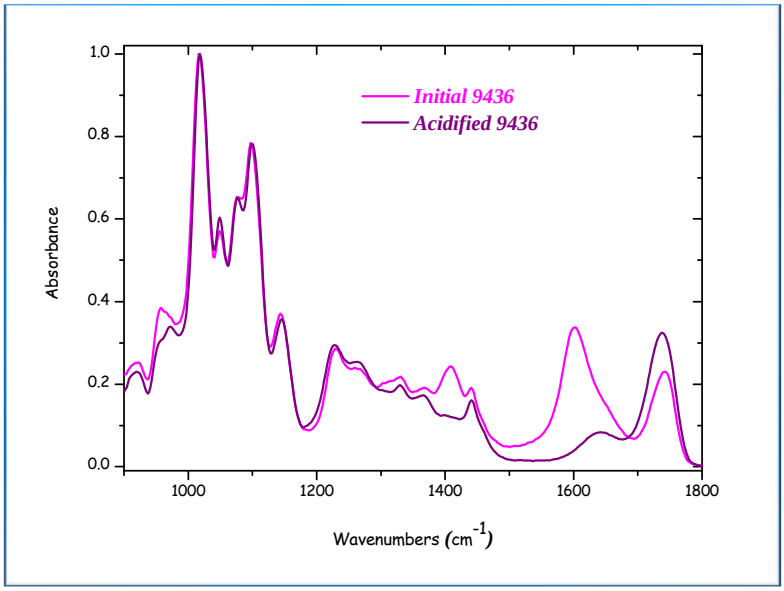

Fig. 3. 2. Effect of drying of pectin from acidified solutions on the measured IR spectrum.

This may seem an unusual procedure in deference to attempting to manipulate the sample conditions in order to obtain all charged and no protonated groups, as following this suggested acid treatment the protonated and methylesterified species essentially absorb at the same frequency and the originally proposed method is no longer applicable. However, another alternative now becomes possible, which completely eliminates problems introduced by the presence of the signals from hydration water.

Previous IR studies on pectins have suggested that the esterified CH_3 group presents bands in the 1350–1450 cm^{-1} range, one at 1380 cm^{-1} corresponding to the symmetric stretching of CH_3 and one at around 1440 cm^{-1} corresponding to the asymmetric stretching modes of CH_3 (Synytsya et al., 2003). Therefore, rather than attempting to quantify the bands corresponding to the absorption of the carboxylic ester and the carboxylic acid groups; and to the absorption of the carboxylic anion, we investigated whether the DM could be calculated simply by using the intensity of the asymmetric stretching of CH_3 at 1440 cm-1 relative to a backbone vibration at 1010 cm^{-1}. While pectin samples can contain small amounts of neutral sugars (for example in rhamnogalacturonan as described in Section III.A), the backbone vibration band is largely due to the homogalacturonan and a reasonably good correlation with the classically measured DM could still be expected.

In fact it was found that in order to perform the reliable quantification of the proposed band over a large DM range, acidification of the sample (which limits the interference of the symmetrical stretching of the carboxylate group (Fig. 3.2.)), and robust peak fitting, as described in Section III.B, were both required. While some preliminary progress was made previously by examining the asymmetric stretching modes of CH_3 (Strom, 2006), it is now clear that without properly accounting for the underlying intensity owing to the symmetric modes of any charged carboxylic groups the method struggles to be useful for samples with DM values below 40% (Fig. 3.3.).

However, under the conditions suggested herein, employing acidification and robust peak fitting, a linear relationship was established between the degree of methylesterification of the pectin samples and the ratio of the peak areas from bands at 1440 cm^{-1} and at 1010 cm^{-1}, (DM = ((455 ± 20) * ratio) + (2 ± 5)), which yielded a considerably improved R^2 value (0.975) and furthermore within experimental uncertainties a reassuring zero intercept (Fig. 3.3.). Using the given 95% confidence limits in the relationship the DM of an unknown sample can confidently be recovered to around ±7%.

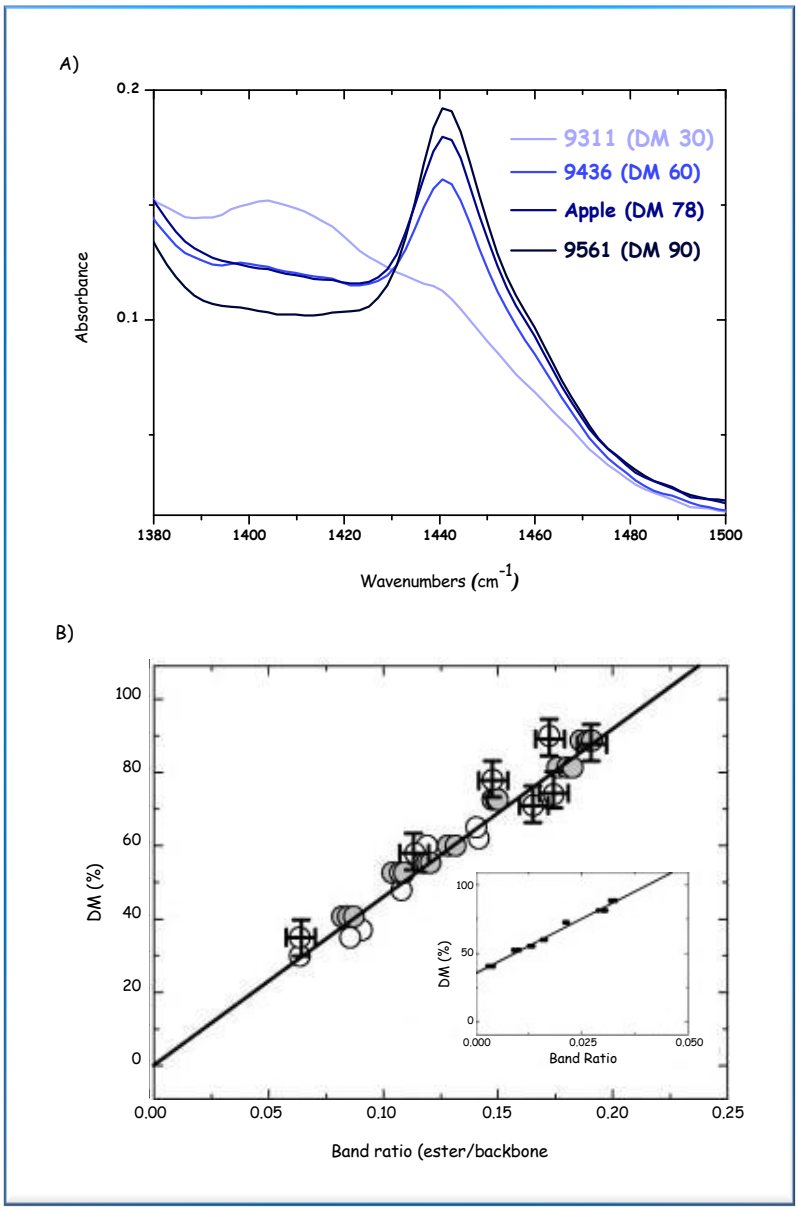

Fig. 3. 3. A) ATR/FT-IR spectra of pectins with different DM, as in the inset of Fig. 3.1, but in the region of 1380–1500 cm^{-1} B) Regression analysis for dried acidified samples using the ratio of asymmetric CH_3 stretches and the 1010 cm^{-1} backbone vibration band (open circles); also compared with previous work (Ström, 2006) on un-acidified samples (filled circles-inset), and scaled to take into account underlying intensity of the neighbouring band (grey circles).

In order to gain further confidence in the proposed methodology, and additionally to investigate the success of DFT in capturing the essential experimental details, a number of calculations were performed. Full quantum chemical calculations were used to generate theoretical FT-IR spectra of

the monomer, dimer and trimer of a-D galacturonic acid and their methylesterified analogues (Fig. 3.4A, B and C).

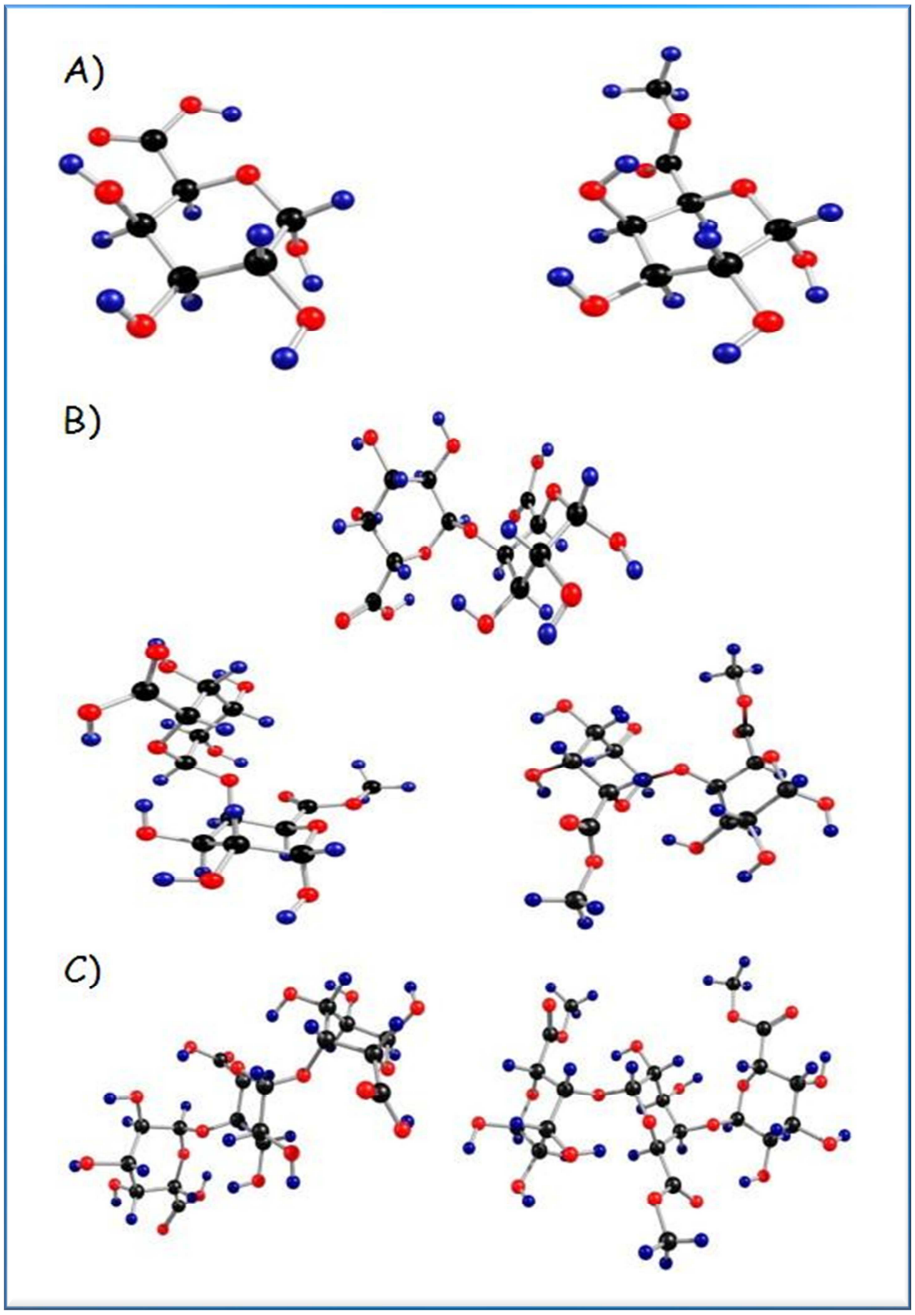

Fig. 3. 4. A) Pure monomer of a-d-galacturonic acid and its methylester analogue. (b) Galacturonic acid dimers of 0%, 50% and 100% DM depending on the number of the esterified groups in the molecule. (c) Trimers of a-d-galacturonic acid and its completely methylesterified analogue.

The experimental IR spectra of 0% and 90% DM pectin samples and simulated spectra of the monomer, dimer and the trimer of a-D-galacturonic acid and their fully methylesterified counterparts were first compared (Fig. 3.5.).

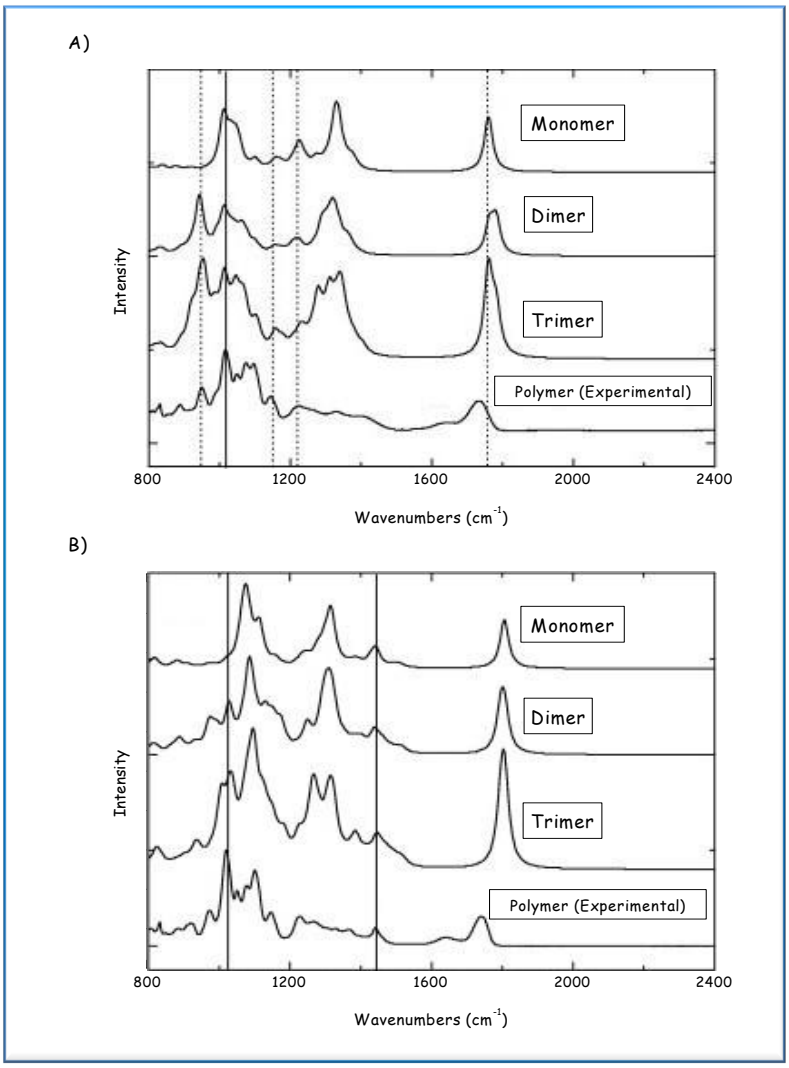

Fig. 3. 5. A) Comparison of experimental IR spectra of a 0% DM pectin polymer with calculations of monomer, dimer and trimer of a-d-galacturonic acid. Bands indicated by lines are assigned in Table 1; B) Comparison of experimental IR spectra of a 90% DE pectin polymer with calculations of 100% methylesterified monomer, dimer and trimer of a-d-galacturonic acid .The lines show the position of the asymmetric CH_3 stretches and the backbone ring vibration exploited by the proposed method.

Fig. 3.5A shows the comparison of the experimental spectra of a 0% DM pectin with the simulated spectra of oligomers of 0% DM of different DPs up to the point at which the calculation become uncomfortably expensive. There is, in general, good accordance between the calculations and the experiment, in particular between the carbonyl group vibrations and the backbone vibration frequencies at (1600–1800 cm^{-1}) and (900–1200 cm^{-1}) respectively. Since the 0% DM pectin samples do not have any methylester groups, we do not find the corresponding vibrations, occurring at around 1430–1490 cm^{-1} as expected; and clearly the water interference in the region at 1600-1650 cm^{-1} in the experimental result is not expected to be present in the calculated spectra. Five bands are specifically highlighted; and their assignments are shown in Table 1.

Table 3. 1. The assignment of relevant IR peaks and comparison of the experimentally measured frequencies with those found directly form the DFT calculation expounded herein (PGA, polygalacturonic acid).

Experimental (cm^{-1})	Raw calculated (cm^{-1})	Assignment
1750	1786	v(C=O), PGA ester
1750	1798	v(C=O), PGA
1630	-	v(C=O), PGA ion
1640	-	δ(HOH)
1440	1497	$v_{as}(CH_3)$, ester CH_3
1380	1442	$v_s(CH_3)$, ester CH_3
1215	1275	v(CO), δ(OCH)
1107	1155	v(CO), v(CC), Ring
1010	1051-1062 (acid and ester)	v(CO), v(CC), δ(OCH), Ring
934	983-1013 (acid and ester)	v(CO) glycosidic

It should noted that such calculations on systems of this size are highly complex, and the fact that the raw calculated frequencies only deviate by some 40 wavenumbers or less from those found experimentally constitutes good agreement. The main reasons for the observed differences result from approximations inherent in the calculations including: they are essentially carried out in vacuum at 0 K, and assume a strictly harmonic form for the relevant potentials. In light of this it is routine to scale the frequency axis by a small amount so as to align major bands with those experimentally observed. The co-alignment of multiple calculated and experimental bands via the same scaling, as seen here, constitutes good agreement.

Fig. 3.5B. shows the comparison between the experimental 90% DM data and simulations, again of varying DP substrates, but here with all residues methylesterified. Here, in addition to observing the pectin peaks in the IR spectra as described for the 0% DM oligomers (including the all-important marked backbone vibration), we do indeed find the $-CH_3$ group vibrations at around 1450 cm^{-1} as indicated in the figure.

In order to look at the difference in the $-CH_3$ group vibrations of different DM pectins, a galacturonic acid dimer was used for simulation, as this is the simplest molecule for which it is possible to study at least three different DMs by simulation. By varying the number of methyl groups along the molecule, we could easily generate a 0%, 50% and 100% DM sample for simulation. Comparing the calculated spectra of these 0%, 50% and 100% dimers (Fig. 3.6A.), a clear increase in the peak areas of the $-CH_3$ group vibrations is observed as the DM increases, validating the philosophy behind our proposed methodology. These simulation results should also be compared with the experimentally determined spectra of different DM pectins (0%, 48% and 90%), which are comparable with the ones obtained through the DFT simulations (Fig. 3.6B.). Again the simulations and the experimental data agree well.

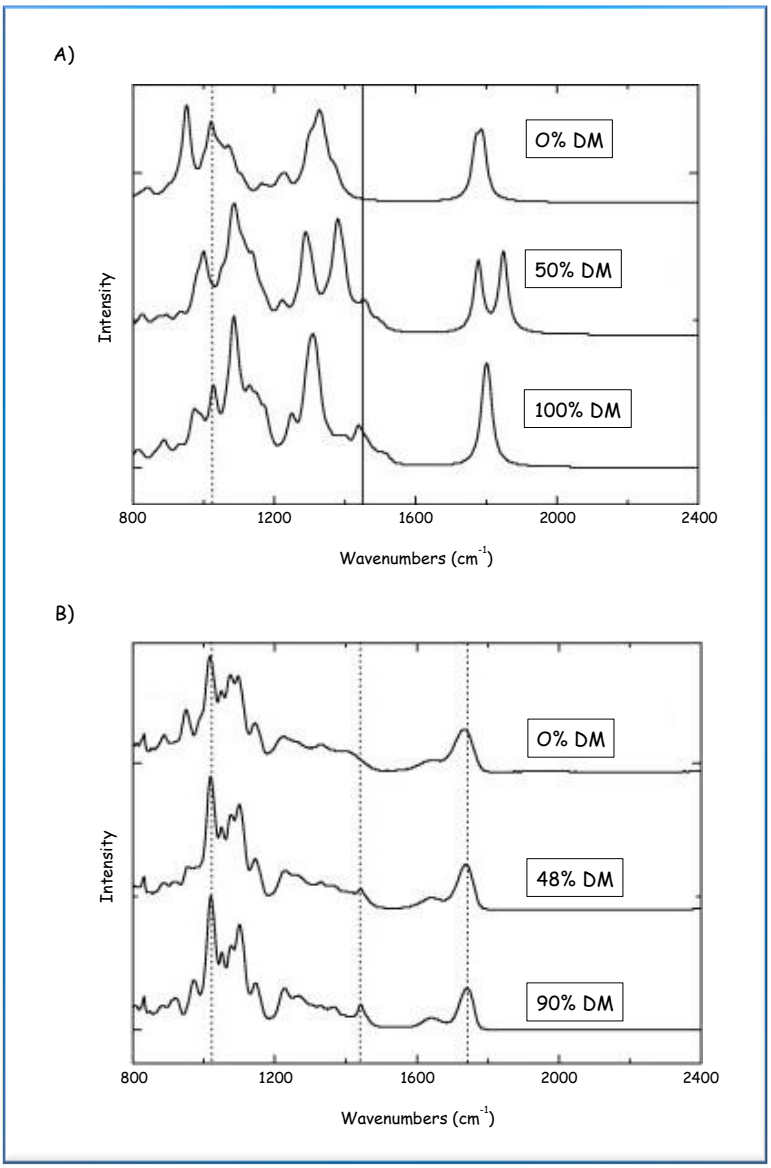

Fig. 3. 6. A) Simulated IR spectra for galacturonic acid dimers of 0%, 50% and 100% DM; and B) Experimental IR spectra of pectins of different (comparable to those simulated) DMs. The dotted lines again highlight discussed bands.

In all the simulated spectra, when compared with those obtained from experiments on the polymeric samples, we could see that particularly the bands owing to the backbone –CH vibrations (1200–1450 cm^{-1}) are much sharper in simulation than in experiment. In order to investigate the origins of this, which we hypothesized was due to the increased complexity in the polymeric backbone (both in terms of possibilities for coupled vibrations and dynamic averaging of

conformations), we took the experimental spectrum of a pure galacturonic acid monomer and dimer (0% DM) and compared them with the polymeric result (Fig. 3.7.).

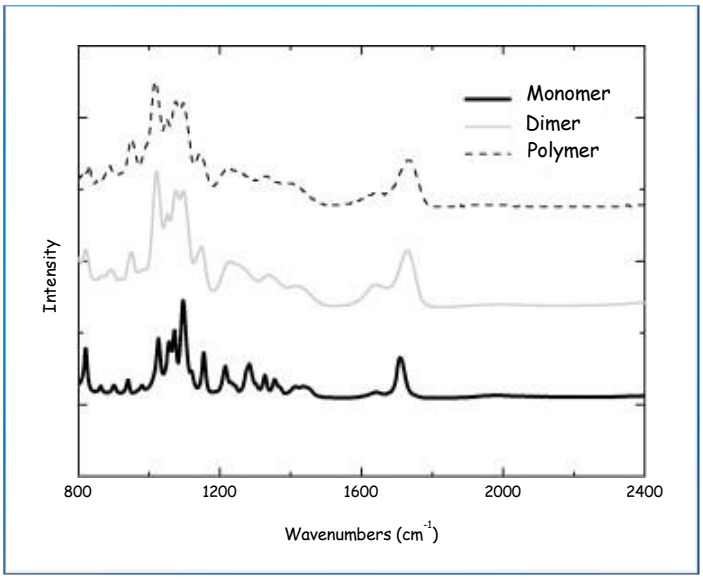

Fig. 3. 7. Comparison of experimental IR spectra recorded for a-d-galacturonic acid monomer, dimer and polymer, illustrating the increasing broadening owing to the increasing degree of polymerization.

It was indeed observed that the experimental spectra of a sole monomer showed sharp regions in 1200–1450 cm^{-1} accounting for the –CH vibrations; and the experimental and the theoretical spectra (shown in Fig. 3.5A.) were in reasonable accordance with each other. Already some broadening of the peaks is seen experimentally as the dimer spectra is measured, suggesting that the broadening of the experimental pectic spectra in this regime (1200–1450 cm^{-1}) is indeed a facet of the increasing degree of polymerisation.

5. CONCLUSION

The FT-IR method described in this study for the determination of the degree of methylesterification of pectins is non-invasive and is significantly more accurate than other reported IR methods; although the expected uncertainty in the measured DM value still stands at around ±7%. In order to get the best results from this method the samples should be treated

(precipitated from acidic solution and dried) as described. The ratio of the intensities of the asymmetric vibrations of the CH3 group and backbone bands can then be used to determine the DM (rather than the commonly used carboxylic bands), which permits the elimination of the interferences from other cell wall components such as water and proteins. In addition, DFT calculations have been shown to reproduce the main features of the experimental spectra, with a clear evolution towards the polymer result as the DP of the saccharide molecule in the calculation was increased from 1 to 2, and ultimately 3. This spectral elucidation makes FT-IR coupled with DFT an analysis method that has the potential to investigate pectin structure in more complex systems, such as post-coupling reactions. This forms part of ongoing work and will be reported next.

6. ACKNOWLEDGEMENTS

The authors would like to gratefully acknowledge Fonterra and FRST, and the Royal Society of New Zealand Marsden Fund for supporting PhD scholarships to A.F. and P.A. respectively. We would like to thank UCSC, Canterbury and their technical staff for help, and the MacDiarmid Institute for Advanced Materials and Nanotechnology for providing access and necessary resources to utilise the computational facilities. Anna Strom and Stephen Schum are acknowledged for initial contributions towards the method development. Yacine Hemar and Don Otter are acknowledged for helpful discussions and encouragement, and Ashton Partridge for access to the ATR assembly for the FT IR spectrometer.

7. REFERENCES

Barros, A.S.; Mafra, I.; Ferreira, D.; Cardoso, S.; Reis, A. and. Lopes da Silva, J.A (2002) Determination of the degree of methylesterification of pectic polysaccharides by FT-IR using an outer product PLS1 regression. *Carbohydrate Polymers*, **50**, 85–94.

Bédouet, L.; Courtois, B. and Courtois, J. (2003) Rapid quantification of O-acetyl and O-methyl residues in pectin extracts. *Carbohydrate Research*, **338** (4), 379–383.

Bociek, S.M. and Welti, D. (1975) The quantitative analysis of uronic acid polymers by infrared spectroscopy. *Carbohydrate Research*, **42**, 217–226.

Chatjigakis, A.K.; Pappas, C.; Proxenia, N.; Kalantzi, O.; Rodis, P. and Polissiou, M. (1998) FT-IR spectroscopic determination of the degree of esterification of cell wall pectins from stored peaches and correlation to textural changes. *Carbohydrate Polymers*, **37**, 395–408

Gnanasambandam, R. and Proctor, A. (2000) Determination of pectin degree of esterification by diffuse reflectance Fourier transform infrared spectroscopy. *Food chemistry*, **68**, 327–332.

Haas, U. and Jager, M. (1986) Degree of esterification of pectins determined by photoacoustic near infrared spectroscopy. *Journal of Food Science*, **51**, 1087–1088.

Huisman, M.M.H.; Oosterveld, A. and Schols, H.A. (2004) Fast determination of the degree of methylesterification of pectins by head-space GC, *Food Hydrocolloids*, **18** (4), 665–668.

Korolevich, M.V. and Zhbankov, R.G. (1998) A theoretical study of vibrational spectra of tetranitrate-methyl-β-d-glucopyranoside and 2,3-di-O-nitro-methyl-β-d-glucopyranoside. *Journal of Molecular Structure*, **440**, 247–263.

Korolevich, M.V. and Zhbankov, R.G. (1999) Theoretical study of the influence of structure on the vibrational spectra of crystalline nitrates of substituted glucopyranosides. *Journal of Molecular Structure*, **474**, 187–196.

Krishnakumar, V.; Keresztury, G.; Sundius, T. and Ramasamy, R. (2004) Simulation of IR and Raman spectral based on scaled DFT force fields: A case study of 2-(methylthio)benzonitrile, with emphasis on band assignment. *Spectrochemica Acta Part A*, **71**, 449–457.

Maness, N.O.; Ryan, J.D. and Mort, A.J. (1990) Determination of the degree of methylesterification of pectins in small samples by selective reduction of esterified galacturonic acid to galactose. *Analytical Biochemistry*, **185** (2), 346–352.

Massiot, P.; Perron, V.; Baron, A. and Drilleau, J.F. (1997) Release of methanol and depolymerisation of highly methylesterified apple pectin with an endopolygalacturonase from Aspergillus niger and pectin methylesterases from A. niger or from orange. *Food Science and Technology*, **30** (7), 697–702.

Monsoor, M.A.; Kalapathy, U. and Proctor, A. (2001) Improved method for determination of pectin degree of esterification by diffuse reflectance Fourier transform infrared spectroscopy. *Journal of Agricultural and Food chemistry*, **49**, 2756–2760.

Ralet, M.C. and Thibault, J.-F. (2002) Interchain heterogeneity of enzymatically deesterified lime pectins. *Biomacromolecules*, **3**, 917–925.

Rosenbohm, C.; Lundt, I.; Christensen, T.M.I.E. and Young, N.W.G. (2003) Chemically methylated and reduced pectins: Preparation, characterization by ^{1}H NMR spectroscopy, enzymatic degradation and gelling properties. *Carbohydrate Research*, **338,** 637–649.

Schulz, T.H. (1965) Methods in carbohydrate chemistry, *Academic Press*.

Ström, A. and Williams, M.A.K. (2004) On the separation, detection and quantification of pectin derived oligosaccharides by capillary electrophoresis. *Carbohydrate Research*, **339**, 1711–1716.

Ström, A.; Ralet, M.C.; Thibault, J.F. and Williams, M.A.K. (2005) Capillary electrophoresis of homogeneous pectin fractions. *Carbohydrate Polymers*, **60**, 467–473.

Ström, A. (2006). Characterization of pectin fine structure and its effect on supramolecular properties, *PhD Thesis*, University of Cork.

Synytsya, A.; Čopíková, J.; Matějka, P. and Machovič, V. (2003) Fourier transform Raman and infrared spectroscopy of pectins. *Carbohydrate Polymers*, **54**, 97–106

Venyaminov, S.Y. and Kalnin, N.N. (1990) Quantitative IR spectroscopy of peptide compounds in water solutions. 1. Spectral parameters of amino acid absorption bands. *Biopolymers*, **30**, 1243–1257.

Vincent, R.R.; Cucheval, A.; Hemar, Y. and Williams, M.A.K. (2009) Bio-inspired network optimization in soft materials – Insights from the plant cell wall. *The European Physical Journal E*, **28**, 79–87.

Vincent, R. R., & Williams, M. A. K. (2009). Microrheological investigations give insights into the structure and functionality of pectin gels. *Carbohydrate Research*, **344**, 1863-1871.

Vincken, J.P.; Schols, H.A.; Oomen, R.J.F.J.; McCann, M.C.; Ulvskov, P. and Voragen, A.G.J. (2003) If homogalacturonan were a side chain of rhamnogalacturonan I. Implications for cell wall architecture. *Plant Physiology*, **132** (4), 1781–1789.

Voragen, A.G.J.; Pilnik, W.; Thibault, J.-F.; Axelos, M.A.V. and Renard, C.M.G.C. (1995) In A.M. Stephen, Editor, Food polysaccharides and their applications, *Marcel Dekker*, New-York, 287–339.

Voragen, A.G.J.; Schols, H.A. and Pilnik W. (1986) Determination of the degree of methylation and acetylation of pectins by HPLC. *Food Hydrocolloid*, **1**, 65–70.

Williams, M.A.K.; Foster, T.J. and Schols, H.A. (2003) Elucidation of pectin methylester distributions by capillary electrophoresis. *Journal of Agricultural and Food Chemistry*, **51** (7), 1777–1782.

Williams, M.A.K.; Marshall, A.T.; Anjukandi, P. and Haverkamp, R.G. (2007) Investigation of the effects of fine structure on the nanomechanical properties of pectin. *Physical Review E*, **76**, 021927.

Zhong, H.J.; Williams, M.A.K.; Keenan, R.D.; Goodall, D.M. and Rolin, C. (1996) Separation and quantification of pectins using capillary electrophoresis: A preliminary study. *Carbohydrate Polymers*, **32**, 27–32.

Zhong, H.J.; Williams, M.A.K.; Goodall, D.M. and Hansen, M.E. (1998) Capillary electrophoresis studies of pectins, *Carbohydrate Research*, **308**, 1–8.

CHAPTER 4.

SUBSTRATES FUNCTIONALIZATION : PECTIN SPECIFIC ATTACHMENT

This chapter has been accepted for publication as:

Fellah, A.; Anjukandi, P.; Hemar, Y.; Otter, D. and Williams, M.A.K. (2009) Towards polysaccharide handles for single molecule experiments: Spectroscopic evidence for the selective covalent coupling of terminal sugar residues to desired substrates. *Carbohydrate Polymers*.

1. ABSTRACT

Single molecule force spectroscopy (SMFS) has recently given access to an unprecedented level of information regarding the stress-response of a host of biopolymers at the single chain level. However, the difficulty of designing handles for the specific attachment of the different ends of polysaccharide chains to substrates, such as piezoelectric scanners, cantilevers or microbeads; particularly in contrast to nucleotides and proteins, has meant that progress in more sophisticated single carbohydrate measurements has been relatively slow. Herein, methods for generating specific covalent attachments of the terminal sugar residue at one end of a pectin chain to polystyrene microspheres are demonstrated. Using FT-IR spectroscopy in combination with density functional theory (DFT) calculations the attachment was unequivocally shown to be mediated by the introduction of a C–N bond between the reducing end of the polysaccharide chain and a pre-aminated bead.

2. INTRODUCTION

In the simplest type of single molecule force spectroscopy experiment two spatially separated points on a molecule are held by two separate contacts, for example a micro-cantilever and a substrate (AFM experiments), or a pair of micron-sized beads (Optical Tweezers (OT) experiments) (Sarid, 1991; Fisher et al., 1999; Jansho et al., 2000; Butt et al., 2005; Buchachenko, 2006). One of the points is then moved away from the other one in a controlled manner, typically using a piezoelectric scanner to translate the substrate or a steered laser beam to move a bead, and the force involved is directly measured via the induced displacement of a tethered cantilever or optically trapped bead. Such technologies allow pN forces to be applied to the contact points and their displacements to be controlled and monitored in the nanometer range. Making controllable connections between these nano-scale force-transducers and the molecules of interest is key, not only to facilitating simple force-extension measurements, but also in expanding these tools into the realms of more sophisticated experiments such as those monitoring interactions and real-time kinetics. While nucleotides and proteins both intrinsically present termini that have distinct chemistries at each end of the chain and furthermore have manipulation possibilities afforded by

the developed tools of molecular biology (Kellermayer et al., 1997; Bustamante et al., 2000) developing such "handles" for the end residues of polysaccharides presents more of a challenge.

Certainly great progress has been made in single polysaccharide force spectroscopy and work has yielded particularly interesting data, including the observation of force-induced conformational transitions of the constituent sugar rings (Marszalek et al., 1999; Marszalek et al., 2001; Marszalek et al., 2002; Haverkamp et al., 2005; Zhang et al., 2005; Haverkamp et al., 2007). Such monomer transitions during stretching, from classical chair forms of the pyranose ring to more elongated arrangements, increase the polymer's contour length and thus produce characteristic deviations in the slope of the force-extension curve. Despite this unique behavior, owing to the difficulty of designing handles for the specific attachment of the different ends of polysaccharide chains as described, the majority of studies have been carried out with the polymer in question physisorbed to the substrates between which it is stretched, with a minority held through physical interactions between covalently attached binding pairs (Marszalek et al., 1998), or at best with one contact chemically attached to a substrate via a covalent bond (Khner et al., 2006), but at an uncontrolled location along the length of the molecule.

Consequently, polysaccharide stretching experiments to date have been largely dependent on picking up physisorbed polymers by chance from different surfaces, and attempting to locate favourable solution conditions for achieving the best stretches (Maurice & Matthai, 1999). In these circumstances definitive interpretation can be exacerbated by a lack of knowledge about the nature of the physisorbed contact points. Physisorption on surfaces is generally considered to be weak, owing to the intrinsic lack of strength of physical forces such as the Van Der Waals forces, and indeed many studies report peeling of molecules from surfaces. However, occasionally a contact is made that is strong enough to suffice for a significant stretch to ensue, presumably because of some pinning induced by a surface feature of the substrate or by another overlapping chain. It follows that a large number of scans are needed in order to detect an effective stretch by such a methodology, involving tedious trials of several solvent conditions, making it particularly difficult to perform multiple scanning and stretch reversal studies.

If, alternatively, known points on the polysaccharide molecules, ideally the terminal residues, could be functionalized with handles to which the nano-scale force transducers (cantilevers or beads) could be attached, this would significantly improve the potential of this type of experiment. As mentioned, with nucleotides and proteins the abundance of functional groups with well-

differentiated chemistry makes such an endeavor comparatively easy, while in sugars and carbohydrates, owing to the large number of functional –OH groups in the system, it becomes a complex procedure to perform chemistry at preferred positions. Nevertheless, herein, we have made an effort in this direction, attempting to convincingly attach one end of a polysaccharide molecule, pectin, to micro-beads, and to characterize the specific covalent bond formed using spectroscopy supported by quantum chemical calculations.

The particular polysaccharide, pectin, was selected as:

(i) the typical force-extension behavior of this important polysaccharide presents two force induced conformational transitions that make it a particularly interesting case (Williams et al., 2007);

(ii) recent work on coupling low molecular weight pectic oligomers to substrates presented an opportunity to examine whether any of these reported couplings could be effectively used for polymeric compounds (Guillaumie et al., 2002);

(iii) recent work carried out using ATR/FT-IR coupled with density functional theory (DFT) calculations for the analysis of pectin substrates seemed ripe for extension into the examination of coupling (Fellah et al., 2009).

For the purpose of this work pectin can be considered as a polymer of alpha 1–4 linked galacturonic acid sugar rings, each of which is capable of carrying a methyl group as an ester at the C-6 position (Ralet & Thibault, 2002). The previous study described the determination of the degree of methylesterification of pectins based on measurements of the ratio of the intensities of the CH_3 and backbone bands originating from linkages within the sugar rings. This permitted the elimination of the interferences from other cell wall components such as water and proteins that are found in a commonly used alternative method that employs monitoring the intensity of carboxylic bands (Haas & Jager, 1986; Gnanasambandam & Proctor, 2000; Monsoor et al., 2001; Synytsya et al., 2003). In order to validate proposed assignments, and confirm the frequencies associated with the new proposed methodology, IR spectra were calculated using DFT. Of late, there have been extensive studies of the IR and Raman properties of molecular systems using theoretical simulations (Krishnakumar et al., 2004; Krishnakumar & Prabhavathi, 2008) and the revolutionary development in recent years in available computational facilities and large clusters have made the simulations of comparatively large systems, such as several sugar rings, possible (Fellah et al., 2009).

Herein, the use of this robust spectroscopy method supported by DFT calculations is investigated for its potential for validating specific bond formation in proposed coupling reactions involving pectin macromolecules and substrates, carried out in order to facilitate various single molecule biophysical experiments. While many indirect methods can assess the "sticking" of polymers to substrates, we aimed to investigate whether FTIR spectroscopy could allow the detection of specific newly formed bonds with surfaces. Such functionalization of different surfaces with pectin molecules could be utilized as the starting step for AFM and Optical Tweezers studies to obtain high-resolution structural and mechanical properties of these functionally important molecules.

3. EXPERIMENTAL

3.1. Materials

Pectin was obtained from Fluka. It had an anhydrogalacturonic acid content of 85%, a degree of methylesterification of 78% and a molecular weight of 30–100 kDa. All other chemicals were purchased from Acros Organics except SnCl2 from Scharlau, Boc-Cys(trt)-OH from Bachem and hydrazine monohydrate from Alfa Aesar. Polystyrene beads (nominally 100 and 500 nm, 2.5% (w/v) solids aqueous suspension, Polysciences, USA) used in the experiments were first washed, removed from their respective solutions by centrifugation, and subsequently dried.

3.2. Coupling scheme

The immobilization of pectins onto pre-aminated beads was carried out via reductive amination (RA) or thiazolidine formation (TF). These methods have been successfully carried out for pectin oligomers (Guillaumie et al., 2002), but to our knowledge this is the first time they have been applied to polymeric molecules. Beads were selected as the substrate in preference to flat surfaces so as to increase the available surface area and thus the number of coupled species, in order to maximize the IR absorption. Polystryrene beads were selected as the major focus of the study (i) owing to their availability and common use in biophysical experiments and (ii) the complementarity of their IR spectra with that of pectin.

3.3. Polystyrene beads Amination

266 mg of polystyrene beads in a nitrating mixture of 0.532 mL of HNO_3 and 1.33 mL of H_2SO_4, were stirred at 60 °C for 30 min. The mixture was then poured over cold water in a refrigerated bath and washed several times with distilled water to remove excess acid. The polystyrene beads were then transferred to a mixture of 2.8 g of $SnCl_2$, 2.34 mL of HCl, and 2.6 mL of ethanol, and refluxed for 10 h at 90 °C. Upon completion of the reaction, the aminated polystyrene beads were washed with distilled water and 2 M NaOH, removed from solution by centrifugation and dried overnight under reduced pressure.

3.4. Immobilization of pectin

3.4.1. Reductive Amination

Dried amino-terminated beads (50 mg) were washed with DMF. Succinic anhydride (320 mg, 3.2 mmol) and hydroxybenzotriazole (HOBt) (320 mg, 2.4 mmol) were dissolved in DMF (15 mL). N-N-Diisopropylethylamine (DIEA) (600 µL, 3.6 mmol) was added and the solution was added to the beads. The mixture was then stirred at room temperature for 1.5 h. Excess reagents and solvents were filtered off and the beads were washed with DMF, centrifuged and dried overnight under reduced pressure. The dried carboxylic acid-terminated beads synthesized were transferred and washed with DMF. O-Benzotriazole-NNN'N'tetramethyl-uronium-hexaflurophosphate (HBTU) (200 mg, 0.5 mmol) and HOBt (360 mg, 2.7 mmol) were dissolved in DMF (15 mL). DIEA (540 µL, 3.24 mmol) was then added, followed by hydrazine monohydrate (180 µL, 3.6 mmol) and the mixture was added to the beads. After 2 h coupling at room temperature, solvents and unreacted compounds were removed by filtration and the beads were washed with DMF, centrifuged and dried overnight under reduced pressure. Dried hydrazide-terminated beads were transferred and washed with DMF. Subsequently, pectin was dissolved in DMF-AcOH (acetic acid) (99:1), 0.5% (w/w); 3 mL of this solution was then added to the beads, and following addition of $NaBH_3CN$ (30 mg, 0.48 mmol), the mixture was then stirred at room temperature. After 24 h, the solvent and excess reagents were filltered off and the beads were washed with DMF, centrifuged and dried overnight under reduced pressure. The entire procedure is shown schematically in Fig. 4.1.

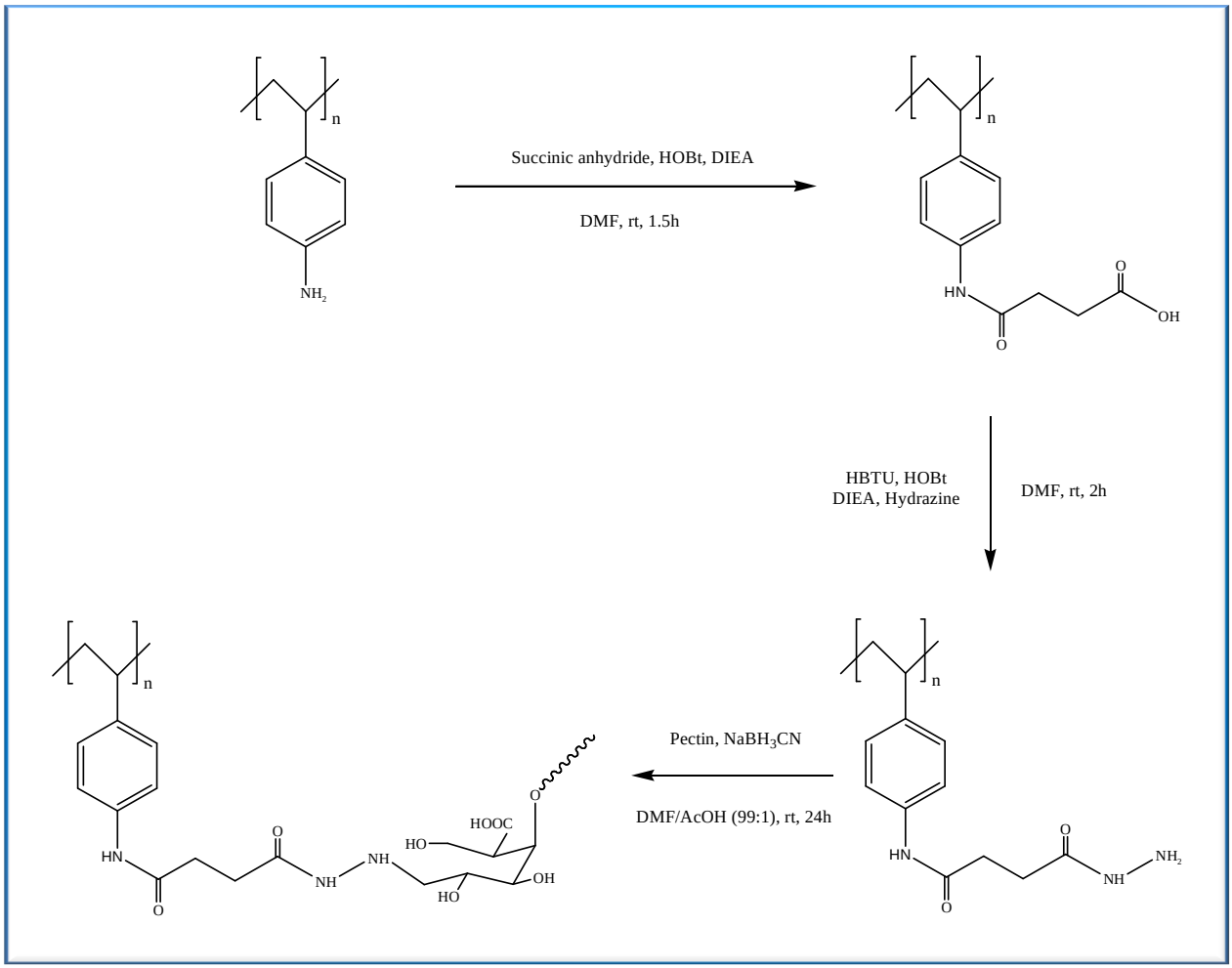

Fig. 4. 1. A schematic of the reductive amination (RA) reaction scheme used for the attachment of the terminal sugar residue of pectin to aminated polystyrene.

3.4.2. Thiazolidine Formation

Dried amino-terminated beads (15 mg) were washed with DMF. Boc-Cys(trt)-OH (100 mg, 0.22 mmol) was coupled in the presence of benzotriazol-1-yl-oxytripyrrolidinophosphonium hexaflurophosphate (PyBOP) (80 mg, 0.15 mmol), HOBt (15 mg, 0.12 mmol) and DIEA (30 µL, 0.18 mmol) in DMF (5 mL) at room temperature. After 1 h, the beads were washed with DMF, centrifuged and dried overnight under reduced pressure. Deprotection of Boc and trt groups was accomplished with TFA-CH_2Cl_2 (1:1) (5 mL) in the presence of Et_3SiH (50 µL, 0.3 mmol) for 1 h at room temperature. The beads were washed with CH_3CN, centrifuged and dried overnight under reduced pressure. Dried cys-terminated beads were transferred and washed with CH_3CN. Pectin

was dissolved into CH_3CN–H_2O (1:2), 0.5% (w/w), and the solution, whose pH was decreased to 4 with 0.2 M HCl, was added to the beads. After 48 h at room temperature, the beads were washed with CH_3CN, centrifuged and dried overnight under reduced pressure. The entire procedure is shown schematically in Fig. 4.2.

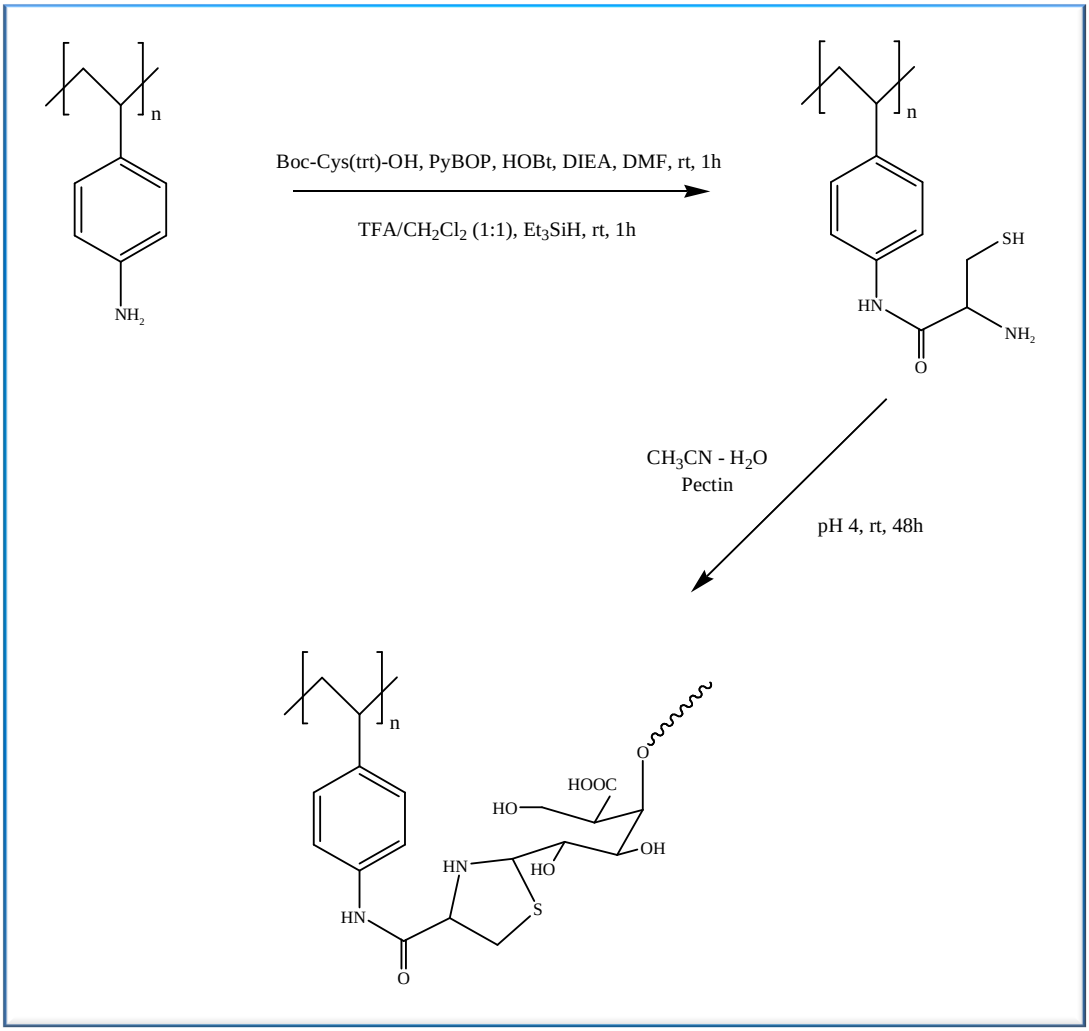

Fig. 4. 2. A schematic of the thiazolidine formation (TF) reaction scheme used for the attachment of the terminal sugar residue of pectin to aminated polystyrene.

3.5. Spectroscopy

Spectral acquisition was performed on solid samples using a Nicolet 5700 FT-IR spectrometer equipped with Omnic software (version 7.1) and a Smart Omni-Sampler (ATR cell with single

reflectance germanium crystal). Each recorded spectrum is the average of 32 scans with a spectral resolution of 4 cm^{-1} from 400 to 4000 cm^{-1}, with a background spectrum recorded before each analysis.

3.6. Light scattering

Dynamic light scattering (DLS) experiments were carried out using a monochromatic polarized beam of laser light from a 2W Argon laser of wavelength 488 nm. The beam was incident on the sample and scattered light was collected at 90° with respect to the incident beam. A single mode fibre optic was used to direct the collected light to a photomultiplier tube (PMT) used as a detection system. The PMT was connected to a flex99 multiple tau digital correlator (www.correlator.com), where the correlation function was calculated and output to a local computer. Prior to the measurements, the sample was placed in a 1 cm^2 cuvette and the concentration of the sample was diluted enough such that only single scattering took place in the measurements. The cuvette was placed into a scattering chamber filled with water as an index matching fluid and measurements were taken at room temperature in a temperature-controlled room (25 °C).

4. RESULTS AND DISCUSSION

Fig. 4.3. and Fig. 4.4. show the calculated IR spectra of galacturonic acid dimers (Fellah et al., 2009), bead (styrene-monomer) intermediates, and galacturonic acid dimers covalently coupled onto the polystyrene beads intermediates via the two methods discussed above. The (green) dotted lines indicate spectral features clearly associated with pectin while the (blue) dashed lines indicate those originating from the bead intermediate.

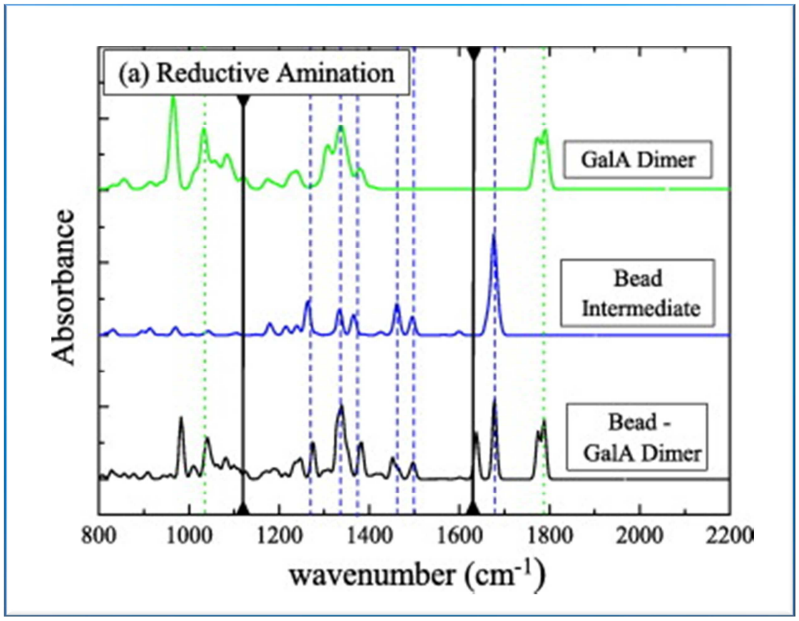

Fig. 4. 3. The simulated IR spectra for a pectin model (galacturonic acid dimer) immobilized on a polystyrene bead model (functionalized styrene monomer) by the reductive amination method described herein. (For molecular models see Appendix)

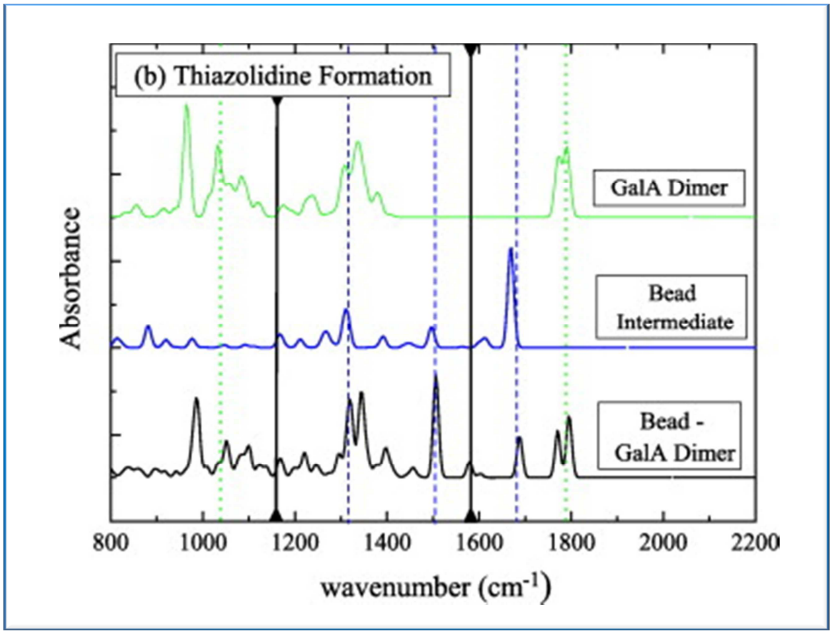

Fig. 4. 4. The simulated IR spectra for a pectin model (galacturonic acid dimer) immobilized on a polystyrene bead model (functionalized styrene monomer) by the thiazolidine formation method described herein. (For molecular models see Appendix).

The origin of these features is reported in Table 4.1 and Table 4.2.

Table 4. 1. The assignment of relevant IR peaks for the reductive amination reaction and the comparison of the experimentally measured frequencies with those found directly from DFT calculation expounded herein (PIB: pectin immobilized on beads, AB: aminated intermediate beads, PGA: polygalacturonic acid).

PIB Calc. (cm^{-1})	PIB Exp. (cm^{-1})	AB Calc. (cm^{-1})	AB Exp. (cm^{-1})	Assignment
1795	1720	-	-	ν(C=O), PGA
1720	1660	1735	1660	ν(C=O), Bead
1650	1520	1635	1520	ν, Benzene ring
1230	1210	-	-	ν(CO), ν(CC), Pectin ring
1125	1145	-	-	ν(CN), Bead
1610	1660	-	-	ν(CN), new covalent coupling
1040	1010	-	-	ν(CO), ν(CC), δ(OCH) Ring

Table 4. 2. The assignment of relevant IR peaks for the thiazolidine immobilization reaction and the comparison of the experimentally measured frequencies with those found directly from DFT calculation expounded herein (PIB: pectin immobilized on beads, AB: aminated intermediate beads, PGA: polygalacturonic acid).

PIB Calc. (cm^{-1})	PIB Exp. (cm^{-1})	AB Calc. (cm^{-1})	AB Exp. (cm^{-1})	Assignment
1815	1760	-	-	ν(C=O), PGA
1720	1680	1720	1660	ν(C=O), Bead
1620	1550	1620	1520	ν, Benzene ring
1267	1210	-	-	ν(CO), ν(CC), Pectin ring
1202	1210	1205	1215	ν(CN), Bead
1125	1145	-	-	ν(CN), new covalent coupling
1590	1610	-	-	ν(C=N), new covalent coupling
1040	1010	-	-	ν(CO), ν(CC), δ(OCH) Ring

While the intensities of the simulated bands should not be taken literally as predictions of the strengths of experimental features the calculated spectra can be interrogated in order to locate the relative frequencies of distinct vibrational features associated with the specific bonds proposed to have been introduced in the trialed coupling schemes. The simulated spectra of the

coupled systems therefore highlight the potential locations of distinct peaks associated with any newly formed bonds after pectin immobilization in the experimental spectra. For example, it can clearly be seen that beads successfully attached to the end residue of the pectin chain bead are predicted to exhibit a newly formed C-N bond.

Fig. 4.5. and Fig. 4.6. show the measured experimental IR spectra of (a) pectin, (b) described bead-intermediates directly prior to pectin attachment, and (c) the beads with putative pectin coupling, via the reductive amination and thiazolidine formation, respectively. Once again (green) dotted lines indicate spectral features clearly associated with pectin while the (blue) dashed lines show vibrational frequencies originating from features of the bead intermediates. The assignment of these bands is detailed in Table 1 and Table 2 (Venyaminov & Kalnin, 1990; Momany and Willett, 2000; Appell et al., 2004; Momany et al., 2004; Krishnakumar et al., 2004; Krishnakumar & Prabhavathi, 2008).

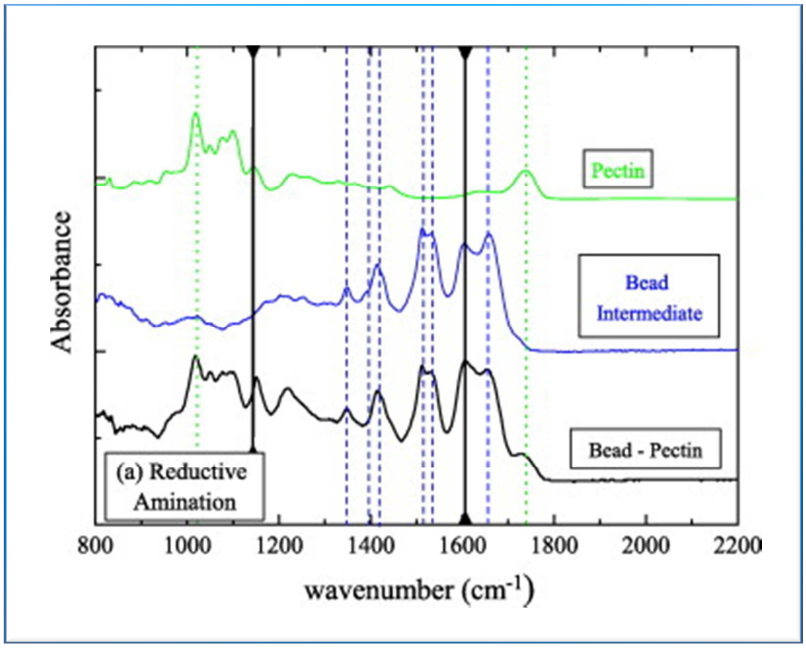

Fig. 4. 5. Experimental IR spectra measured for pectin, and pectin immobilized on polystyrene beads using reductive amination, compared with the functionalized inter-mediate beads. The black solid lines indicate the positions at which the DFT calculations indicate vibrations relating to the newly formed covalent coupling are expected to occur.

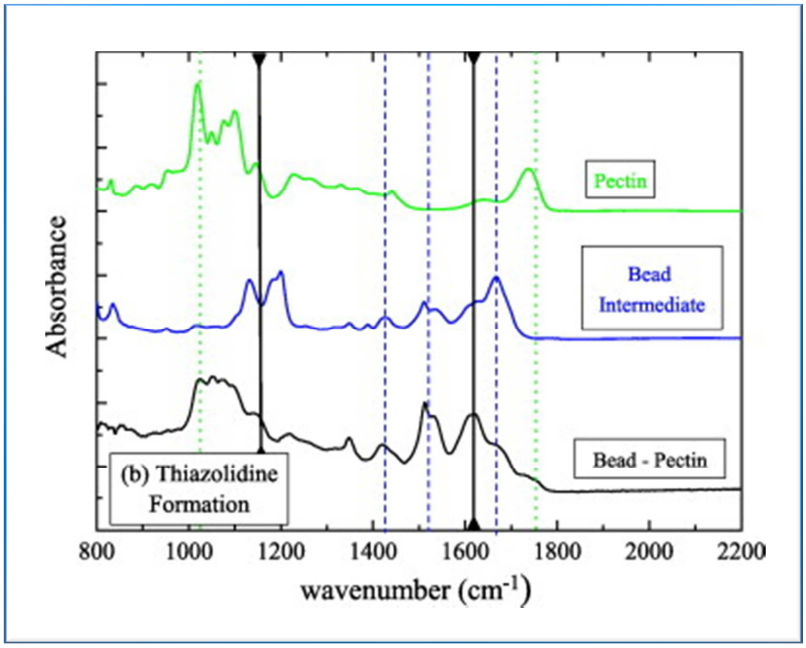

Fig. 4. 6. Experimental IR spectra measured for pectin, and pectin immobilized on polystyrene beads using thiazolidine formation, compared with the functionalized intermediate beads. The black solid lines indicate the positions at which the DFT calculations indicate vibrations relating to the newly formed covalent coupling are expected to occur.

While the presence of pectin on the bead substrates following the described procedures could be inferred from washing assays and the results of the light scattering experiments, the goal of the spectroscopy experiments was the detection of the specific covalent bond formed in coupling and hence confirmation that the desired coupling chemistries had been successful and that specifically the terminal sugar residue was attached (thereby potentially maximizing the length of polymer stretched in single molecule experiments). As mentioned both coupling modalities were expected to involve the formation of a new –C–N bond after the pectin immobilization that potentially could be monitored in the IR spectrum. In the case of the reductive amination technique, this new pectin-substrate bond is unique as it is the only –C–N bond in the system while there is a pre-existing –C–N bond in the thiazolidine coupled system intermediate prior to pectin attachment that has to be considered. Such C–N bonds are expected to show clear signatures at around 1120–1150 cm^{-1} and additional vibrations around 1580–1670 cm^{-1} that reflect the delocalised character of the –C–N; being coupled with –C=O in the reductive amination case and strained in the five-membered ring formed in the thiazolidine case. The black lines in the experimental figures indicate the position of the predicted signature vibrations arising from the new bond formed on

coupling and there can indeed be seen to be extra intensity at these frequencies in the experimental data, consistent with coupling the polysaccharide moiety via newly formed chain-end covalent bonds. This is particularly clear for the RA case, while with TF it is less clear-cut with the new-bond intensity predominantly broadening pre-existing peaks.

Despite the fact that, owing to the crystalline, single-unit nature of the substrate in the simulations, peaks in the simulated spectra are sharp compared with typical experimental bands, the coincidence of the calculated end-residue-covalent-coupling bands, indicated by the (black) solid lines, with extra experimentally detected intensity is strong evidence supporting the proposed nature and position of the attachment. It should also to be noted that the simulations correspond to vacuum conditions and 0 K, unlike the experiments that are performed at the room temperature, and the absolute values of the calculated frequencies do typically deviate slightly from the experimental ones by up to 50 wave numbers. It is routine to scale the frequency axis by a small amount so as to align major bands with those experimentally observed and the co-alignment of multiple calculated and experimental bands via the same scaling, as seen here, is typically taken to constitute good agreement.

Other prominent bond vibrations seen in the experimental IR spectra, as detailed in Table 1 and Table 2, are those corresponding to a set of carbonyl (–*C*=*O*) groups in the system at around 1650–1750 cm^{-1} and the benzene ring vibrations at around 1550 cm^{-1}. In the case of pectin and pectin-functionalized beads, the pectin backbone vibrations can be seen at 1000–1100 cm^{-1}. The addition of a new shoulder peak in the IR spectra, owing to the –*C*=*O* stretching of the pectin entity at around 1715 cm^{-1} also adds support to the attachment of the pectin molecules on the beads (although not to the nature of the bond). Once again similar behavior was found in the simulated IR spectra.

Finally the RA method described was trialed using 200 nm diameter silica beads (the initial step again involving amination, followed by the identical coupling chemistry described for the aminated polystyrene beads). DLS was used to estimate the size of the beads, (i) pre- and (ii) post chemical treatment, and (iii) post washing steps with urea, found to remove purely physisorbed material. The experimental results indicated sizes of (i) 238 nm; (iii) 508 nm and (iii) 659 nm; indicating that indeed post-RA a layer of some 210 nm was introduced onto the bead that could not be removed by washing, suggesting that the RA method was also successful with silica substrates as the starting material.

5. CONCLUSION

It was recently suggested that vibrational spectroscopy coupled with quantum chemical calculations might be a useful tool to examine the success of particular coupling schemes designed for the attachment of biopolymers to substrates as part of an effort to facilitate modern biophysical experiments. It has been shown herein that indeed FT-IR results, when considered with predictions from DFT calculations, can provide strong evidence for the success of specific coupling schemes. A good general agreement between the experimental and simulated spectra pre-, as well as post-, coupling confirm the reliability of this technique. In particular, this work provides evidence that by following the protocols described not only can the pectin chain be attached to microbeads, but that the coupling is via the formation of a specific recognizable C–N bond, with pectin coupled at its reducing end. It is hoped that the availability of such a technique will encourage further work on specific coupling and will ultimately facilitate more sophisticated biophysical experiments to be carried out on polysaccharides and their interactions.

6. ACKNOWLODGEMENT

The authors would like to gratefully acknowledge Fonterra and FRST, and the Royal Society of New Zealand Marsden Fund for supporting PhD scholarships to AF and PA, respectively. We would like to thank UCSC, Canterbury and their technical staff for help, and the MacDiarmid Institute for Advanced Materials and Nanotechnology for providing access and necessary resources to utilise the computational facilities. Mark Waterland is thanked for access to the ATR assembly and FT-IR spectrometer, and Dave Harding for help with supplying reagents for the coupling reaction.

7. REFERENCES

Appell, M.; Strati, G.; Willett, J.L. and F.A. Momany (2004) B3LYP/6-311++G** study of α- and β D-glucopyranose and 1,5-anhydro-D-glucitol: $^4C_1$ and $^1C_4$ chairs, ^{3,0}B and B^{3,0} boats, and skew boat conformations. *Carbohydrate Research*, **339**, 537–551.

Buchachenko, A.L. (2006) New horizons of chemistry: Single molecules. *Russian Chemical Reviews*, **75** (1), 122.

Bustamante, C.; Smith, S.B.; Liphardt, J. and Smith D. (2000) Single-molecule studies of DNA mechanics. *Current Opinion in Structural Biology*, **10**, 279–285.

Butt, H.J.; Cappella, B. and M. Kappl (2005) Force measurements with the atomic force microscope: Technique, interpretation and applications. *Surface Science Reports*, **59** (152), 2005.

Fellah, A.; Anjukandi, P., Waterland, M.R. and Williams, M.A.K. (2009) Determining the degree of methylesterification of pectin by ATR/FT-IR: Methodology optimisation and comparison with theoretical calculations. *Carbohydrate Polymers*, **78** (4), 847–853.

Fisher, T.E.; Marszalek, P.E.; Oberhauser, A.F.; CarrionVazquez, M. and Fernandez J.M. (1999) The micro-mechanics of single molecules studied with atomic force microscopy. *Journal of Physiology*, **50**, 5.

Guillaumie, F.; Thomas, O.R.T. and Jensen, K.J. (2002) Immobilization of pectin fragments on solid supports: Novel coupling by thiazolidine formation. *Bio-conjugate Chemistry*, **13**, 285–294.

Gnanasambandam, R. and Proctor, A. (2000) Determination of pectin degree of esterification by diffuse reflectance Fourier transform infrared spectroscopy. *Food chemistry*, **68**, 327–332.

Haas, U. and Jager, M. (1986) Degree of esterification of pectins determined by photoacoustic near infrared spectroscopy. *Journal of Food Science*, **51**, 1087–1088.

Haverkamp, R.G.; Williams, M.A.K. and Scott, J.E. (2005) Stretching single molecules of connective tissue glycans to characterise their shape maintaining elasticity. *Biomacromolecules*, **6**, 1816.

Haverkamp, R.G., Marshall, A.T. and Williams, M.A.K. (2007) A model for stretching elastic biopolymers which exhibit conformational transformations. *Physical Review E*, **75**, 021907.

Jansho, A.; Neitzert, M.; Oberdrfer, Y. and Fuchs, H. (2000) Force spectroscopy of molecular systems—single molecule spectroscopy of polymers and biomolecules. *Angewandte Chemie*, **39**, 3212–3237.

Kellermayer, M.S.Z., Smith, S.B., Granzier, H.L. and Bustamante, C. (1997) Folding unfording transitions in single titin molecules characterized with laser tweezers. *Science*, **276**, 1112.

Khner, F.; Erdmann, M. and H. Gaub (2006) Scaling exponent and kuhn length of pinned polymers by single molecule force spectroscopy. *Physical Review Letters*, **97**, 218301.

Krishnakumar, V.; Keresztury, G.; Sundius, T. and Ramasamy, R. (2004) Simulation of IR and Raman spectral based on scaled DFT force fields: A case study of 2-(methylthio)benzonitrile, with emphasis on band assignment. *Spectrochemica Acta Part A*, **71**, 449–457.

Krishnakumar, V. and Prabhavathi, N. (2008) Simulation of IR and Raman spectral based on scaled DFT force fields: A case study of 2-amino 4-hydroxy 6-trifluoromethylpyrimidine, with emphesis on band assignment. *Spectrochemica Acta Part A*, **71**, 449–457.

Marszalek, P.E.; Oberhauser, A.F.; Pang, Y.P. and Fernandez, J.M. (1998) Polysaccharide elasticity governed by chair-boat transitions of the glucopyranose ring. *Nature*, **396**, 661–664.

Marszalek, P.E.; Pang, Y.P.; Li, H.; Oberhauser, F.A.; Yazal, J.E. and Fernandez, J.M. (1999) Atomic levers control pyranose ring conformations. *Proceedings of National Academy of Sciences*, **96**, 7894–7898.

Marszalek, P.E., Li, H. and Fernandez, J.M. (2001) Fingerprinting polysaccharides with single molecule atomic force microscopy. *Nature Biotechnology*, **19**, 258.

Marszalek P.E.; Li. H.; Oberhauser, F.A. and Fernandez, J.M. (2002) Chair-boat transitions in single polysaccharide molecules observed with force-ramp AFM. *Proceedings of National Academy of Sciences the United States of America*, **99**, 4278–4283.

Maurice, R.G. and Matthai, C.C. (1999) Force-extension curves for a single polymer chain under varying solvent conditions. *Physical Review E*, **60**, 3165–3169.

Momany, F.A. and Willett, J.L. (2000) Computational studies on carbohydrates: I. Density functional ab-Initio geometry optimisation on maltose conformations. *Journal of Computational Chemistry*, **21**, 1204–1219.

Momany, F.A., Appell, M., Strati, G. and Willett, J.L. (2004) B3LYP/6-311++G** study of a- and β-d-glucopyranose hydrogen bonding, stress energies, and effect of hydration on internal coordinates, *Carbohydrate Research,* **339**, 553–567.

Monsoor, M.A., Kalapathy, U. and Proctor, A. (2001) Improved method for determination of pectin degree of esterification by diffuse reflectance Fourier transform infrared spectroscopy. *Journal of Agricultural and Food chemistry*, **49**, 2756–2760.

Ralet, M.C. and Thibault, J.-F. (2002) Interchain heterogeneity of enzymatically deesterified lime pectins. *Biomacromolecules*, **3**, 917–925.

Sarid, D. (1991) Scanning force microscopy, *Oxford University Press*, New York.

Synytsya, A.; Čopíková, J., Matějka, P. and Machovič, V. (2003) Fourier transform Raman and infrared spectroscopy of pectins. *Carbohydrate Polymers*, **54**, 97–106.

Venyaminov, S.Y. and Kalnin, N.N. (1990) Quantitative IR spectroscopy of peptide compounds in water solutions. 1. Spectral parameters of amino acid absorption bands. *Biopolymers*, **30**, 1243–1257.

Williams, M.A.K.; Marshall, A.T.; Anjukandi, P. and Haverkamp, R.G. (2007) Investigation of the effects of fine structure on the nanomechanical properties of pectin. *Physical Review E*, **76**, 021927.

Zhang, Q.; Lee, G. and Marszalek, P.E. (2005) Atomic cranks and levers control sugar ring conformations, *Journal of Physics: Condensed Matter*, **17**, S1427.

CHAPTER 5.

PECTIN FUNCTIONALIZED SURFACES : APPLICATION TO SINGLE MOLECULE FORCE SPECTROSCOPY

This chapter has been submitted for publication as:

Fellah, A.; Belmiloud, N.; Haverkamp, R.; Hemar, Y.; Otter D. and Williams, M.A.K. (2011) Facilitating high-force single-polysaccharide stretching using covalent attachment at one end of the chain. *Carbohydrate Polymers*.

1. ABSTRACT

Single polysaccharide force spectroscopy has yielded particularly interesting data, the interpretation of which requires the marriage of statistical-mechanical theories of polymer physics to the complexities afforded by possible force-induced conformational transitions of the constituent sugar rings. However, the difficulty of designing handles for the specific attachment of the different ends of polysaccharide chains to substrates, such as piezoelectric scanners, cantilevers or microbeads has meant that the majority of studies to date have been carried out with the polymer physisorbed to the substrates between which it is stretched, or at best chemically attached via bonds formed at uncontrolled locations along the length of the molecule. This means that the lengths of obtained polysaccharide stretches, as well as the forces that can be placed on the molecule without generating detachment, are generally smaller than those obtainable for polymers that offer the ability to be covalently attached to substrates specifically at their ends. As a consequence it is troublesome and tedious to record a statistically significant number of force curves that extend chains to high enough forces to investigate certain conformational transitions, such as the boat-to-inverted chair, exhibited by polysaccharides such as pectin.

Herein, single molecule force-extension curves have been measured for the several pectin samples using AFM. The results are compared when either i) the polymers have been physisorbed between the cantilever and the surface of the piezo-electric scanner, under several different solvent conditions of pH and ionic strength, or ii) the polymer molecule has been chemically attached at one end to the piezo surface using a recently reported coupling procedure. In fact, using such a chemical attachment to tether the end of the polysaccharide, reduced the frequency of successful stretching events obtained in a particular location, confirming the role of surface diffusion in the physisorbed experiments. Nevertheless, when polymer stretches were successfully recorded, the force that could be applied before detachment was significantly increased, indicating that this methodology has great potential for improving the acquisition of data reporting on force-induced conformational transitions of the sugar ring that require the application of significant stresses.

2. INTRODUCTION

Modern biophysical instrumentation allows forces in the pN - nN range to be applied to molecular chains and their displacements to be controlled and measured to nm precision. However, making controllable connections between the active nano-manipulators (cantilevers, beads or piezo-ceramics) and the molecules of interest is key, not only to facilitating force-extension measurements, but also in expanding these tools into the realms of more sophisticated experiments such as those monitoring interactions and real-time kinetics. While nucleotides and proteins both intrinsically present termini that have distinct chemistries at each end of the chain and have manipulation possibilities afforded by the developed tools of molecular biology (Kellermayer et al., 1997; Bustamante et al., 2000) developing such "handles" for the end residues of polysaccharides presents more of a challenge.

Certainly great progress has already been made in single polysaccharide force spectroscopy and work carried out with the atomic force microscope (AFM) has yielded particularly interesting data, the interpretation of which requires the marriage of statistical-mechanical theories of polymer physics to the complexities afforded by possible force-induced conformational transitions of the constituent sugar rings (Marszalek et al., 1999; 2001; 2002; Zhang et al., 2005; Haverkamp et al., 2005; 2007). Such monomer transitions during stretching, from classical chair forms of the pyranose ring to more elongated arrangements increase the polymer's contour length and thus produce characteristic deviations (or "clicks") in the slope of the force-extension curve. However, owing to the difficulty of designing handles for the specific attachment of the different ends of polysaccharide chains as described, the majority of studies have been carried out with the polymer in question physisorbed to the substrates between which it is stretched, with a minority held through physical interactions between covalently attached binding pairs (Marszalek et al., 1998), or at best with one contact chemically attached to a substrate via a covalent bond (Khner et al., 2006), but at an uncontrolled location along the length of the molecule.

Polysaccharide stretching studies to date then have been largely focused on AFM and on picking up lengths of physisorbed polymers by chance from different surfaces. Such work typically attempts to locate the most favourable solution conditions for achieving stretches with desired properties (Maurice & Matthai, 1999). Difficulties are exacerbated by a lack of knowledge about the nature of the physisorbed contact points. Physisorption on surfaces is generally considered to

be weak, owing to the intrinsic lack of strength of physical forces such as the Van Der Waals forces, and many studies report the peeling of molecules from surfaces. Indeed adhesion and desorption of polymers from surfaces has become of great interest in its own right (Hugel et al., 2001; Cui et al., 2003; 2004; Seitz at al., 2003; Kierfeld, 2006; Sonnenberg et al., 2008; Geisler et al., 2008; 2009; Francius et al., 2009; Staple et al., 2011). If stretching is rapid enough interactions can persist until higher forces (Ray et al., 2006; 2007; Sonnersberg et al., 2007; Sletmoen et al., 2004); and if pinning is induced by a surface feature of the substrate or by another overlapping chain then occasionally a contact is made that is strong enough to suffice for a significant stretch to ensue. In general however, when such a methodology is applied, a large number of scans can be needed in order to achieve an effective stretch, involving tedious trials of several solvent conditions, and making it particularly difficult to perform, for example, multiple scanning and stretch reversal studies.

While for AFM studies specifically covalently attaching both ends of a polysaccharide molecule to a substrate and cantilever tip respectively remains the ultimate goal, a methodology has recently been reported that makes some progress in this direction by convincingly demonstrating, using spectroscopy supported by quantum chemical calculations, the specific covalent bonding of one end of a pectin chain to microbeads (Fellah et al., 2011). Pectin can be considered for the purposes herein as a polymer of alpha 1-4 linked galacturonic acid sugar rings, each of which is capable of carrying a methyl group as an ester at the C-6 position (Ralet & Thibault, 2002). This polysaccharide was selected for study here as it presents two force-induced conformational transitions upon straining that make it a particularly interesting case (Williams et al., 2007). Furthermore, one of these transition, hypothesized to be a boat-to-inverted chair transition, occurs at reasonable large forces (> 700 pN), making this feature difficult to observe in experiments in which the polymer is physisorbed between contacts. Herein, this recently-reported coupling methodology was supplemented and applied in order to covalently link one of the terminal sugar residues of the pectin chains onto substrates that were subsequently mounted onto a piezo-electric scanner. Attempts were then made to physisorb the trailing end of the chain to an AFM cantilever using advance and retract cycles of the piezo in the usual fashion and the results obtained from a statistical sample of stretch attempts were compared when using (i) purely physisorption of both ends under different solvent conditions or (ii) where the one end was specifically chemically bound to the piezo-surface as described.

3. EXPERIMENTAL

3.1. Materials

Pectin samples with different fine structures were used, the origin, the degree of methylesterification (DM), the anhydrogalacturonic acid content (GA) and the molecular weight (M_w) of which are given in Table 1. All other chemicals were purchased from Acros Organics except Boc-Cys(trt)-OH from Bachem, and hydrazine monohydrate from Alfa Aesar. Water used throughout this study was purified with a MilliQ water purification system (Millipore) giving a water resistivity 18.2 MΩ.cm. Circular glass coverslips were supplied by Warner Instruments LLC and used as substrates onto which the polymer chains were attached. AFM experiments were performed using gold tipped silicon nitride cantilevers (Ultrasharp CSG11/Au, NT-MDT Co). (Additional preliminary scouting experiments found similar behaviour to that reported here for physisorbed experiments when using mica and gold-coated surfaces).

Table 5. 1. The characteristics of the pectin samples used; degree of methylesterification (±3); galacturonic acid content (±5); and molecular weight as quoted by the manufacturer.

Pectin	Origin	DM (%)	GA (%)	M_w (kDa)
LM 12	CP Kelco (Denmark)	35	90	130
Kelco 8A	CP Kelco (Denmark)	65	87	150
Apple pectin	Fluka Biochemical (Switzerland)	78	90	30 - 100
P9561	Sigma Aldrich (St Louis, USA)	90	≥75	~ 31

3.2. Polymer coupling

3.2.1.Pre-treatment

The preparation and the cleanliness of substrates were found to be of critical importance in these experiments. Prior to pectin physisorption or chemical treatment the glass cover slides were sonicated in dried toluene for 10 min, cleaned in freshly prepared Piranha solution (a mixture of 30% hydrogen peroxide and 70% sulfuric acid) for 1 h, rinsed in de-ionized water and toluene exhaustively, dried under vacuum and finally irradiated for 1 hour in a UV/O_3 surface decontamination chamber (PSD / UV Novascan Technology). The cleaned surfaces were stored in dried toluene for further treatment as detailed below.

3.2.2. Physisorption

Samples of physisorbed polymers were prepared by applying 20 µl of 0.1 or 0.01 w/w % pectin solution in deionized H_2O to cleaned discs, which were then dried at 11.3 % relatively humidity overnight. These were then extensively rinsed with deionized H_2O leaving only tightly bound molecules. These glass substrate discs were mounted on the piezo-electric ceramic of the AFM and a "liquid cell", consisting of a perspex chamber sealed with an O-ring, and containing the pre-mounted cantilever, was placed on top of the substrate. Several channels in the wall of the chamber allowed different solvents to be introduced above the sample in-situ, in which the stretching experiments were conducted. Measurements were made in de-ionized water at pH 3, or in 10 mM or 100 mM phosphate buffer at pH 7.0 as described in more detail below.

3.2.3. Chemisorption

In order to prepare the glass substrate for the ensuing attachment chemistry 3-aminopropyltriethoxysilane (APTES) films were prepared on the surface by incubating clean slides in a fresh APTES solution (1% APTES, 99% dried toluene) under sonication and in the presence of 1,1-diisopropylethylamine (DIEA), for 30 min at room temperature. Subsequently, the surfaces were ultrasonically washed with anhydrous toluene twice for 10 min to remove loosely physisorbed

APTES. The resultant silanized amino-terminated surfaces were subsequently rinsed with a 1mM anhydrous acetic acid solution and used in the following chemical coupling scheme.

The immobilization of pectins onto surfaces was carried out via a reductive amination (RA) reaction previously described for use with oligogalacturonides, (Guillaumie et al., 2002) and more recently for polymers (Fellah et al., 2011) using microbeads as substrates. Herein the reaction is carried out in order to attach pectin molecules to flat substrates, specifically at the reducing end of the chains. The freshly amino-terminated substrates prepared as above were washed with dimethylformamide (DMF). Then succinic anhydride (30 mg) and hydroxybenzotriazole (HOBt) (30 mg) were dissolved in DMF (5mL) with DIEA (70µL) and this solution was added to the substrates and subsequently ultrasonicated at room temperature for 1.5 hours. Thus carboxylic acid-terminated substrates are formed and were then washed thoroughly with DMF. Next, O-Benzotriazole-NNN'N'tetramethyl-uronium hexaflurophosphate (HBTU) (70 mg) and HOBt (120 mg) were dissolved in DMF (5 mL) with DIEA (180 µL) and hydrazine monohydrate (60 µL). This mixture was then added to the carboxylic acid-terminated surfaces and ultrasonicated. After 2 hours coupling at room temperature, solvents and unreacted compounds were removed and the surfaces washed thoroughly with DMF, leaving the surfaces hydrazide-terminated. Pectin was dissolved in DMF / AcOH (v/v=99:1) at 0.5 % w/w. Subsequently 5 mL of this solution was added to the hydrazide-terminated surfaces and, following addition of $NaBH_3CN$ (50 mg), the mixture was ultrasonicated at room temperature. After 24 hours, solvent and excess reagents were removed and the substrates were washed with DMF and dried overnight under reduced pressure. The entire procedure is shown schematically in Fig. 5.1. After preparation the sample was mounted in the AFM and the liquid cell described above was filled with the appropriate solvent just prior to carrying out the force-curve measurements.

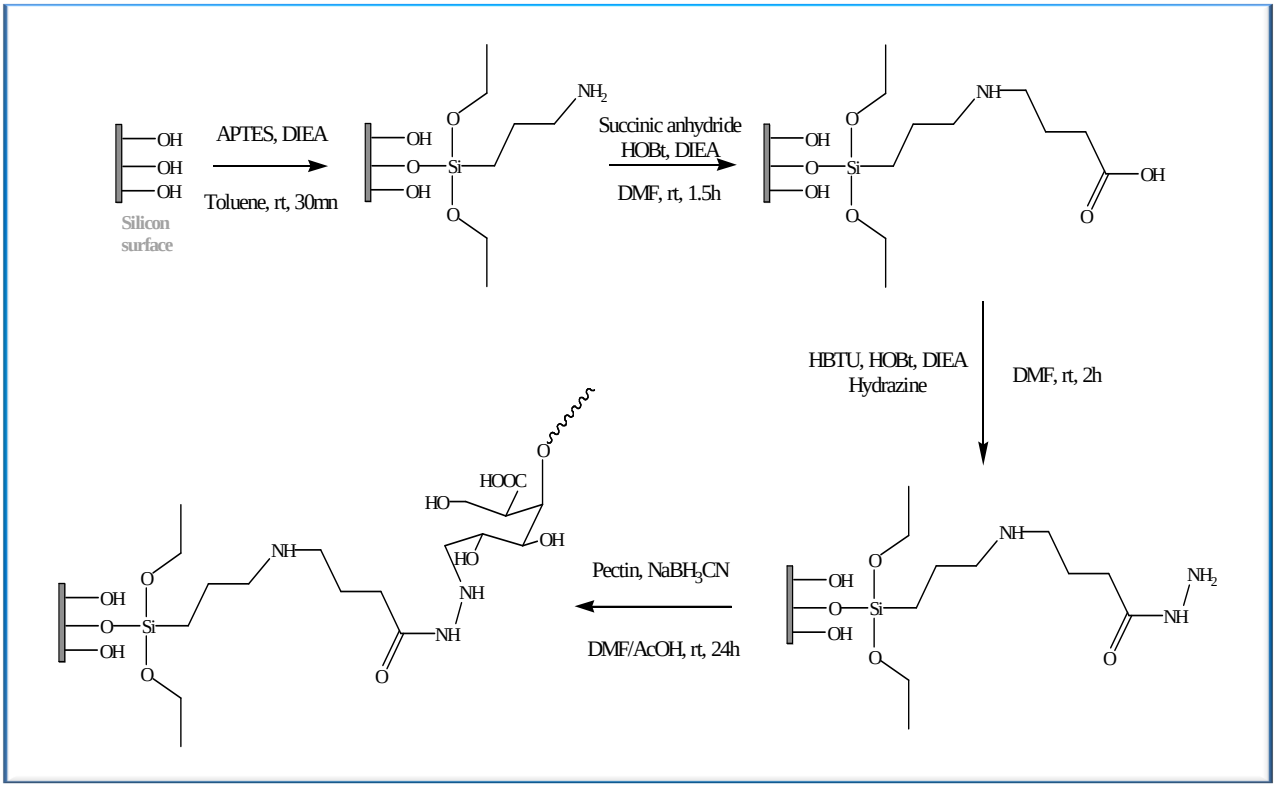

Fig. 5. 1. A schematic of the scheme developed herein for the covalent attachment of the terminal sugar residue of pectin to hydrazide-functionalized surfaces via reductive amination (RA).

3.3. AFM

Force-distance curves were recorded by pulling the molecules at 0.5-4 $\mu m.s^{-1}$ using the scanning probe microscope head from a Veeco Nanoscope E, with a home-built laptop-based controller driving the stepper-motor and the piezoelectric scanner, based on a feedback-signal generated from a Quadrant Photodiode (QPD) (Belmiloud, 2011). Briefly, I / O voltages were generated and recorded simultaneously, every microsecond. A voltage booster was constructed in order to increase the available voltage of the output signal, without supplying appreciable power, which preserved I / O synchronization and gave a control system with a spatial resolution estimated at 1 nm.

Prior to each experiment cantilevers were cleaned in a mixture of ammonia and hydrogen peroxide (v/v=2:1) for 1 h, rinsed thoroughly with de-ionized water and absolute ethanol, dried under a stream of nitrogen gas and finally exposed to ultraviolet light in a UV/O_3 decontamination chamber for 30 min. They were then calibrated using the well-documented thermal method (Sader

et al., 2005). This measurement was made in air so the first resonance of the cantilever was not damped and was easily isolated from the other modes. Gold-coated cantilevers were preferred and maximized the QPD sensitivity. Typical cantilever force constants were 50 pN nm^{-1}.

In order to facilitate the acquisition of a large set of experimental data a custom-designed software protocol was written in LabView that allowed on the-fly-filtering of the dataset, as reported elsewhere (Belmiloud, 2011). Briefly, the first step of analysis was to obtain the cantilever deflection in nm from the QPD signal, and then from this deflection, the force in nN was obtained using the spring constant of the cantilever as obtained from the thermal calibration method. To calibrate the deflection it was assumed that, in an absence of deformation of the sample, and neglecting a light elastic hysteresis of the piezoceramics, that when the piezo-mounted substrate contacts the cantilever and subsequently bends it before retraction, (the compliance region), that the deflection of the cantilever is equivalent to the distance travelled by the piezo. With the slope of the compliance region and the spring constant of the cantilever in hand, force–extension curves can be measured. The developed protocol detects the compliance region automatically and also monitors localized jumps in the force curve, assessing local standard deviations in a sliding window and comparing them statistically with the baseline and user-defined confidence intervals. Thus the user can be notified if likely single-molecule stretching events occur and data that correspond to possible events can be saved for post-run processing. Additionally the developed software reports the detachment force and the approximate value of the stretch length.

4. RESULTS AND DISCUSSION

In the present work coupling chemistry was developed to permit the direct covalent attachment of pectin to glass surfaces and was accomplished by first functionalizing the surface with amine groups. These were ultimately modified to hydrazide groups that were subsequently used to attach specifically the reducing end of pectin molecules via reductive amination. Starting with the introduction of an amine functionality onto the surface is the most widely used approach to functionalizing solid supports with biomolecules as amines have high nucleophilicity and a wide variety of amine-based coupling chemistries exist. In order to attach the prerequisite amine groups to the surface the use of APTES, widely used as a coupling agent in order to enhance the adhesion between polymeric matrices and inorganic solids (Crampton et al, 2005), was investigated. A general

consensus regarding APTES film formation on a silica substrate holds that silanization begins with the hydrolysis of ethoxy groups in APTES, a process catalyzed by water, leading to the formation of silanols, which then condense with surface silanols forming a monolayer of APTES via a lateral siloxane network in which amino groups are oriented away from the underlying silicon surface (Simon et al., 2002; Howarter et al., 2006). It is well known that the properties of the resultant APTES films are affected by preparation conditions such as the cleaning procedure, the choice of reaction solutions (APTES concentration, solvent) and the deposition time. It was important to ensure that APTES deposited as a smooth uniform thin film and did not experience aggregation at the surface or the deposition of multi-layers. Different combinations of the following parameters were therefore trialed during the work reported herein: cleaning procedures (HCl / H_2SO_4, MeOH / HCl, UV/O_3), solvents (toluene, chloroform, ethanol), APTES concentrations (1%, 5%), reaction times (30 min, 1 hr, 24 hr), and temperatures (20°C, 60°C).

In brief, it was found that the wet cleaning methods employed effectively cleaned the surfaces and produced a highly hydrophilic interface. DIEA promoted the hydrolysis of hydroxyl groups in order to allow covalent siloxane bonding. The APTES deposition reaction is potentially not limited to exclusively monolayer formation but can continue through polymerization at the surface (because of the favourable head-and-tail group interactions, APTES can form zwitterions in solution and at the film surface, resulting in multilayer formation as reaction is extended). However, using ultrasonic waves polymerization of the free ethoxy-groups of APTES near the surface during the reaction was found to be prevented and any physisorbed material, which may hinder the chemical reaction itself, was removed. The AcOH activates the silane to form a network on the surface, and results in any silane material not strongly bound to the surface being rinsed off. In summary, a surface amination procedure was developed that ultimately resulted in good single molecule force curves (H_2SO_4 / H_2O_2, toluene, 1%, 30 min and 20°C) with the other variations investigated leading, to various extents, to peeling the attached layer off the surfaces, that we attribute to the formation of heterogeneous multilayers.

With a successfully optimized functionalization of glass substrates in hand experiments focused on finding the physisorption conditions that yielded the best single molecule stretches (in terms of frequency, length and detachment force), so that subsequently results obtained thus could be compared with those obtained from substrates modified as described with the terminal sugar residue at one end of the chain chemically attached to the surface.

Fig. 5.2. shows typical single molecule force-extension curves recorded from pectin during the course of this work. The results agree well with previous work and in particular clearly show "clicks", the characteristic deviations in the force extension curve arising from force-induced conformational transitions in the sugar rings (Marszalek et al, 1999; Williams et al, 2007).

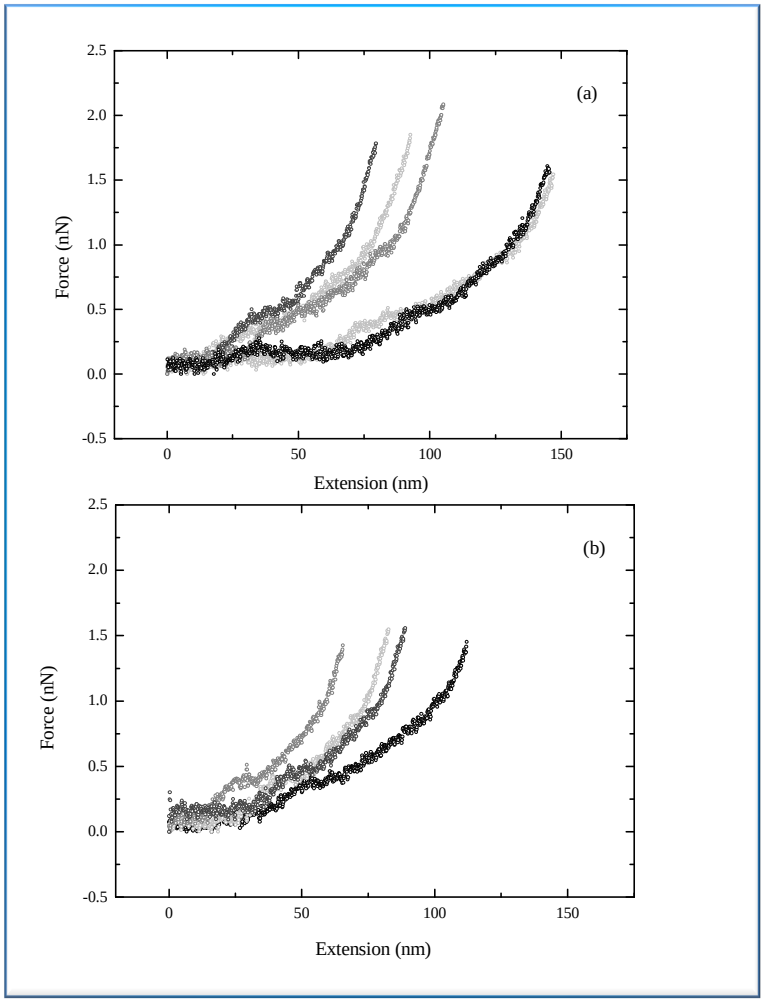

Fig. 5. 2. Single polysaccharide force-extension curves measured for apple pectin when either (a) covalently bound at the reducing end to a silica substrate, or (b) physisorbed (pH 7, 100 mM phosphate buffer).

Fig. 5.3-6. show the distribution of detachment lengths obtained from experiments carried out on pectins of ~35%, 55%, 75% and 90% DM respectively when physisorbed between glass and a gold-coated AFM tip under different solvent (de-ionized water (pH3); 10 and 100 mM phosphate buffer (pH7)) and preparation conditions (dried solution 0.01 or 0.1%).

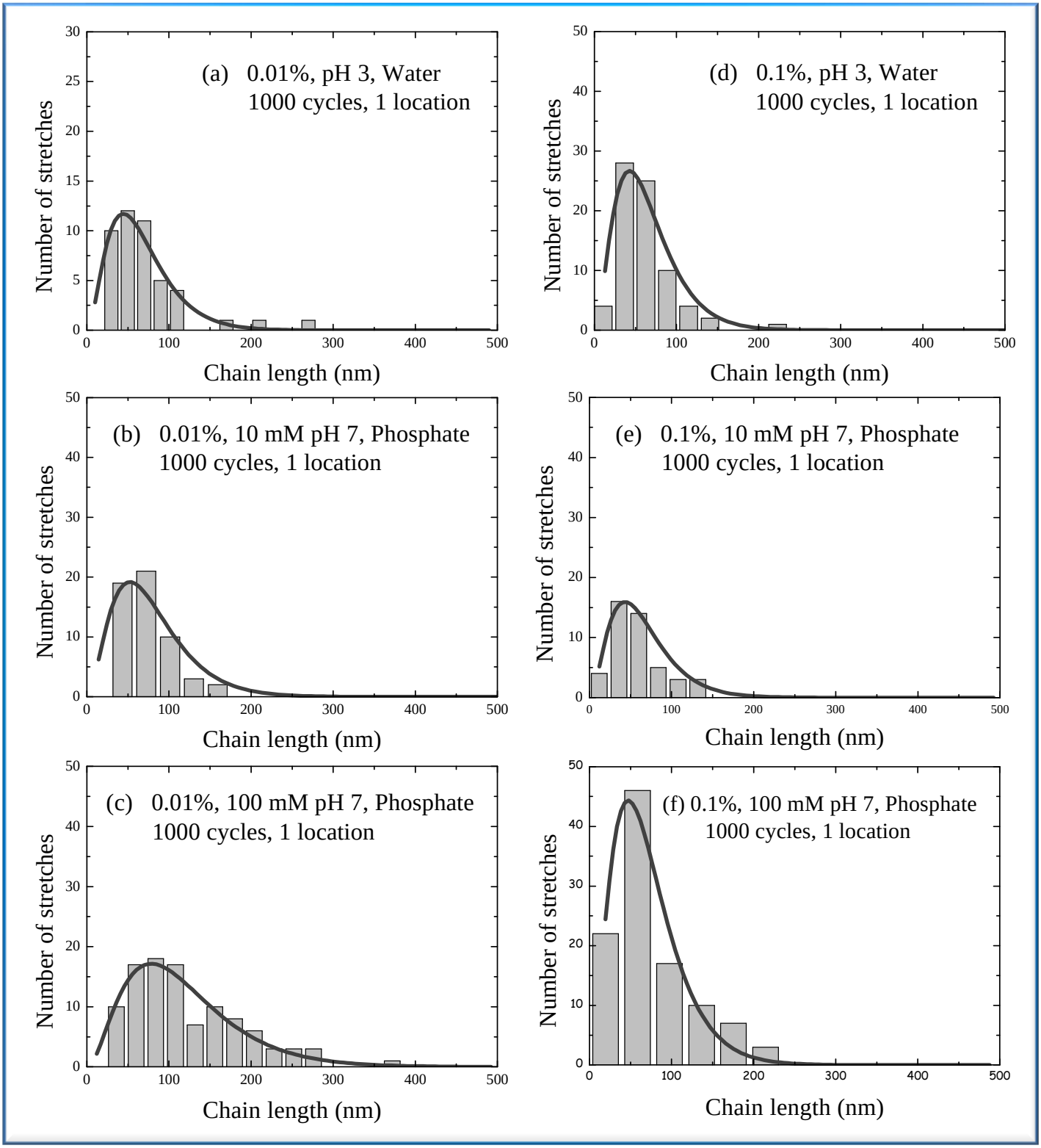

Fig. 5. 3. Distribution of single-molecule detachment lengths found for LM 12 pectin in different experimental conditions: (a) 0.01% polymer, pH 3 (b) 0.01% polymer, pH 7 10mM (c) 0.01% polymer, pH 7 100mM (d) 0.1% polymer, pH 3 (e) 0.1% polymer, pH 7 10mM (f) 0.1% polymer, pH 7 100mM. The solid lines are fits to the data described in the text.

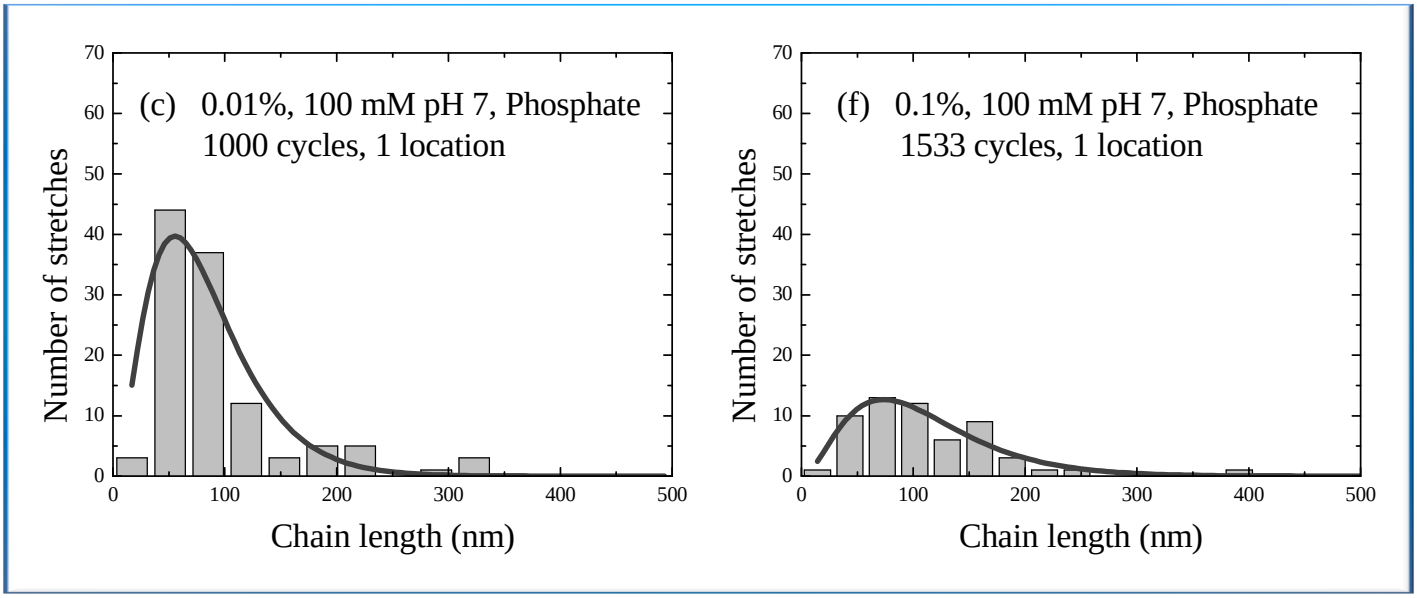

Fig. 5. 4. Distribution of single-molecule detachment lengths for Kelco8A pectin in different experimental conditions: (c) 0.01% polymer, pH 7 100mM (f) 0.1% polymer, pH 7 100mM. The solid lines are fits to the data described in the text.

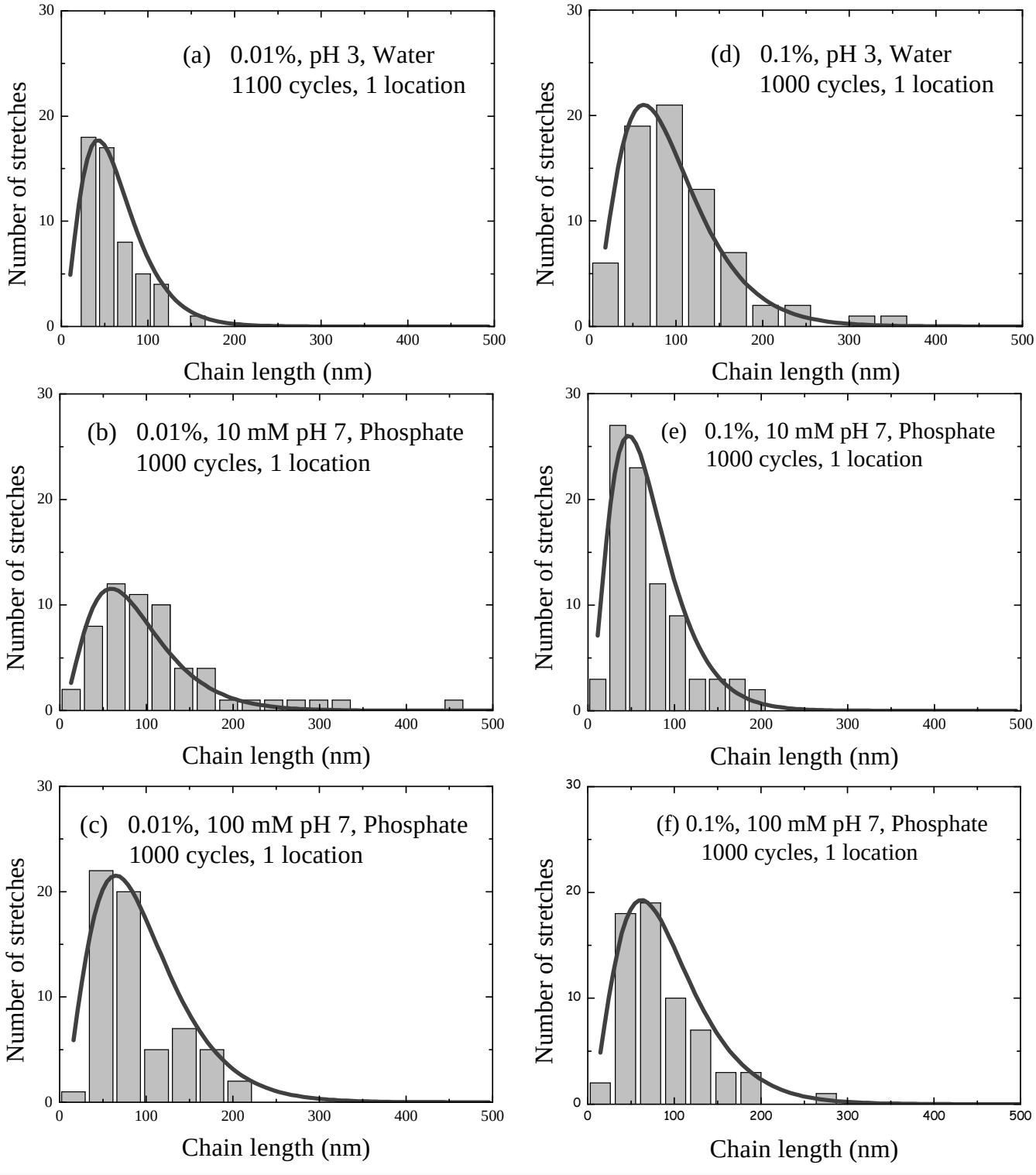

Fig. 5. 5. Distribution of single-molecule detachment lengths for Apple pectin in different experimental conditions: (a) 0.01% polymer, pH 3 (b) 0.01% polymer, pH 7 10mM (c) 0.01% polymer, pH 7 100mM (d) 0.1% polymer, pH 3 (e) 0.1% polymer, pH 7 10mM (f) 0.1% polymer, pH 7 100mM. The solid lines are fits to the data described in the text.

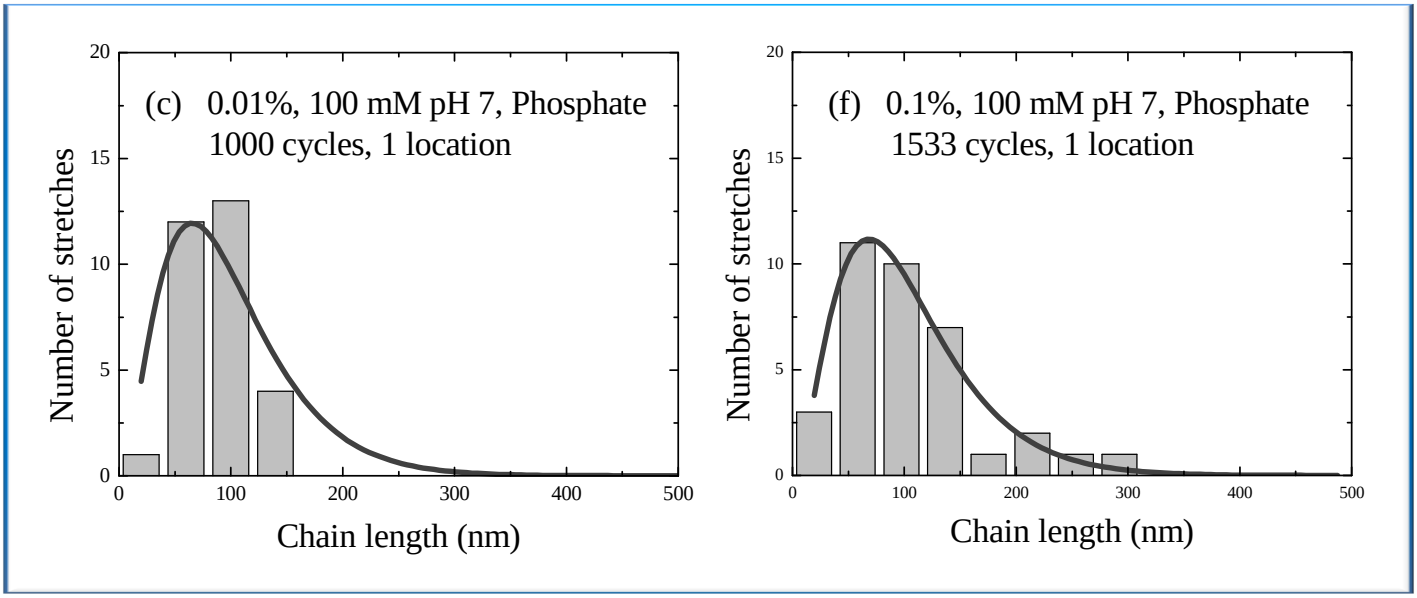

Fig. 5. 6. Distribution of single-molecule detachment lengths for P9561 pectin in different experimental conditions: (c) 0.01% polymer, pH 7 100mM (f) 0.1% polymer, pH 7 100mM. The solid lines are fits to the data described in the text.

Perhaps the most striking observation is the reasonably small effect that these variations in solvent conditions had on the results obtained in the range investigated. The forms of the histograms obtained are similar to those obtained from other studies on physisorbed polymers (Grandbois et al., 1999; Oritz & Hadziioannou, 1999; Mueller et al., 1999; Li et al., 1999; Zou et al., 2005; Nakajima et al., 2006; Valle et al., 2008; Kocun et al., 2011). Furthermore, similar relative insensitivities to salt and pH have also been reported (Roiter & Minko, 2007; Pirzer et al., 2009). While some of this previous work was focused on measuring surface desorption by continuously peeling molecules, it can be argued that the length distribution obtained in such a manner should have a similar functional form to that obtained in experiments of the type described here, with the terminal positions of the adsorbed or "picked-up" sections being determined randomly (Sonnenberg et al., 2008).

The resulting histograms have been fitted to a simple model of the form $A \times DP^2 \times e^{-B \times DP}$; with DP, the degree of polymerization. This successfully captures the hypotheses that a) attachment of the chain to the substrate or the cantilever tip in a manner such that a successful stretch follows is a random event and can occur at any residue with an equal probability; hence yielding an exponential

distribution of stretch lengths; and b) that the lengths should also be weighted by the possible proximity of a polymer attachment point to the AFM tip onto which it may physisorb; longer sections of chain have a larger chance to be picked up in each extend-retract cycle as they sample an area of the surface proportional to the square of their length.

It can be seen that given the limited dataset these fits provide a reasonable description of the experimental data. A similar model has previously been described (Sonnenberg et al, 2008), although it is noteworthy that modelling such experimental histograms has generally not been undertaken in much of the previously reported work. The modelling performed herein allows the estimation of the probability for the attachment of a single residue to the substrate from the value of the parameter B, and hence an estimate of the binding energy can be made. As expected from the appearance of the raw data remarkably little variation was found between the results from experiments employing different sets of conditions, with the values spanning 2.3 - 2.9 kT. This corresponds to a range of 56-63 meV, which indeed falls well within the expected range for physisorption phenomena, typically between 10 and 100 meV. While it should also be remembered that, as shown in Table 2, a large number of stretch attempts did not yield a single molecule stretch, the relevant fit parameters, and thus estimates of the probabilities and binding energies that result from the analysis of the data obtained when stretches are successfully measured, are given in Table 2.

Table 5. 2. Single molecule stretch experiments: polymer; concentration; solvent conditions; attachment (physisorbed (P), covalently end-tethered (C)); event frequency; probability of residue adhesion, calculated as described in the text, and attachment energy.

Polymer	Polymer Conc (%)	Conditions of experiment	Attachment Method	Stretch frequency (%)	Attachment Probability	Binding Energy (k_BT)
LM 12	0.01	pH 3 (a)	P	5	0.093±0.004	2.27±0.05
LM 12	0.1	pH 3 (d)	P	8	0.095±0.004	2.25±0.05
LM 12	0.01	pH 7, 10 mM (b)	P	5	0.079±0.005	2.45±0.06
LM 12	0.1	pH 7, 10 mM (e)	P	5	0.095±0.002	2.25±0.03
LM 12	0.01	pH 7, 100 mM (c)	P	10	0.053±0.004	2.88±0.05
LM 12	0.1	pH 7, 100 mM (f)	P	10	0.087±0.003	2.34±0.04
LM 12	0.1	pH 7, 100 mM (g)	C	10	0.055±0.003	2.84±0.04
Kelco8A	0.01	pH 7, 100 mM (c)	P	11	0.075±0.005	2.50±0.06
Kelco8A	0.1	pH 7, 100 mM (f)	P	4	0.057±0.002	2.80±0.03
Kelco8A	0.1	pH 7, 100 mM (g)	C	10	0.055±0.004	2.84±0.05
Apple	0.01	pH 3 (a)	P	5	0.097±0.006	2.22±0.08
Apple	0.1	pH 3 (d)	P	7	0.067±0.004	2.62±0.05
Apple	0.01	pH 7, 10 mM (b)	P	6	0.069±0.005	2.59±0.06
Apple	0.1	pH 7, 10 mM (e)	P	8	0.089±0.005	2.32±0.06
Apple	0.01	pH 7, 100 mM (c)	P	6	0.065±0.004	2.66±0.05
Apple	0.1	pH 7, 100 mM (f)	P	6	0.067±0.003	2.62±0.04
Apple	0.1	pH 7, 100 mM (g)	C	10	0.053±0.006	2.88±0.08
9561	0.01	pH 7, 100 mM (c)	P	3	0.063±0.006	2.69±0.08
9561	0.1	pH 7, 100 mM (f)	P	4	0.061±0.002	2.73±0.03
9561	0.1	pH 7, 100 mM (g)	C	15	0.055±0.006	2.84±0.08

While the effects of the solvent and preparation conditions appear minor the trends observed are nonetheless consistent with expectations. Firstly, the effect of the concentration of polymer used to create the dried layer appears minimal. However, both the polymer concentrations used are in excess of that required to provide a monolayer, (surface coverage would be equivalent to a chain every few nm), and as such previously reported work suggesting that washing as described in the experimental section removes all but a strongly-bound monolayer (Marszalek et al., 1999; 2001) would seem pertinent. This suggests that by the time the substrates are introduced into the liquid cell for experiments the coverage is likely to be the similar in both cases. Secondly, for the most charged (lowest DM) polymers the most favourable conditions for yielding stretches appear to be pH 7, 100 mM phosphate where, while both surface and polymer are negatively charged, the

relatively high ionic strength facilitates attachment. Lastly, DM appears to have only a very minimal effect under these conditions, consistent with the screening of charge effects, but also suggesting that the presence of methylesterified residues does not play a dominant role.

Fig. 5.7-10 show: a) the distribution of detachment lengths obtained from experiments carried out on pectins of ~35%, 55%, 75% and 90% DM respectively when physisorbed between glass and a gold-coated AFM tip under the optimum solvent conditions investigated, (100 mM phosphate buffer (pH7)); b) the distribution of detachment lengths obtained from experiments carried out on the same pectins in the same solvent conditions as in (a), but where the reducing end of the pectin molecule is covalently attached to the glass substrate; and c) the distribution of forces achieved at detachment for the same pectins under both physisorbed conditions and when possessing the described chemical coupling. With the goal in mind of facilitating further study on the force-induced conformational transitions of polysaccharides the measured maximum forces applied before detachment are simply considered in three bins corresponding to forces less than 300 pN; between 300 and 800 pN; or greater than 800 pN, thus corresponding to stretches that would allow the investigation of 0, 1 or 2 of the manifest conformational transitions in pectin respectively.

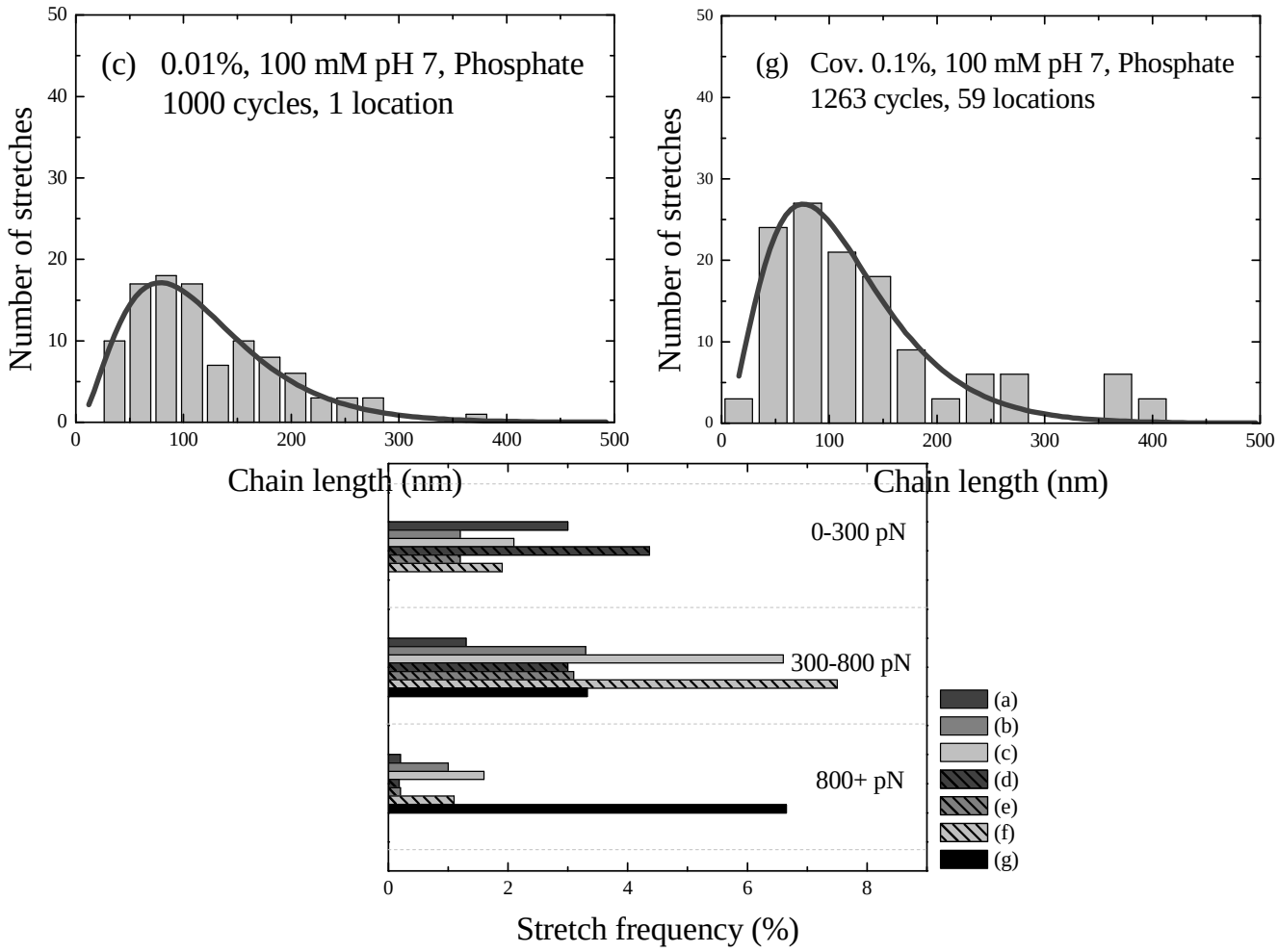

Fig. 5. 7. Distribution of single-molecule detachment lengths obtained from experiments carried out on LM 12 pectin when (c) physisorbed and (f) covalently attached under the same optimum solvent conditions investigated (100 mM phosphate buffer (pH7)) and distribution of forces achieved at detachment for the same pectin under both physisorbed and covalent attachment conditions. The labelling reflecting the physisorbed conditions is constant throughout (i.e. see Fig. 5.3.).

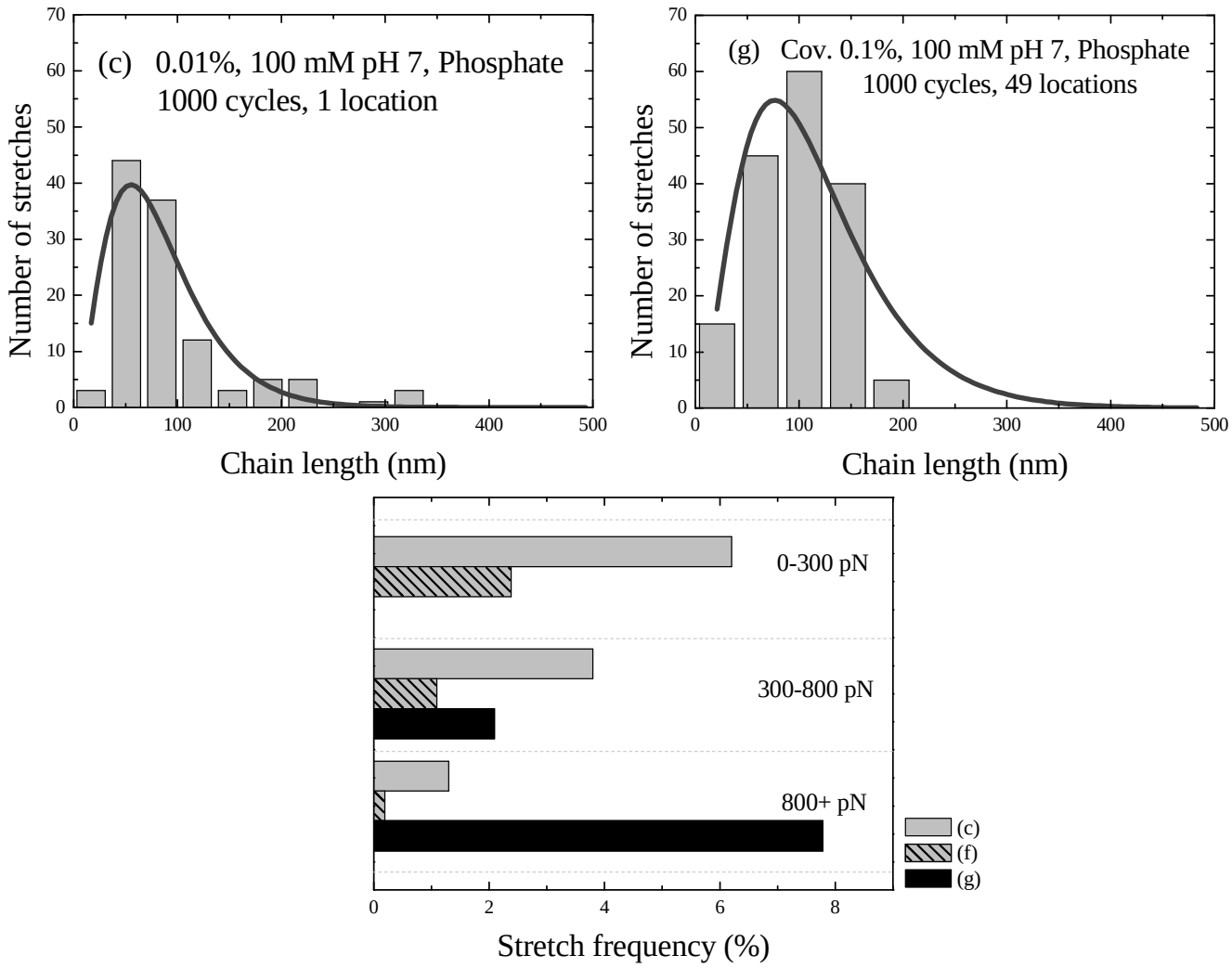

Fig. 5. 8. Distribution of single-molecule detachment lengths obtained from experiments carried out on Kelco8A pectin when (c) physisorbed and (f) covalently attached under the same optimum solvent conditions investigated (100 mM phosphate buffer (pH7)) and distribution of forces achieved at detachment for the same pectin under both physisorbed and covalent attachment conditions. The labelling reflecting the physisorbed conditions is constant throughout (i.e. see Fig. 5.3.).

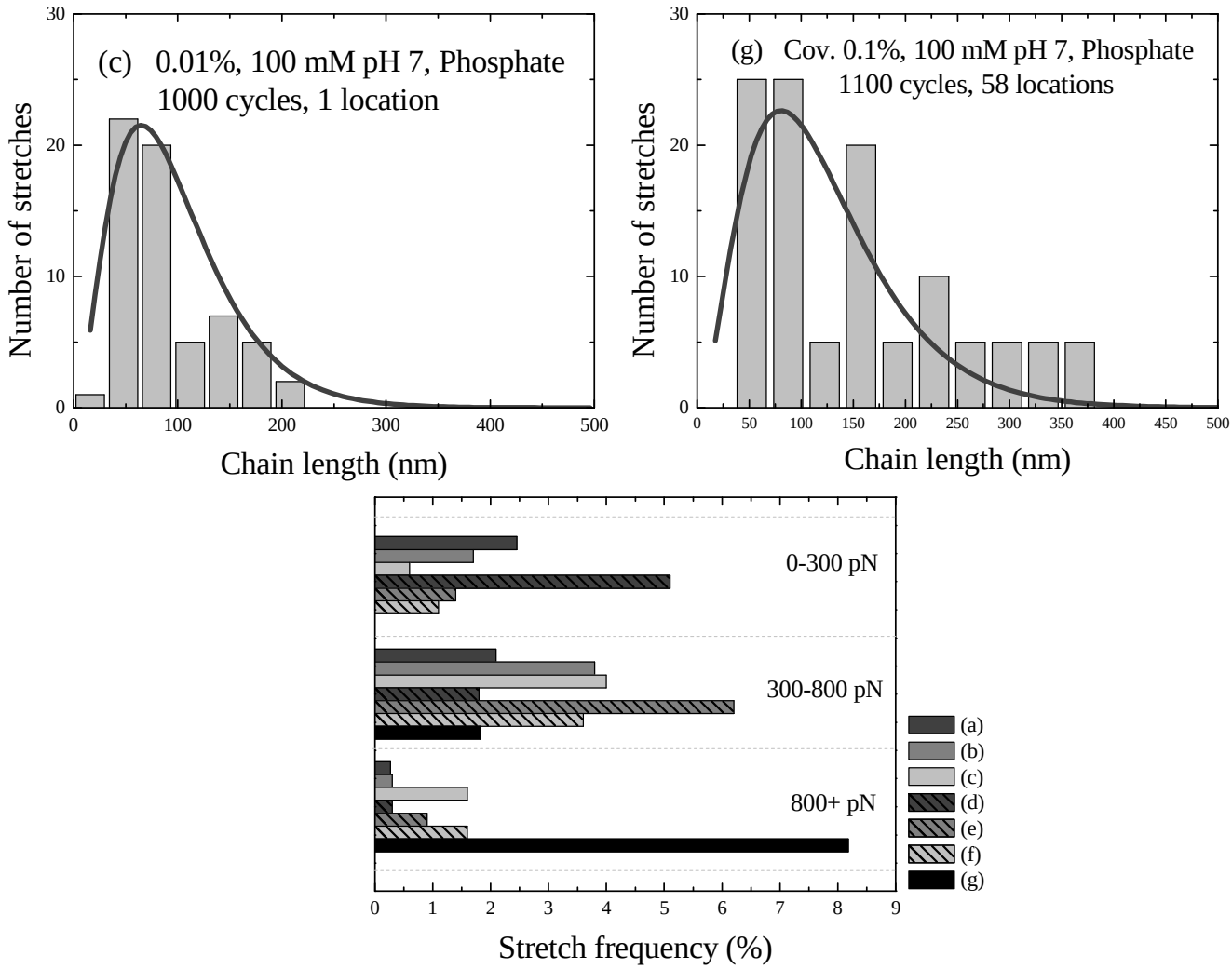

Fig. 5. 9. Distribution of single-molecule detachment lengths obtained from experiments carried out on Apple pectin when (c) physisorbed and (f) covalently attached under the same optimum solvent conditions investigated (100 mM phosphate buffer (pH7)) and distribution of forces achieved at detachment for the same pectin under both physisorbed and covalent attachment conditions. The labelling reflecting the physisorbed conditions is constant throughout (i.e. see Fig. 5.3.).

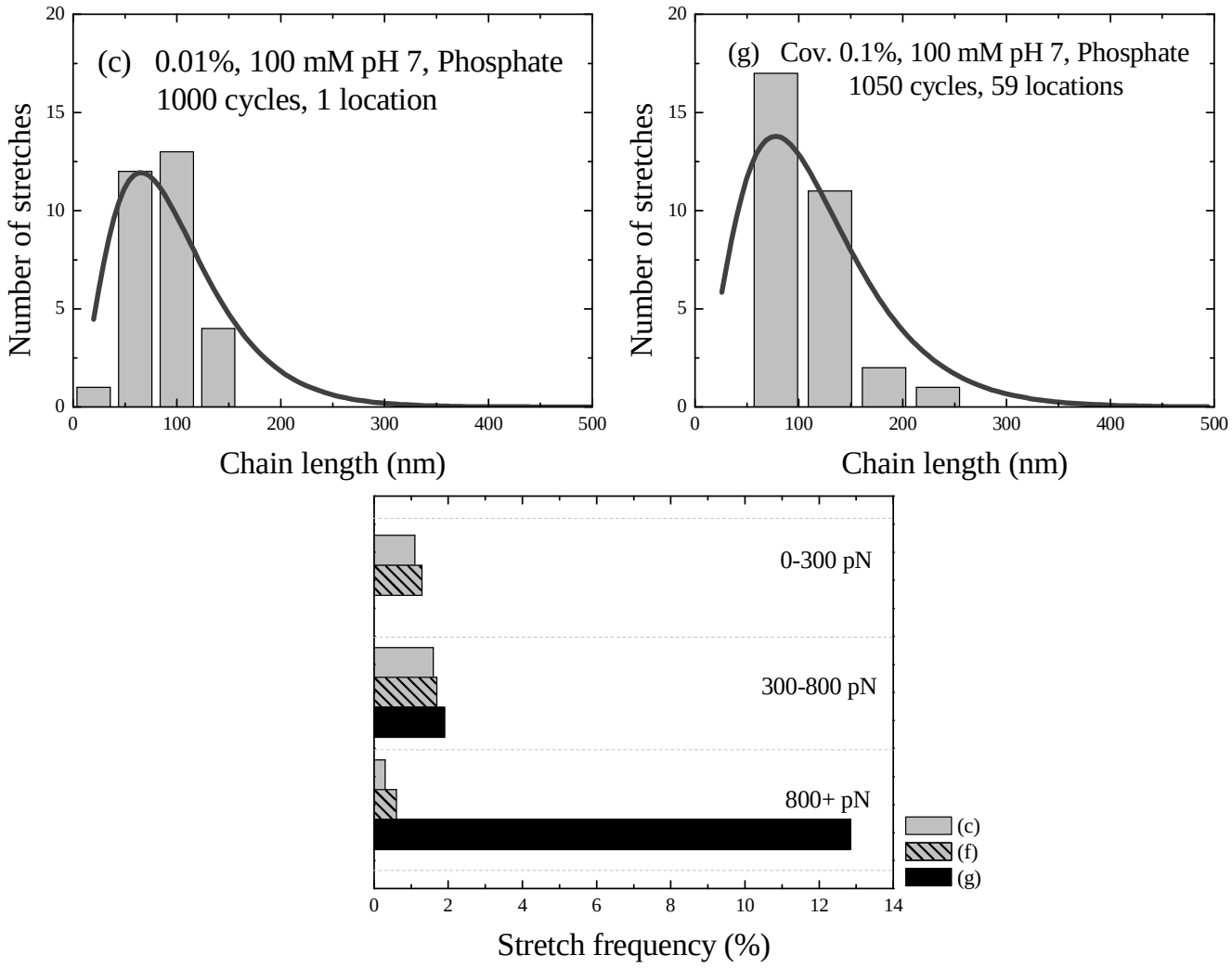

Fig. 5. 10. Distribution of single-molecule detachment lengths obtained from experiments carried out on P9561 pectin when (c) physisorbed and (f) covalently attached under the same optimum solvent conditions investigated (100 mM phosphate buffer (pH7)) and distribution of forces achieved at detachment for the same pectin under both physisorbed and covalent attachment conditions. The labelling reflecting the physisorbed conditions is constant throughout (i.e. see Fig. 5.3.).

The data convincingly reveal that the forces obtained before detachment are substantially larger for the chemically end-tethered chains. There is also an indication, particularly in the data shown in Fig. 5.7., 5.9. and 5.10., that there is a slight increase in the average lengths of the sections picked up when one end is chemically attached, as might be expected. It should however also be noted that the fits to the data from the chemically end-tethered experiments are, in general, of poorer quality compared to the physisorbed experiments owing largely to the increasingly good statistics required to reliably sample the tail of the predicted exponential distribution as the lengths increase. It is also important to state that while the data from the physisorbed experiments was acquired from only one location per sample, the chemically attached polymers required some fifty different locations to be probed to achieve the same number of successful stretch events. It appears that tethering the end of the chain to the surface prevents surface diffusion that might well be expected in the physisorbed case (Gunning at al., 2004) and therefore limits the number of chains that can be picked up during repeated extend-retract cycles of the AFM tip in an initially barren region of the substrate.

It is also to be noted that the major obstacle to single-molecule force spectroscopy experiment on chemically modified surfaces is the strong attraction of the tip to the surface after chemical coupling. While a good "spot" gives a large number of force-curves for physisorbed substrates, for a covalent surface this number is only limited to about 20, due to the drifting of the QPD signal. Fig. 5.11. shows a mixed population of single and aggregated polymers that are distinguishable by height measurements. The aggregates are present even at low concentrations where few single polymers can be seen, suggesting that they are not simply superposition's or entanglements of polymers but multi-polymer complexes held together by intermolecular interactions.

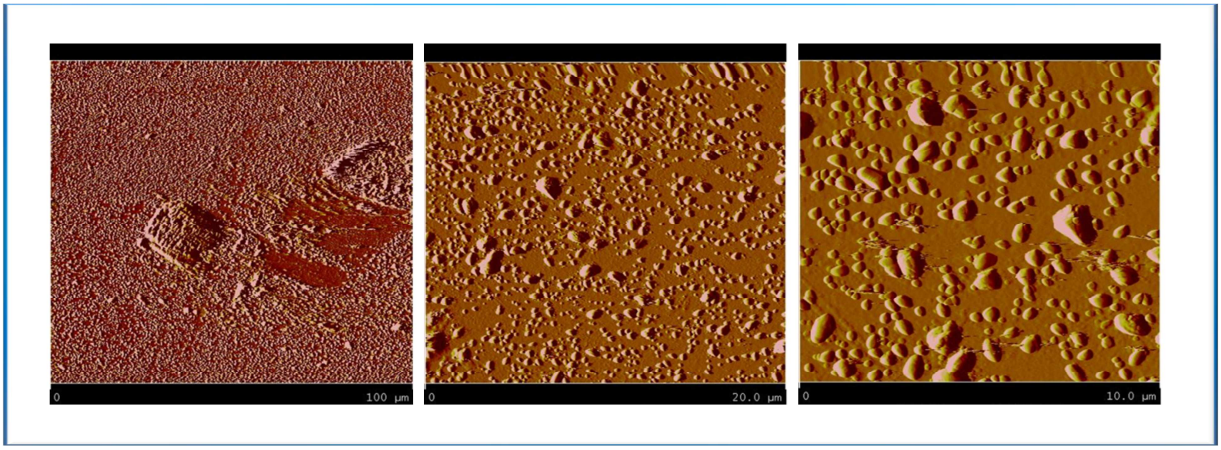

Fig. 5. 11. AFM images of a pectin chemically functionalized surface (scan sizes 100x100 µm, 20x20 µm and 10x10 µm).

The surface coverage after chemical coupling is heterogeneous, which may be an explanation for the difference in location probability and the difficulty in picking up a chain and achieving good stretches. This heterogeneity truly depends on the amination experimental conditions as stated previously.

Finally the RA method described was trialed using 200 nm diameter silica beads (the initial step again involving amination, followed by the identical coupling chemistry described for the aminated polystyrene beads). DLS was used to estimate the size of the beads, (i) pre- and (ii) post chemical treatment, and (iii) post washing steps with urea, found to remove purely physisorbed material. The experimental results indicated sizes of (i) (230±30) nm; (iii) (350±30) nm and (iii) (370±30) nm; indicating that indeed post-RA a layer of some 60 nm was introduced onto the bead that could not be removed by washing, suggesting that the RA method was also successful with silica substrates as the starting material.

5. CONCLUSION

In summary, if maximising the frequency of successful polysaccharide stretch events in a particular spatial location of the substrate is paramount then chemically attaching both ends of the

polysaccharide is still a necessary goal. Nevertheless, this work represents a substantial step in that direction. The approach taken here by chemically tethering one-end of the chain does appear to increase the average stretched length, but also dramatically improves the fraction of successful stretches that yield high forces, thus offering a method to facilitate the study of conformational transitions requiring large strains.

6. REFERENCES

Bustamante, C.; Smith, S.B.; Liphardt, J. and Smith, D. (2000) Single-molecule studies of DNA mechanics. *Current Opinion in Structural Biology*, **10**, 279-285.

Belmiloud, N.; Fellah, A.; Haverkamp, R.G. and Williams, M.A.K. (2011) Facilitating nanomechanical measurements on physisorbed biopolymers with automated on-the-fly monitoring of single-molecule force curves. *Advanced Science Letters*, **4**, 1-4.

Crampton, N.; Bonass, W.A.; Kirkham, J. and Thomson, N.H. (2005) Formation of amino-silane-functionalized mica for atomic force microscopy imaging of DNA. *Langmuir*, **21**, 7884-7891.

Cui, S.; Lui, C.; Zhang, W.; Zhang, X. and Wu, C. (2003) Desorption force per polystyrene segment in water. *Macromolecules*, **36** (11), 3779-3782.

Fellah, A.; Anjukandi, P.; Hemar, Y.; Otter, D and Williams, M.A.K. (2011) Towards polysaccharide handles for single molecule experiments: Spectroscopic evidence for the selective covalent coupling of terminal sugar residues to desired substrates. *Carbohydrate Polymers*, **86** (1), 105-111.

Friedsam, C.; Gaub, H.E. and Netz, R.R. (2006) Probing surfaces with single-polymer atomic force microscope experiments. *Biointerphases*, **1** (1), 1-121.

Francius, G.; Alsteens, D.; Dupres, V.; Lebeer, S.; DeKeersmaecker, S.; Vanderleyden, J.; Gruber, H.J and Dufrene, Y.F. (2009) Stretching polysaccharides on live cells using single molecule force spectroscopy. *Nature Protocols*, **4** (6), 939-946.

Geisler, M.; Pirzer, T.; Ackerschott, C.; Lud, S.; Garrido, J.; Scheibel, T. and Hugel, T. (2008) Hydrophobic and Hofmeister effects on the adhesion of spider silk proteins onto solid surfaces: an AFM-based single molecule study. *Langmuir*, **24**, 1350-1355.

Geisler, M.; Horinek, D and Hugel, T. (2009) Single molecule adhesion mechanics on rough surfaces. *Macromolecules*, **42**, 9338-9343.

Grandbois, M.; Beyer, M.; Reif, M.; Clausen-Schaumann, H. and Gaub, H.E. (1999) How strong is a covalent bond? *Science*, **283**, 1727-1730.

Guillaumie, F.; Thomas, O.R.T. and Jensen, K.J. (2002) Immobilization of pectin fragments on solid supports: novel coupling by thiazolidine formation. *Bioconjugate Chemistry*, **13**, 285-294.

Gunning, A.P.; Kirby, A.R. and Mackie, A.R. (2004) Watching molecular processes with the atmic force microscope: dynamics of polymer adsorption and desorption at the single molecule level. *Journal of Microscopy*, **216**, 52-56.

Haverkamp, R.G.; Williams, M.A.K. and Scott, J.E. (2005) Stretching single molecules of connective tissue glycans to characterize their shape maintaining elasticity. *Biomacromolecules*, **6**, 1816.

Haverkamp, R.G.; Marshall, A.T. and Williams, M.A.K. (2007) A model for stretching elastic biopolymers which exhibit conformational transformations. *Physical Review E*, **75**, 021907.

Howarter, J.A. and Youngblood, J.P. (2006) Optimization of silica silanization by 3-aminopropyltriethoxysilane. *Langmuir*, **22**, 11142-11147.

Hugel, T.; Grosholz, M.; Clausen-Schaumann, H.; Pfau, A.; Gaub, H.E. and Seitz, M. (2001) Elasticity of single polyelectrolyte chains and their desorption from solid supports studied by AFM based single molecule force spectroscopy. *Macromolecules*, **34** (4), 1039-1047.

Kellermayer, M.S.Z.; Smith, S.B.; Granzier, H.L. and Bustamante. C. (1997) Folding-unfording transitions in single titin molecules characterized with laser tweezers. *Science*, **276**, 1112-1116.

Khner, F.; Erdmann, M. and Gaub., H. (2006) Scaling exponent and Kuhn length of pinned polymers by single molecule force spectroscopy. *Physical Review Letters*, **97**, 218301.

Kierfeld, J. (2006) Force-induced desorption and unzipping of semi-flexible polymers. *Physical Review Letters*, **97** (5), 058302-1.

Kocun, M.; Grandbois, M. and Cuccia, L.A. (2011) Single molecule atomic force microscopy and force spectroscopy of chitosan. *Colloids and Surfaces B: Biointerfaces*, **82**, 470-476.

Li, H.; Bingbing, L.; Zhang, X.; Gao, C.; Shen, J. and Zou, G. (1999) Single-molecule force spectroscopy on poly(acrylic acid) by AFM. *Langmuir*, **15**, 2120-2124.

Marszalek, P.E.; Oberhauser, A.F.; Pang, Y.P. and Fernandez, J.M. (1998) Polysaccharide elasticity governed by chair-boat transitions of the glucopyranose ring. *Nature*, **396**, 661-664.

Marszalek, P.E.; Pang, Y.P.; Li, H.; Oberhauser, F.A.; Yazal, J.E. and Fernandez, J.M. (1999) Atomic levers control pyranose ring conformations. *Proceedings of National Academy of Sciences*, **96**, 7894-7898.

Marszalek, P.E.; Li, H. and Fernandez, J.M. (2001) Fingerprinting polysaccharides with single molecule atomic force microscopy. *Nature Biotechnology*, **19**, 258

Marszalek, P.E.; Li, H.; Oberhauser, F.A. and Fernandez, J.M. (2002) Chair-boat transitions in single polysaccharide molecules observed with force-ramp AFM. Proceedings of National Academy of *Sciences*, **99**, 4278-4283.

Maurice, R.G. and Matthai, C.C. (1999) Force-extension curves for a single polymer chain under varying solvent conditions. *Physical Review E*, **60**, 3165-3169.

Mueller, H.; Butt, H-J. and Bamberg, E. (1999) Force measurements on myelin basic protein adsorbed to mica and lipid bilayer surfaces done with the atomic force microscope. *Biophys. J.*, **76**, 1072-1079.

Nakajima, K.; Watabe, H. and Nishi, T. (2006) Single polymer chain rubber elasticity investigated by atomic force microscopy. *Polymer*, **47,** 2505-2510.

Oritz, C. and Hadziioannou, G. (1999) Entropic elasticity of single polymer chains of poly(methacrylic acid) measured by atmoc force microscopy. *Macromolecules*, **32**, 780-787.

Pirzer, T.; Geisler, M.; Scheibel, T. and Hugel, T. (2009) Single molecule force measurements delineate salt, pH and surface effects on biopolymer adhesion. *Phys. Biol.*, **6**, 1-8.

Ralet, M.C. and Thibault, J.F. (2002) Interchain heterogeneity of enzymatically deesterified lime pectins. *Biomacromolecules*, **3**, 917-925.

Ray, C.; Brown, J.R. and Akhremitchev, B.B. (2006) Single-molecule force spectroscopy measurements of "hydrophobic bond" between tethered hexadecane molecules. *J. Phys. Chem. B*, **110**, 17578-17583.

Ray, C.; Brown, J.R. and Akhremitchev, B.B. (2007) Correction of systematic errors in single-molecule force spectroscopy with polymeric tethers by atomic force microscopy. *J. Phys. Chem. B*, **111**, 1963-1974.

Roiter, Y. and Minko, S. (2004) Single molecule force spectroscopy on polyelectrolytes: effect of spacer on adhesion force and linear charge density on rigidity. *Macromolecules*, **37**, 946-953.

Roiter, Y. and Minko, S. (2007) Adsorption of polyelectrolyte versus surface charge: in-situ single molecule atomic force microscopy experiments on similarly, oppositely, and heterogeneously charged surfaces. *J. Phys. Chem. B*, **111**, 8597-8604.

Sader, J.E.; Pacifico, J.; Green, C.P. and Mulvaney, P. (2005) General scaling law for stiffness measurement of small bodies with applications to the atomic force microscope. *Journal of Applied Physics*, **97**, 124903.

Seitz, M.; Friedsam, C.; Jostl, W.; Hugel, and Gaub, H.E. (2003) Probing solid surfaces with single polymers. *ChemPhysChem*, **4**, 986-990.

Simon, A.; Cohen-Bouhacina, T.; Porte, M.C.; Aime, J.P. and Baquey, C. (2002) Study of two grafting methods for obtaining a 3-aminopropyltriethoxysilane monolayer on silica surface. *Journal of Colloid and Interface Science*, **251**, 278-283.

Sletmoen, M.; Skjak-Braek, G. and Stokke, B.T. (2004) Single molecular pair unbinding studies of mannuronan C-5 epimerase algE4 and its polymer substrate. *Biomacromolecules*, **5**, 1288-1295.

Sonnenberg, L.; Parvole, J.; Kuhner, F.; Billon, L. and Gaub, H.E. (2007) Choose sides: Differential Polymer Adhesion. *Langmuir*, **23**, 6660-6666.

Sonnenberg, L.; Billon, L. and Gaub, H.E. (2008) Competitive adhesion reduces effective bridging length of polymers. *Macromolecules*, **41**, 3688-3691.

Staple, D.B.; Geisler, M.; Hugel, T.; Kreplak, L. and Kreuzer, H-J. (2011) Forced desorption of polymers from interfaces. *New Journal of Physics*, **13**, 013025.

Valle, F.; Zuccheri, G.; Bergia, A.; Ayres, L.; Rowan, A.E.; Nolte, R.J.M. and Samori, B. (2008) A polymeric molecular handle for multiple AFM-based single-molecule force measurements. *Angewandte Chemie*, **47**, 2431-2434.

Williams, M.A.K.; Marshall, A.T.; Anjukandi, P. and Haverkamp, R.G. (2007) Investigation of the effects of fine structure on the nanomechanical properties of pectin. *Physical Review E*, **76**, 021927.

Zhang, Q.; Lee, G. and Marszalek, P.E. (2005) Atomic cranks and levers control sugar ring conformations. *Journal of Physics : Condensed Matter*, **17**, S1427.

Zhang, L.; Wang, C.; Cui, S.; Wang, Z. and Zhang, X. (2003) Single-molecule force spectroscopy on curdlan: unwinding helical structures and random coils. *Nano-letters*, **3** (8), 1119-1124.

Zou, S.; Schonherr, H. and Vansco, G.J. (2005) Stretching and rupturing individual supramolecular polymer chains by AFM. *Angewandte Chemie International Edition*, **44** (6), 956-959.

CHAPTER 6

CONCLUSION AND FURTHER WORK

1. SUMMARY AND CONCLUSION

Prior to the study of its covalent attachment, the structure of pectin was investigated using an IR spectroscopy technique. This ATR technique used belongs to a group of instrumental methods for the determination of the degree of methylesterification of pectins needing minimal processing and has the main advantage of simplicity and accuracy when compared to other reported IR methods; although the expected uncertainty in the measured DM value still stands relatively high. In order to get the best results samples should be treated (acidification and drying). Results showed that the use of the ratio of the intensities of the ester vibrations and those occurring in the backbone fingerprint region allowed the prediction of the DM, while eliminating the interferences from other cell wall components such as water and proteins. In addition, theoretical calculations were shown to reproduce the main features of the experimental spectra, with a clear evolution towards the polymer result as the degree of polymerization of the saccharide molecule in the calculation was increased from monomer to dimer, and ultimately trimer.

Subsequently, vibrational spectroscopic investigations coupled with predictions from quantum mechanical calculations were demonstrated as a well-suited method for monitoring the progress of particular schemes designed for the attachment of biopolymers to beads. A good general agreement between the experimental and simulated spectra pre-, as well as post-, coupling confirmed the reliability of this technique. In particular, this work provided evidence that, by following the protocols described, not only could the pectin chain be attached to microbeads, but that the coupling was via the formation of a specific recognizable newly formed bond, with pectin immobilized at its reducing end.

In order to study the effect of covalent attachment on single-molecule stretching with Atomic Force Microscopy, the coupling method was also applied to glass surfaces. Pectin was successfully immobilized onto the surface via silanization, hydrazidation and pectin attachment through its reducing end. A number of relevant parameters of the silanization reaction were systematically studied. Among them, deposition time and silane agent concentration were shown to be crucial and

have to be controlled during the reaction process. When using the optimal experimental conditions described, one can obtain high-quality mono-layers.

The pectin covalent linkage was adapted to these mono-layers in order to generate substrates for use in single molecule stretching experiments.
Specifically the length and detachment force of recorded stretches was compared when either 1) the polymers were physisorbed between cantilever and the surface of the piezo-electric scanner or 2) specifically one end of the polymer molecule was chemically attached to the piezo surface. It has been shown that in the case of the chemical attachment, while more searching of the surface was required before stretching events were revealed, owing to the limited translational diffusion of the end-tethered species, the mean length of the polymer extended and in particular the force applied before detachment were significantly increased.

2. FURTHER WORK

This study demonstrated the utility of AFM for investigating the conformational changes of pectins, which may open a new field for studying their stereochemistry and provide new insight into the nanomechanical properties of biologically important polysaccharides and processes.
If maximising the frequency of successful polysaccharide stretch events in a particular spatial location of the substrate is paramount then chemically attaching both ends of the polysaccharide is still a necessary goal. Successful experiments require that the binding of the biomolecules to both probe and substrate is much stronger that the intermolecular force being studied.
It is hoped that the availability of the technique described here will encourage further work on specific coupling of the free end to cantilevers, and will ultimately facilitate more sophisticated biophysical experiments to be carried out on polysaccharides and their interactions by maximizing the length of the chain that might be manipulated.

Preliminary attemps were made to hold a stretched pectin chain under tension(Fig. 6.1.), but the physisorbed end of the chain detached in a matter of seconds.

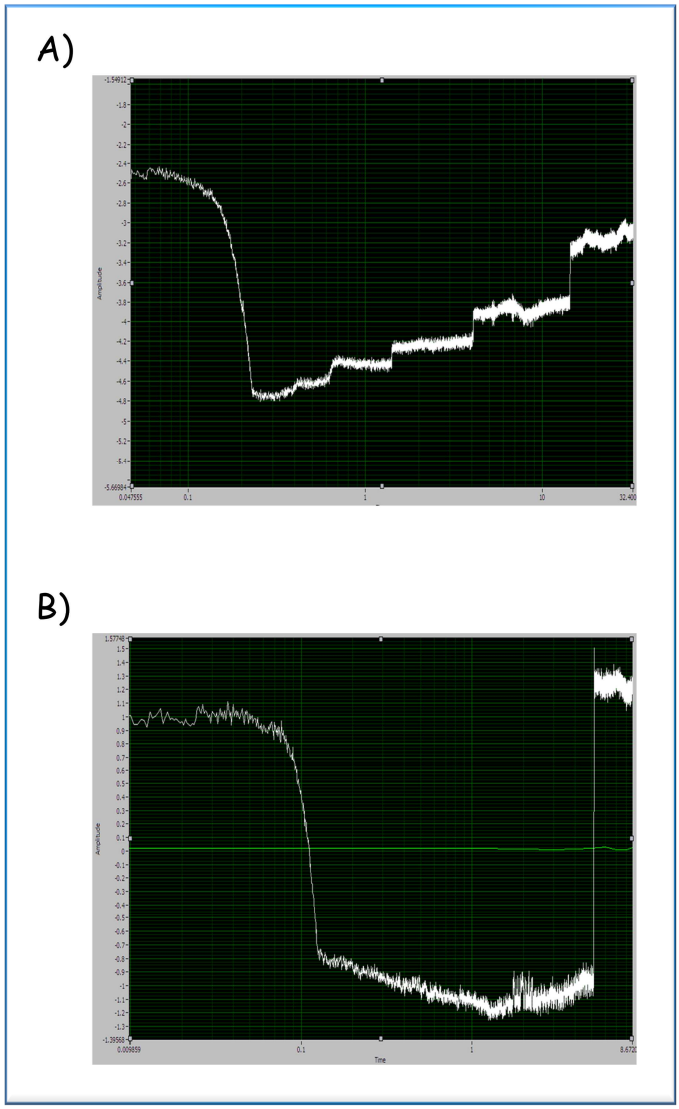

Fig. 6. 1. Amplitude vs. Time spectrum. A) multiple chains (or single chain anchored at several points) are held stretched for about 10 seconds. B) a single chain is held stretched for about 5 seconds.

If both ends were covalently linked to the tip and the surface, the single molecule could be held stretched for longer allowing time to inject reactants into the system, i.e. an enzyme, and study the effect of modifying the pectin fine structure on the physical properties of the pectin.

Another interesting route would be to gain further information on the attractive weak interactions between proteins and pectins with single molecule force experiments by coating the surface with pectin and the tip with proteins. The functionality of these complexes, which can serve as fat replacer or texturing agents and stabilizers, could then be studied, for example hydration, structuration, interfacial and adsorption properties.

ANNEXE 1

DFT CALCULATIONS

1. MONOMER, DIMER AND TRIMER OF GALACTURONIC ACID

Complete Hessian calculations were performed on a monomer, dimer and trimer of a-D-galacturonic acid and their methylesterified analogues using DFT calculations implemented in the Gamess US package (Pople & Gordon, 1967). The computational facilities used were an IBM-Bluegene cluster sited at the University of Canterbury, NZ.

Bluegene/L nodes have two processors and two modes of execution are supported: co-processor (CO) and virtual node (VN) modes. In CO mode the first processor runs the program and the second processor handles I/O and communication on behalf of the first processor. In virtual node mode, both processors run the program. In CO mode all node memory is allocated to the first processor, while in the VN mode, the node memory is shared between the two processors. The single rack system we utilized provides a maximum of 1024 processors with 512 MB of RAM each, or 2048 processors with 256 MB of RAM each; with the calculations reported herein exploiting the first option. Initially, the respective systems were placed in standard pyranose $^4C1$ configurations, completely optimized in the semi-empirical basis AM1, and were then geometry optimized using the B3LYP/6-31G* basis. These ground-states were then subsequently subjected to a complete optimization and Hessian calculation using the B3LYP/6-311++G** basis set, (Appell et al., 2004; Momany et al., 2004), incorporating the diffuse functionals. All simulations were performed at 0 K and in vacuum. The convergence criteria in the energy minimization for energy differences between cycles of optimization were less than 10^{-6} Hartree, with the gradient set to be less than 10^{-4} a.u, as in our previous work (Williams et al., 2007). The scaling and assignment of the vibrational modes was carried out using the *Chemcraft* program (Zhurko, 2009).

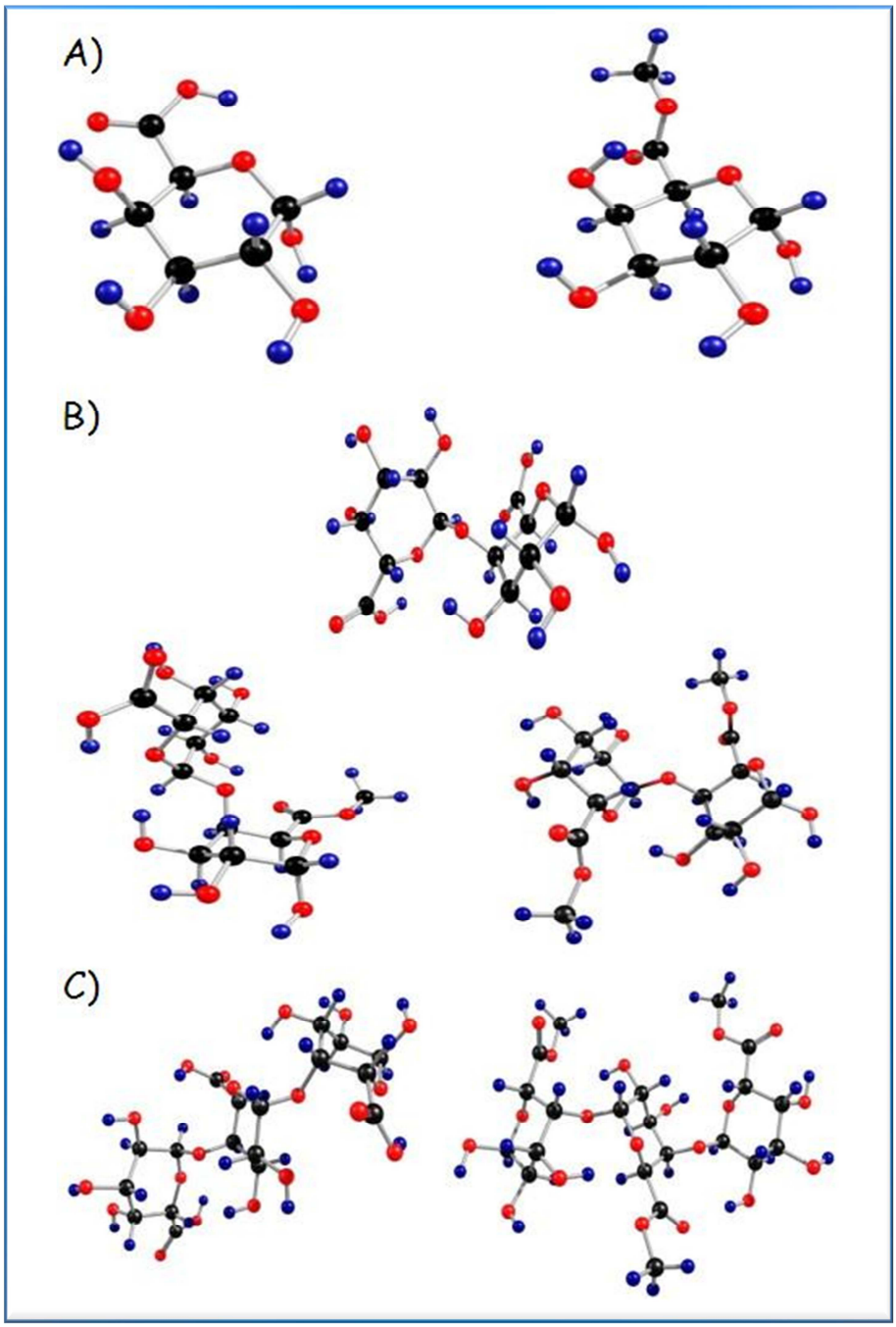

Fig. 7. 1. A) Pure monomer of a-d-galacturonic acid and its methylester analogue. (b) Galacturonic acid dimers of 0%, 50% and 100% DM depending on the number of the esterified groups in the molecule. (c) Trimers of a-d-galacturonic acid and its completely methylesterified analogue.

2. PECTIN COUPLING TO BEADS

DFT calculations were investigated for their usefulness in predicting changes in the IR spectra resulting from the coupling of pectins to polystyrene beads. Molecular models for the pectin moiety immobilized on polystyrene beads (by reductive amination as well as thiazolidine formation) were built using Ghemical (Hassinen & Perakyla, 2001) and these were subsequently energy-minimized using the semi-empirical AM1 basis set. To make the system computationally less expensive, a pectinic acid dimer molecule attached to one unit of polystyrene was considered. The free valencies of the single styrene-monomer were satisfied by H atoms. Fig. 7.2. and Fig. 7.3. show the models used for the calculations of the vibrational spectra of the proposed intermediates and pectin-functionalized polystyrene beads respectively (a) during reductive amination and (b) during thizolidine formation.

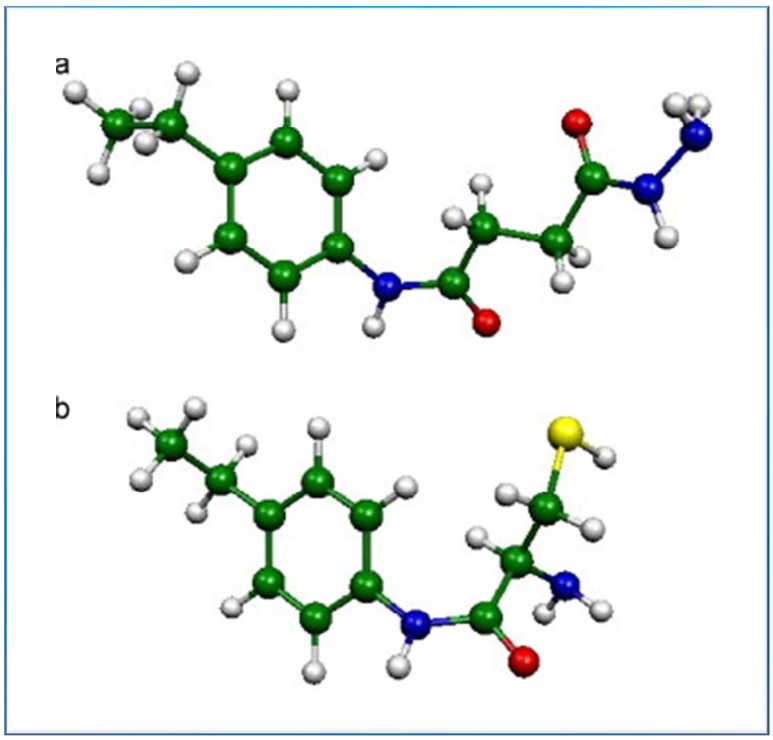

Fig. 7. 2. Models for the intermediates formed (a) during the reductive amination pathway and (b) during thizolidine formation (carbon: green; oxygen: red; hydrogen: white; nitrogen: blue; suphur: yellow).

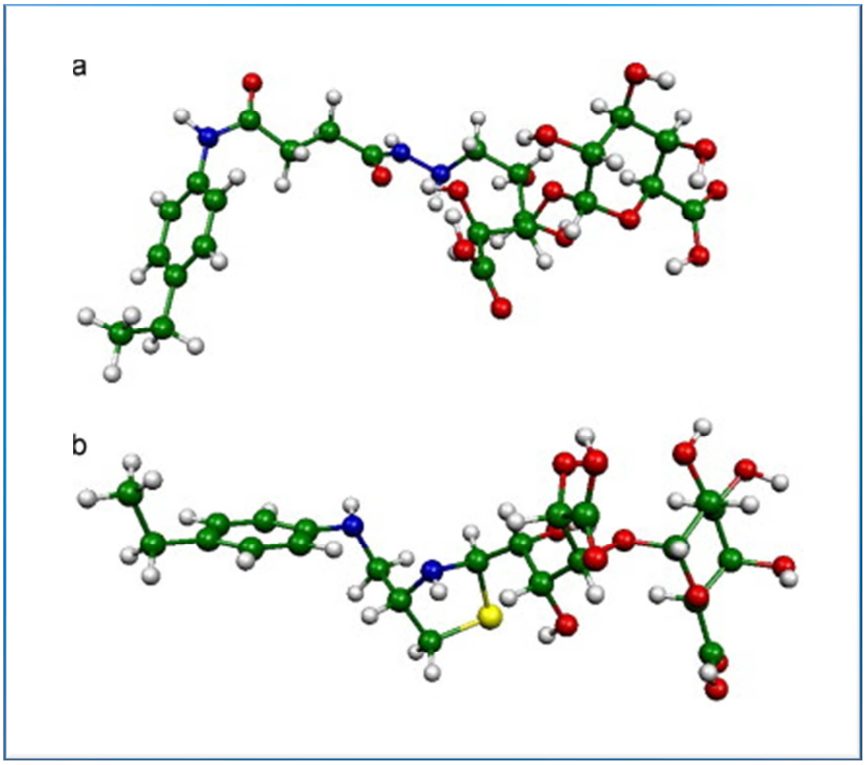

Fig. 7. 3. Models of an immobilized pectin dimer coupled to a 'polystryrene bead' (a) by reductive amination and (b) via thizolidine formation, used in the DFT calculations of the vibrational spectra. (carbon: green; oxygen: red; hydrogen: white; nitrogen: blue; suphur: yellow).

DFT calculations were implemented in the Gamess U S package (Pople & Gordon, 1967). The computational facilities used consisted of an IBM-Bluegene cluster sited at the University of Canterbury, NZ. Bluegene/L nodes have two processors and two modes of execution are supported: co-processor (CO) and virtual node (VN) modes.

The structures of the reaction intermediates were first geometry optimized using the B3LYP/6-31G* basis and subsequently a complete optimization and Hessian calculation was undertaken using the B3LYP/6-311++G** basis set, incorporating the diffuse functionals. All simulations were performed at 0 K and in vacuum condition. The convergence criteria in the energy minimization for energy differences between cycles of optimization were less than 10^{-6} Hartree with the gradient set to be less than 10^{-4} a.u. The scaling and assignment of the vibrational modes were carried out using the Chemcraft program (Zhurko, 2009).

3. REFERENCES

Appell, M.; Strati, G.; Willett, J.L. and F.A. Momany (2004) B3LYP/6-311++G** study of α- and β D-glucopyranose and 1,5-anhydro-D-glucitol: $^{4}C_{1}$ and $^{1}C_{4}$ chairs, ^{3,0}B and B^{3,0} boats, and skew boat conformations. *Carbohydrate Research*, **339**, 537–551.

Hassinen, T. and Perakyla, M. (2001) New energy terms for reduced protein model simplemented in an off-lattice force field. *Journal of Computational Chemistry*, **22**, 1229–1242.

Momany, F.A.; Appell, M., Strati, G. and Willett, J.L. (2004) B3LYP/6-311++G** study of α- and β-d-glucopyranose hydrogen bonding, stress energies, and effect of hydration on internal coordinates. *Carbohydrate Research*, **339**, 553–567.

Pople, J.A. and Gordon, M.S. (1967) Molecular orbital theory of the electronic structure of organic compounds. I. Substituent effects and dipole moments. *Journal of the American Chemical Society*, **89**, 4253–4261.

Williams, M.A.K.; Marshall, A.T.; Anjukandi, P. and Haverkamp, R.G. (2007) Investigation of the effects of fine structure on the nanomechanical properties of pectin. *Physical Review E*, **76**, 021927.

Zhurko, G. A. (2009) *Chemcraft*, http://www.chemcraftprog.com.

ANNEXE 2

AUTOMATIC DETECTION OF SINGLE MOLECULE STRETCHING

Published as :

Belmiloud, N.; Fellah, A.; Haverkamp, R.G. and Williams, M.A.K. (2011) Facilitating nanomechanical measurements on physisorbed biopolymers with automated on-the-fly monitoring of single-molecule force curves. *Advance Science Letters*, **4**, 1-4.

1. ABSTRACT

Single molecule force spectroscopy has recently given access to an unprecedented level of information regarding the stress response of a host of biopolymers at the single chain level. However, particularly for polysaccharides, where the intrinsic chemistry of the biopolymer complicates the design of chain-end-specific handles, the majority of studies are still carried out with biopolymers physisorbed to the substrates between which they are stretched. This means that the nature of recorded force-curve data is somewhat unpredictable from one scan to the next, making measurements tedious and time-consuming. Herein a methodology is described for use with single polymer force-spectroscopy that ameliorates this experimental inefficiency. The study describes the set-up of both an electronics bench and computational routines that enable accurate and automated measurements to be made despite low-level analog voltages and noisy signals. The length, quality and maximum force of any stretches detected are monitored in real-time and compared with user-defined thresholds, thus filtering the data set on-the-fly. This methodology for the automatic detection of single molecule stretching can be used both as an important time-saving tool in analysis, where many thousands of stretch attempts may be made in a single experiment, and eliminates measurement bias related to subjective choices made by the user. In addition, this tool enables the simple generation of an ensemble of measurements of the properties of studied molecular chains.

2. INTRODUCTION

Despite the fact that several studies in the literature highlight the promising prospects of AFM (Atomic Force Microscopy) for the study of molecular nanomechanics (Fisher et al., 1999; Jansho et al., 2000; Bustamante et al., 2000; Butt et al., 2005), only a few schemes for automatically detecting candidate single-molecule force-curves have been reported. These have been used in screening prerecorded data sets (Levy & Maaloum, 2005; Fuhman & Ros, 2010). In this brief report a low-cost protocol using a home-built laptop-based AFM control system and analysis software, integrated with a Veeco Nanoscope E, is described that is dedicated to performing single molecule force spectroscopy and that is capable of monitoring potential stretch-events in real-time. In such single-molecule techniques nano-scale stochastic events such as conformational changes, which can

be masked in measurements carried out on ensembles, may be observed. Typically, molecules are either adsorbed (physisorption) or covalently bonded (chemisorption) onto a substrate and are subsequently picked up by a nanoscopic tip that is located at the end of an elastic silicon microcantilever. The principle of a force measurement by AFM is simple: the polymer-laden substrate is mounted on a piezoelectric ceramic which is repeatedly extended towards, and subsequently retracted away from the microcantilever, whilst the induced deflection of the cantilever is concurrently recorded as a function of the piezo displacement. If a tether is formed between the cantilever and the substrate during their contact, then the retraction of piezo results in a force being exerted on the cantilever, mediated by the polymeric tether. The generated deflection of the cantilever increases up to a rupture point where the connection between cantilever and piezo scanner is lost. When physisorbed polymers form the tether several molecules may adsorbed onto the tip and multiple bridges can form during the contact with the substrate, resulting in unbinding traces with multiple saw-toothed patterns, with the molecules losing attachment successively. Each "tooth" consists of a part with a rising deflection followed by a sudden jump. The detailed shape of the curve before the rupture reflects the elasticity of the bridge. The jumps that occur on detachment or breakage of the linkage correspond to the breaking of bridges and can provide an estimate of the rupture force, the time needed for severing or detaching of the bridge, and the corresponding distance between the tip and the surface (Fig. 8.1.).

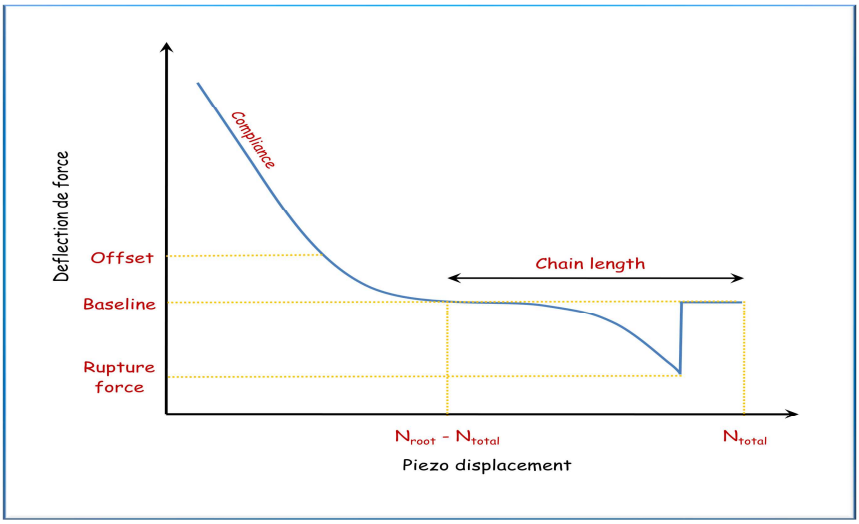

Fig. 8. 1. A schematic illustrating the parameters used in the force-curve detection algorithm: baseline, offset, compliance, and rupture force.

In this paper, we focus on describing simple protocols for the automatic analysis of force-curves in real-time. Studies using force spectroscopy on polysaccharide molecules have yielded particularly interesting data, the interpretation of which requires the marriage of statistical-mechanical theories of polymer physics to the complexities afforded by possible force-induced conformational transitions of the constituent sugar rings (Marszalek et al., 1999; 2001; Williams et al., 2007; Haverkamp et al., 2005; 2007; 2009; Zhang et al., 2005). Such monomer transitions during stretching, from classical chair forms of the pyranose ring to more elongated arrangements increase the polymer's contour length and thus produce characteristic deviations in the slope of the force-extension curve. Despite this unique behaviour, progress in the study of such polysaccharide stretching has been comparitively slow. The difficulty of designing handles for the specific attachment of the different ends of polysaccharide chains to substrates, such as piezoelectric scanners or cantilevers, means that the majority of studies have been carried out with the polymer in question physisorbed to the substrates (Maurice et al., 1999) between which it is stretched; with only a minor amount of work using specific ligands as polymer attachment points (Marszalek et al., 1998) or at best chemically attaching one end of the saccharide chain via a bond formed at an uncontrolled location along the length of the molecule (Khner et al., 2006). This means that the nature of recorded force-curve data is somewhat unpredictable from one scan to the next, making measurements tedious and time-consuming. Such a polymer is therefore ideal for our purposes, as its study would clearly benefit enormously from the availability of an automated analysis procedure. The particular polysaccharide pectin was selected as the typical force-extension behavior of this important polysaccharide presents two force induced conformational transitions that make it a particularly interesting case (Williams et al., 2007; Marszalek et al., 2001; Haverkamp et al., 2005; 2007; Zhang et al., 2005).

3. EXPERIMENTAL DETAILS

3.1. Polymer

Pectin was obtained from Fluka and was physisorbed between a silicon cantilever and a glass disc mounted on a piezoelectric scanner. This polysaccharide had an anhydrogalacturonic acid content of 85%, a degree of methylesterification of 78% and a molecular weight of 30–100 kDa. The samples

were prepared by applying 20 μl of 0.1 or 0.01 w/w% solutions in deionized H2O to cleaned discs, which were then dried at 11.3% relatively humidity overnight. This was then extensively rinsed with deionised H2O leaving only the tightly bound molecules on the surface. Measurements were made in water, and in 10 mM and 100 mM phosphate buffer at pH 7.0 as described below.

3.2. AFM

After preparation the sample was mounted in the AFM and a liquid-cell filled with the appropriate solvent just prior to the force curve measurements. Force-distance curves were recorded by pulling the molecules at 0.5–4 $\mu m\ s^{-1}$ using the scanning probe microscope head from a Veeco Nanoscope E, with but with a home-built lab-top based controller driving the stepper-motor and the piezoelectric scanner, based on a feedback-signal generated from the quadrant photodiode (QPD). A 16 bit National Instruments I/O card was used (NI USB 6211), and recording and analysis routines constructed in LabView.

3.3. Cantilever calibration

The silicon cantilever used was calibrated using a thermal method (Sader et al., 2005). Briefly, the thermal spectrum was obtained from a QPD that monitored the position of laser light after being deflected from the cantilever. The data were acquired at a sampling frequency in agreement with the Nyquist theorem; that is, at a rate twice as fast as the highest resonant mode measured. Once the data has been sampled, the power spectral density was obtained by fast Fourier-transform and subsequently, the power spectrum was fitted to a simple harmonic oscillator model (Jing et al., 2007). Through the use of the equipartition function, the model parameters provide a quantitative measure of the spring constant. The measurement was made in air so the first resonance of the cantilever was not damped and was easily isolated from the other modes. Gold-coated cantilevers were preferred and maximized the QPD sensitivity.

3.4. Hardware protocol for force-curve measurement

In order to start outputting the voltage that controls the piezo position at the same time as the QPD signal sampling was initiated, input and the output signals were first synchronized. Hardware synchronization was implemented, which involved physically changing a voltage on one of the control lines to trigger the I/O process. I/O voltages were generated and recorded simultaneously, every microsecond. The input signal was processed to remove noise disturbances and compensate for environmental effects such as low-frequency electronic noise and acoustic vibration. An optical bench set-up was essential to minimize any noise arising from diffraction of the laser from the cantilever beam. Shiny substrates were also avoided to limit interference from unwanted reflections, and a good alignment of the optical pathway was important to minimize any recorded ripple. Having dealt with the input signal an output voltage was generated in order to drive the piezo-scanner based on the processed input value. However, the output voltage range provided by the data acquisition card used was too small to displace the piezo to sufficient amplitudes to be usefully used in SMFS (Single-Molecule Force Spectroscopy). Therefore a voltage booster was constructed in order to increase the available voltage of the output signal, without supplying appreciable power. Filters were then utilized to minimize the ripple in the amplified voltage, which was estimated at less than 2%. This electronics bench preserved I/O synchronization and gave a control system with a spatial resolution estimated at 1 nm.

3.5. Software protocol for real-time force curve analysis

A typical experiment consists of a sequence of attempts to obtain a force-extension curve, each consisting of one extend-retract cycle of the piezo, as shown schematically in Fig. 8.2. This corresponds to a triangular voltage-train being applied to the piezo and in each attempt the rising and descending phases both contain $N_{total}/2$ data points, where N_{total} is the number of datapoints included in each cycle.

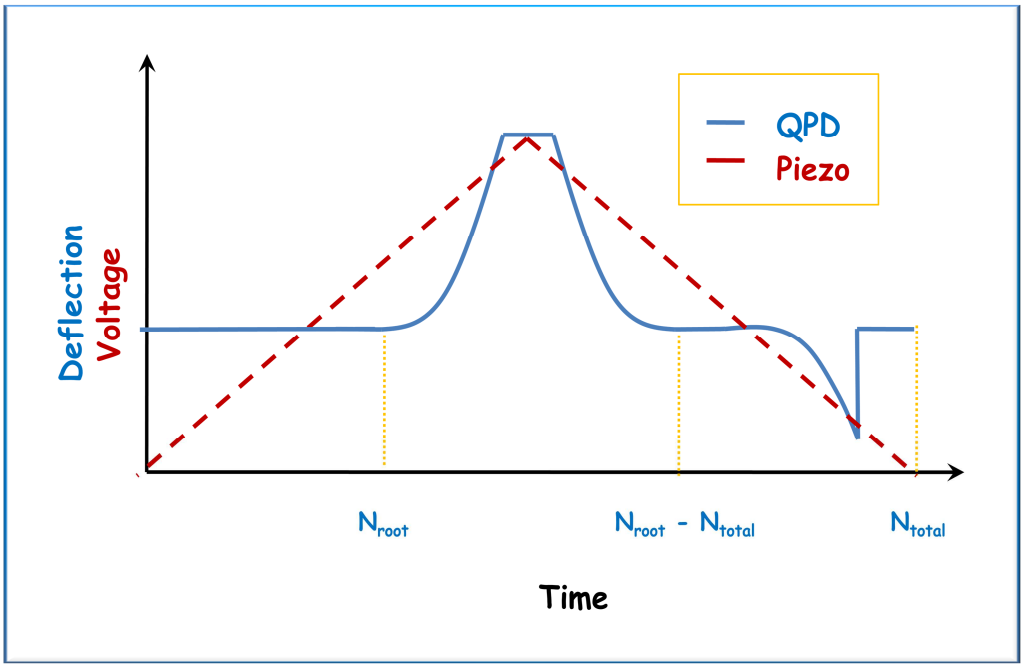

Fig. 8. 2. A schematic of the time-course of the I/O voltages read from the QPD and sent to the piezo, assuming that a single polymer chain is stretched upon retraction.

The desired experimental result in a SMFS AFM experiment is a force curve, F_{exp} (X_i), where F_{exp} is the measured force obtained from the cantilever deflection and X_i is the displacement of the piezo (i.e., the sample) away from the relaxed cantilever at the instant *i*. The first step of analysis is to obtain the cantilever deflection in nm from the QPD signal, and then from this deflection, the force, F_{exp}, is obtained in nN using the spring constant of the cantilever (obtained from calibration as described above). To extract the deflection it is assumed that, in an absence of deformation of the sample, and neglecting a light elastic hysteresis of the piezoceramic, that when the piezomounted substrate contacts the cantilever and subsequently bends it before retraction, (the compliance region), that the deflection of the cantilever is equivalent to the distance traveled by the piezo. Therefore, this compliance region gives a way of relating the measured QPD voltage to a known cantilever deflection in nanometers (the slope S of the compliance region (Fig. 8.1.)). With the slope of the compliance region and the spring constant of the cantilever in hand, force-extension curves can be measured. In order to recognize the compliance region automatically, software was written in LabView that defines a baseline using the start of the data set when the piezo is far away from the cantilever, and then monitors when the data deviate from the baseline

by a chosen offset (introduced to eliminate the nonlinear region corresponding to the deformation of the cantilever owing to capillary forces). This threshold was selected in order to avoid the non-linear response of the sensor and QPD saturation; both of which limit the linear range of the compliance region. The bounded values of the baseline confidence interval were calculated as follows:

$$B^{+} = \frac{1}{N_{start}}\left(\sum_{i}^{N_{start}} F_i + \alpha\sqrt{\frac{1}{N_{start}}\sum_{i}^{N_{start}}(F_i - \bar{F})^2}\right) \qquad (1)$$

$$B^{-} = \frac{1}{N_{start}}\left(\sum_{i}^{N_{start}} F_i - \alpha\sqrt{\frac{1}{N_{start}}\sum_{i}^{N_{start}}(F_i - \bar{F})^2}\right) \qquad (2)$$

where B^{+}, B^{-} are respectively the higher and lower bounds of the 99% confidence interval of the nominal baseline value, F is the mean value of the force for the first N_{start} points, and α the Student's t factor. When $N_{start} > 100$, the Student's t-distribution tends to be normally distributed and $\alpha \approx 3$. When n successive datapoints deviate from the mean value by more than the 99% CI bound then contact between the substrate and cantilever was assumed to have occurred at $i = N_{root}$ (Figs. 8.1. and 8.2.). Additionally, if a polymer-stretch occurs upon retraction, this N_{root} value can be used to approximate zero displacement of the stretch. The main step that finds significant application in the automatic, on-the-fly filtering of datasets is the detection of suitable force curves and ruptures thereof. A rupture is by definition a breakpoint, i.e., an algebraic unsteadiness and, as such, the implemented detection scheme was based on a measure of the dispersion. In order not to exceed the buffer memory size and to increase the speed of the software, the data processing was focused on the area of interest from $i = N_{total} - N_{root}$ up to $i = N_{total}$. The sample standard deviation is computed in a test window of width n that is stepped along the force curve from the instant i to i+n thus:

$$\sigma_i = \sqrt{\frac{1}{n}\sum_{j=i}^{i+n}\left(F_j - \bar{F_i}\right)^2} \qquad (3)$$

The variation in this standard deviation value, σ_i , as the sliding window was translated along the force-curve was used to identify extend-retract cycles of interest. To remove positives due to unwanted experimental noise, a further parameter, σ_{noise}, was introduced, defined as:

$$\sigma_{noise} = \frac{1}{N_{start}} \left(\sum_{i}^{N_{start}} \sigma_i + \alpha \sqrt{\frac{1}{N_{start}} \sum_{i}^{N_{start}} (\sigma_i - \bar{\sigma})^2} \right) \qquad (4)$$

and by comparing this to the value of σ_i a new filtered function was generated as follows :

$$\begin{array}{lll} if\ \sigma_i > \sigma_{noise} & then & \sigma = \sigma_i \\ if\ \sigma_i \leq \sigma_{noise} & then & \sigma = \sigma_{noise} \end{array} \qquad (5)$$

The developed protocol detects localized jumps in the force curve and is able to notify the user if a likely single-molecule stretching event has occurred; or save only data that correspond to possible events for post-run processing. Additionally the developed software reports the rupture force and the approximate value of the stretch length.

4. RESULTS

Fig. 8.3. shows a selection of typical single-molecule forceextension curves measured for pectin, identified automatically from a set of several thousand extend and retract cycles using the set-up described herein.

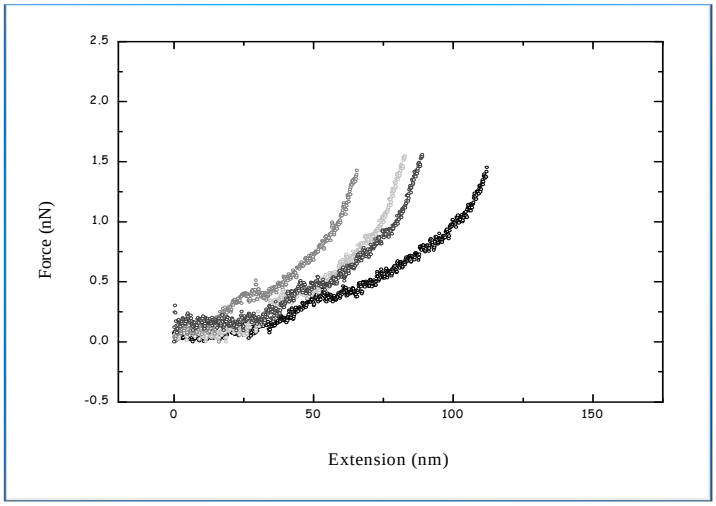

Fig. 8. 3. Force-extension curves measured from a single pectin chain,as described in the experimental section. Two inflections can be seen in the curve, in accordance with the results of previous studies.

Fig. 8.4. shows the real benefit of the method presenting statistical results obtained from the analysis of several entire datasets, showing how (a) the length and (b) the maximum force of the polymer stretches obtained varies under several different solvent conditions.

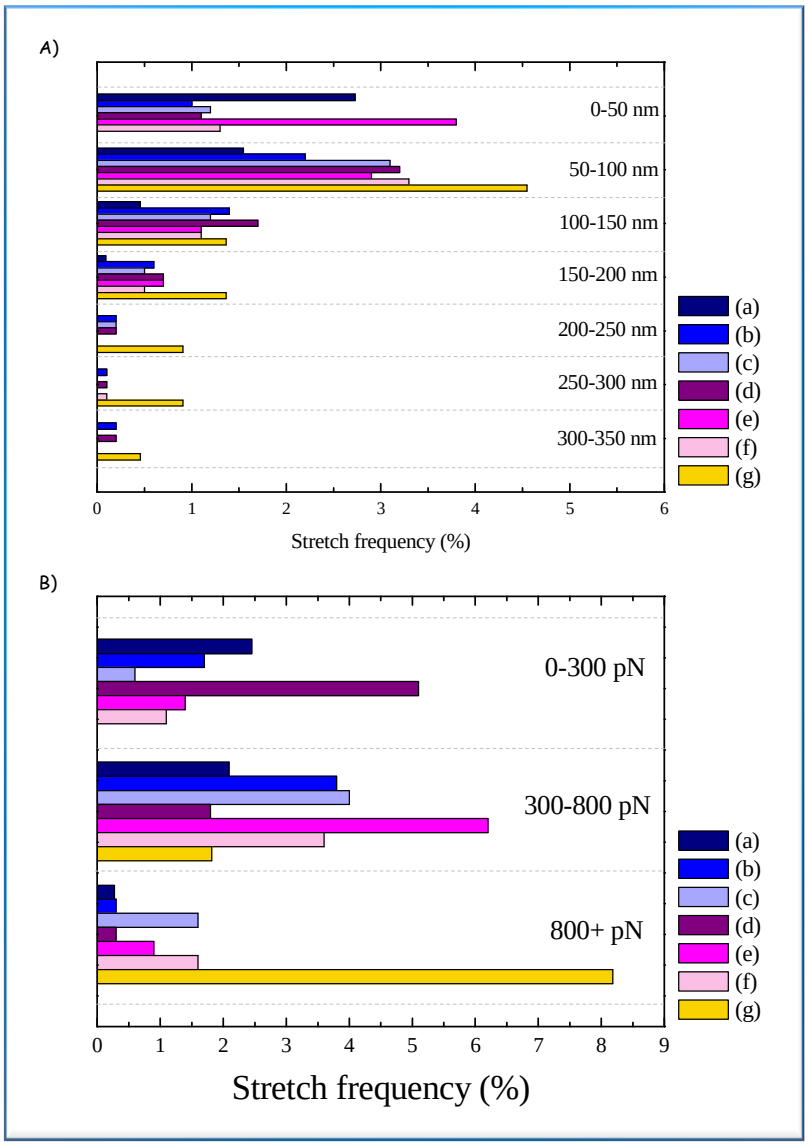

Fig. 8. 4. The frequency of A) the different lengths and B) the different rupture forces of stretch achieved under seven different sets of experimental conditions. (a) 0.01% polymer, pH 3, H2O; (b) 0.01% polymer, pH 7, 10 mM phosphate buffer; (c) 0.01% polymer, pH 7, 100 mM phosphate buffer; (d) 0.1% polymer, pH 3, H2O; (e) 0.1% polymer, pH 7, 10 mM phosphate buffer; (f) 0.1% polymer, pH 7, 100 mM phosphate buffer; (g) 0.1% polymer, pH 7, 100 mM phosphate pre-attached to substrate at reducing end of the polysaccharide chain.

These data represent the outcome of the analysis of some ten thousand extend-retract cycles, a task that would have required a large amount of time and effort had each extend-retract cycle required individual screening, and give a clear indication of differences between the solvent conditions. The methodology described herein enables such studies on physisorbed biopolymers to

be carried out in a significantly more efficient manner than has been possible to-date by screening datasets on-the-fly. With slight modifications it was also demonstrated that this simple methodology is capable of achieving real-time control of polymer stretching, opening up more facile routes to experimental investigation of the interaction of other molecular components with pre-tensioned chains.

5. ACKNOWLEDGEMENTS

The authors would like to gratefully acknowledge Fonterra and FRST for providing a Ph.D. scholarship to Abdenor Fellah, and the Royal Society of New Zealand Marsden Fund for funding (Naser Belmiloud). Dave Lloyd is acknowledged for skillful assistance with the construction of the electronics bench.

6. REFERENCES

Bustamante, C.; Smith, S.B.; Liphardt, J. and Smith, D. (2000) Single-molecule studies of DNA mechanics. *Current Opinion in Structural Biology*, **10**, 279-285.

Butt, H.J.; Cappella, B. and Kappl, M. (2005) Force measurements with the atomic force microscope : technique, interpretation and applications. *Surface Science Reports*, **59** (1-6), 1-152.

Fisher, T.E.; Oberhauser, A.F., Carrion-Vasquez, M.; Marszalek, P.E. and Fernandez, J.M. (1999) The study of protein mechanics with atomic force microscope. *Journal of Physiology*, **50**, 5.

Fuhrmann, A. and Ros, R. (2010) Single-molecule force spectroscopy : a method for quantitative analysis of ligand-receptor interactions. *Nanomedecine*, **5** (4), 657-666.

Haverkamp, R.G., Williams, M.A.K. and Scott, J.E. (2005) Streching single molecules of connective tissue glycans to characterize their shape maintaining elasticity. *Biomacromolecules*, **6**, 1816.

Haverkamp, R.G., Marshall, A.T. and Williams, M.A.K. (2007) A model for stretching elastic biopolymers which exhibit conformational transformations. *Physical Review E*, **75**, 021907.

Haverkamp, R.G. (2009) Nanotechnology provides a new perspective on chemical thermodynamics. *Journal of Chemical Education*, **86** (1), 50.

Janshoff, A.; Neitzert, M.; Oderorfer, Y. And Fuchs, H. (2000) Force spectroscopy of molecular systems – Single molecule spectroscopy of polymers and biomolecules. *Angewandte Chemie – International Edition*, **39** (18), 3213-3237.

Jing, G.Y.; Ma, J. And Yu, D.P. (2007) Calibration of the spring constant of AFM cantilever. *Journal of Electron Microscopy*, **56** (1), 21-25.

Khner, F., Erdmann, M. and Gaub., H. (2006) Scaling exponent and Kuhn length of pinned polymers by single molecule force spectroscopy. *Physical Review Letters*, **97**, 218301.

Levy, R. and Maaloum, M. (2005) New tools for force microscopy. *Ultramicroscopy*, **102** (4), 311-315.

Marszalek, P.E., Oberhauser, A.F., Pang, Y.P. and Fernandez, J.M. (1998) Polysaccharide elasticity governed by chair-boat transitions of the glucopyranose ring. *Nature*, **396**, 661-664.

Marszalek, P.E., Pang, Y.P., Li, H., Oberhauser, F.A., Yazal, J.E. and Fernandez, J.M. (1999) Atomic levers control pyranose ring conformations. *Proceedings of National Academy of Sciences*, **96**, 7894-7898.

Marszalek, P.E., Li, H. and Fernandez, J.M. (2001) Fingerprinting polysaccharides with single molecule atomic force microscopy. *Nature Biotechnology*, **19**, 258

Maurice, R.G. and Matthai, C.C. (1999) Force-extension curves for a single polymer chain under varying solvent conditions. *Physical Review E*, **60**, 3165-3169.

Sader, J.E., Pacifico, J., Green, C.P. and Mulvaney, P. (2005) General scaling law for stiffness measurement of small bodies with applications to the atomic force microscope. *Journal of Applied Physics*, **97**, 124903.

Shusteff, M.; Burg, T.P. and Manalis, S.R. (2006) Measuring Boltzmann's constant with a low-cost atomic force microscope : an undergraduate experiment. *American Journal of Physics*, **74** (10), 873-879.

Williams, M.A.K., Marshall, A.T., Anjukandi, P. and Haverkamp, R.G. (2007) Investigation of the effects of fine structure on the nanomechanical properties of pectin. *Physical Review E*, **76**, 021927.

Zhang, Q., Lee, G. and Marszalek, P.E. (2005) Atomic cranks and levers control sugar ring conformations. *Journal of Physics : Condensed Matter*, **17**, S1427.